POLITECNICO DI MILANO

Facoltà di Ingegneria dei Sistemi
Corso di Laurea Specialistica in Ingegneria Biomedica

MODELING OF ARTICULAR CARTILAGE BEHAVIOR IN UNCONFINED COMPRESSION: COMPARISON WITH EXPERIMENTAL TESTS

Relatore: Prof. Pasquale VENA
Correlatore: Prof. Sam EVANS

Tesi di Laurea Specialistica di

Susanna Piccinelli Matricola 721815

Anno Accademico 2009-2010

Table of Contents

Abstract

1. Introduction

In recent years the interest in the causes that induce cartilage degeneration, such as osteoarthritis (OA), has been increased. OA can be defined as a gradual loss of cartilage that causes pain and sometimes disability. In its severe form joint replacement surgery can be required (Wilson, 2005). The factors that cause this disease are mostly mechanical, but also metabolic and genetic causes can induce cartilage degeneration. In fact, the mechanical loading of cartilage are essential in regulating the activity of chondrocytes. These are, in fact, in turn responsible for maintaining normal extracellular matrix proprieties through the production, organization and degradation of proteoglycans and collagen network, in order to enable the cartilage to perform its main functions. Numerous studies demonstrated that an impulsive load or a non-physiological level of load may result in the onset of osteoarthritis. Examples are the levels of OA found in overweight people, in people that practice high-impact sports, or after a previous trauma to joints.

Articular cartilage (AC) is a connective tissue that covers the diarthrodial joints. Its main functions are to protect the joint from high stress concentration by dissipating the applied load over a larger contact area, through deformation and to facilitate the relative movement between the two articular surfaces, in order to reduce friction and to avoid wear. To carry out these functions, cartilage structure is highly complex. It is manly composed of collagen fibers, proteoglycans (PGs), chondrocytes, water and mobile ions. It is also aneural, avascular and alynphatic. The absence of blood vessels and the low cell concentration increase the difficulty in regeneration, making investigations and studies even more tricky and essential. Some studies demonstrated that OA concerns changes in proteoglycan and collagen concentration and in the spatial arrangement of collagen network. In particular, in

OA the orientation of collagen fibers change from parallel to perpendicular to the articular surface (Julkunen, 2008).

In recent years finite element (FE) analysis has become increasingly important to help the understanding of the causes that lead to degradation of cartilage. Thus, in order to understand these factors FE models of the whole joint, in which the interactions with the surrounding tissues are replied, are needed.

This study is part of a bigger project on the finite element modelling of the knee joint indeed. Articular cartilage was analysed. The purpose of this work was the analysis of the models commonly used in the literature to reproduce the response of cartilage under different mechanical load. In particular, it was required a model that may be accurate in the reproduction of AC response and that may require low computational burden in order to compute the solutions, so as it can be used for a complex finite element model as the whole knee joint. Therefore the analysis started from simple biphasic models, as the BLE model, in which the articular cartilage was reproduced as only composed of a solid matrix and fluid phase, up to more complex models where collagen network and proteoglycans were also modelled in order to increase the accuracy of the structure description. Unconfined compression tests were specially conducted, with the purpose of helping to understand which model best reproduce cartilage behaviour.

A further analysis was led to analyze the causes that induce AC swelling, due to the presence of PGs. This phenomenon can be observed inducing a sudden change of concentration in the bathing solution where the cartilage is stored. This part of the work is a prosecution of a project done by Joanna Li (Li, 2009) in the year 2008/2009 for the Imperial Collage of London. She presented a swelling model based on the analogy between the equation that describe the thermal and mass diffusion. This model was validated with data from the literature. Unfortunately, the data needed to implement the model are not always easy to find in the literature. Thus, unconfined compression tests with a sudden change in the solution concentration were especially performed.

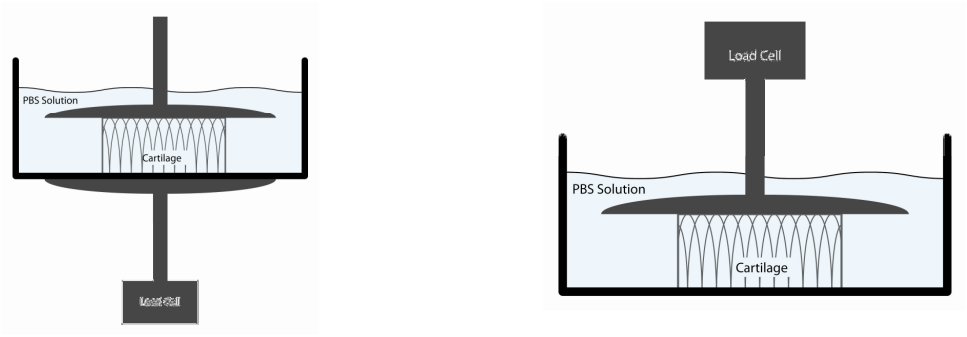

***Figure 1**:Experimental set-up used in the unconfined compression relaxation tests for the analysis of biphasic models (on the left) and for the swelling analysis on the right).*

2. Material and Methods

2.1. Experimental Tests

Unconfined compression tests were performed on six cylindrical AC plugs (with a diameter of 3 mm and a variable thickness. The samples were harvested from the metacarpalphalyngeal joint of a 7-days-old bovine calves. Full thickness AC plugs were first punched with a dermal biopsy punch (diameter of 6 mm) and then separated from the subchondral bone using a razor blade. In order to obtain samples as flat as possible, each AC plug of 6 mm was drilled with a dermal biopsy punch of 3 mm in diameter. All samples were stored for approximately twelve hours in a PBS solution with a sodium chloride concentration of 0.154M (pH 7.4) and at the physiological temperature (37°C). The testing machine (ElectroForce 3200, Bose Corporation, Minnesota, USA) was equipped with a 225N load cell. Ten repeated displacement were applied to each plugs, each one of about 1% strain at a velocity of 1μm/s. Each level of displacement was maintained constant for about 500s to in order to allow AC relaxation. During the test cartilage was bathed in PBS (0.154M NaCl) in order to maintain the hydration.

The experimental tests used to validate the swelling thermal analogy model were unconfined compression relaxation tests. In this case, a displacement of about 10% strain was applied with a velocity of 1 mm/s. After the relaxation (500s) the bathing solution was changed. At the beginning the cartilage was bathed in a 20 ml PBS solution at a physiological concentration equal to 0.154M NaCl. 18 ml of PBS were then removed from the original solution and substituted with 18 ml of distilled water. As a result, the sodium

chloride concentration was changed from the physiological value (0.154M) to an hypotonic one (0.0154M).

In both tests particular attention was paid in order to obtain samples as flat as possible and in the storing method, so as to avoid an alteration of cartilage structure and mechanical properties.

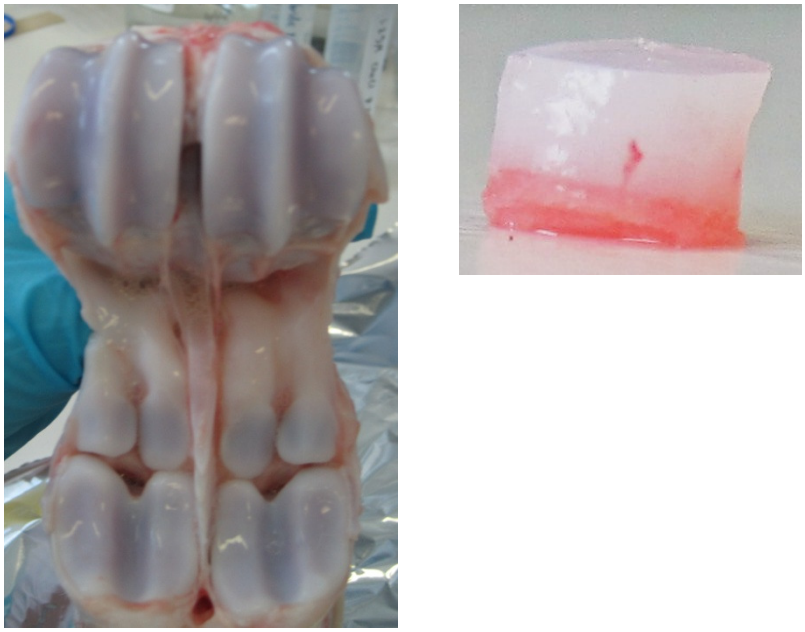

Figure 2*: In the figure is shown the metacarpalphalyngeal joint of a 7-days-old bovine calves from which the AC plugs were harvested (on the left); one example of the obtained samples (diameter of 3 mm), it is possible to notice the presence of the subchondral bone (on the right).*

2.2. Numerical Analysis

The biphasic models analysis were simulated using the commercial FE code FEBio v.1.2.0 (Musculoskeletal Research Laboratories, University of Utah), in a three-dimensional configuration. Instead, the swelling thermal analogy method was validated in axisymmetric condition, using the software ABAQUS v.6.8.1 (ABAQUS Inc., Providence, USA). In both analyses were used geometry, boundary conditions and contact similar to the experimental conditions, in order to allow a comparison between the experimental and the numerical results.

The Young's modulus was obtained from the experimental tests at the end of relaxation. At equilibrium is possible to consider cartilage as composed of only the elastic solid matrix, because the fluid phase is at equilibrium. All the other parameters used for every models

were extracted from a curve-fitting between the reaction forces measured in the unconfined compression tests and the ones predicted numerically.

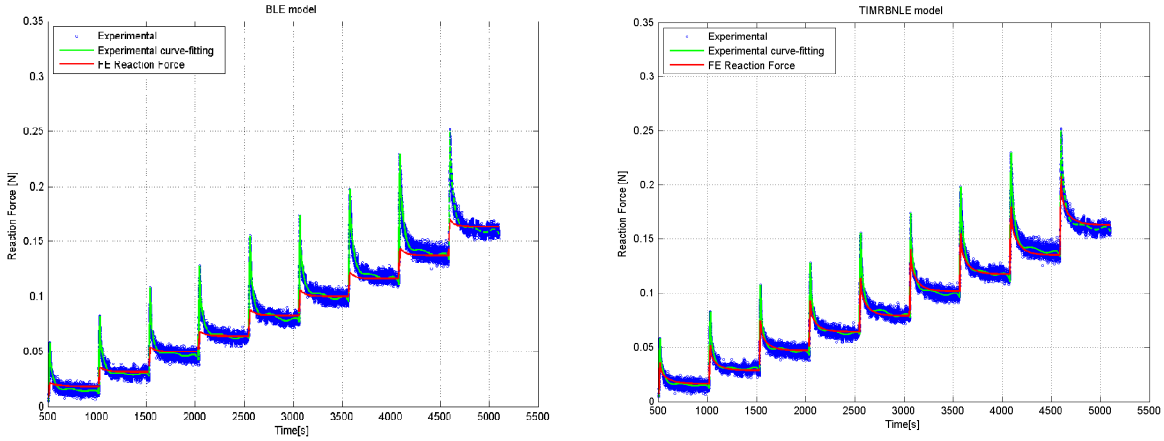

a) *b)*

***Figure 3**: In this figure is shown the predicted history of the reaction force (red) obtained using a BLE model (on the left) and a TIMRBNLE model (on the right). Besides, the history of the experimental reaction force (blue) and its curve-fitting with a polynomial of 5^{th} degrees are shown.*

3. Results and discussion

The simpler and faster models are the linear biphasic (BLE) and the non linear biphasic (BNLE), in which the strain-dependent permeability is considered. Unfortunately, both models cannot accurately reproduce the reaction force of AC (Figure 3a). In particular, the instantaneous peak of reaction force is smaller than the experimental one. If also the presence of collagen fibers is considered, through the implementation of the transversal isotropic Mooney-Rivlin hyperelasticity (Weiss, et al., 1996), the reaction force peak will increase due to the introduction of anisotropy (Figure 3b), however, this value will be still too small. Only the continuum fibers distribution, recently implemented by Ateshian (Ateshian, 2007; Ateshian, et al., 2009) could accurately reproduce the experimental reaction force (Figure 4).

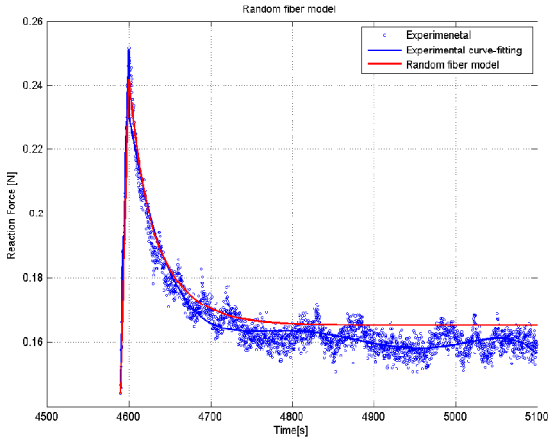

***Figure 4**: In this figure is shown the history of the reaction force numerically predicted (red) using a continuum fiber distribution model. Besides, the history of the experimental reaction force (blue) and its curve-fitting with a polynomial of 5^{th} degrees are shown.*

The difference between the two models is mainly the stricture description of the collagen network. In the former it is represented by a single preferred family of fiber. Instead, in the latter a continuum angular distribution is used to reproduce the collagen network. Thus, in order to accurately reproduce the response of cartilage under different mechanical loading, it is necessary to include in the model numerous families of collagen fiber. In conclusion, it is not possible to find an accurate model that is at the same time fast in the results computation. Thus, the model that can be used for a whole knee joint analysis must be a compromise between accuracy and computational speed.

The swelling thermal analogy model demonstrated to accurately reproduce the experimental swelling tests (Figure 5a). Besides, this FE implementation can be used to separately analyze the two mechanisms that cause cartilage swelling, observations that are not possible to be made experimentally (Figure 5b).

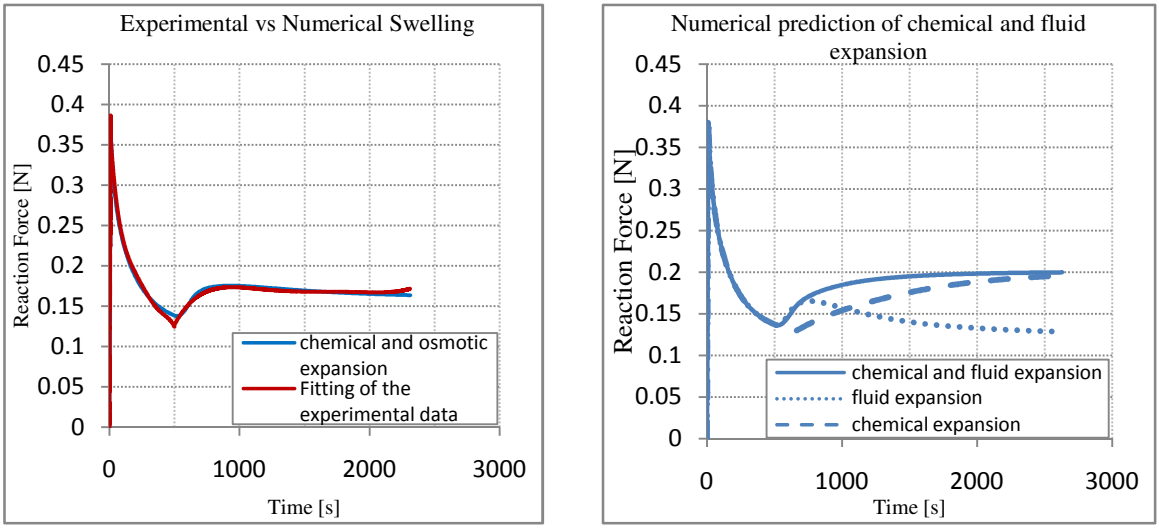

a) *b)*

***Figure 5**: a) Comparison between the numerical results obtained with the swelling thermal analogy and the experimental results obtained with the experimental tests described above.; b) numerical prediction of the AC swelling and of the two mechanisms that cause this phenomenon (Donnan osmotic pressure expansion and charge-to-charge repulsion).*

Besides, particular interest was posed in the study of the effect of non-flat samples on the measured reaction force. If, actually, the contact area is lower than the whole superior surface of the sample, the measured reaction force of AC will be also lower than the one measured when the load is applied on the whole surface. Also the instantaneous peak force will be lower. Thus, mistakes may be done in the extraction of mechanical properties.

Finally, a further analysis was done to study the effect of friction in the specimen/platens interfaces on cartilage response. Generally, friction is considered negligible in order to help the extraction of mechanical parameters of the models through a curve-fitting between the numerical analyses and the experimental tests. Although the platens surfaces are very smooth, friction between the interfaces cannot be neglected. Therefore the mechanical properties obtained considering frictionless surfaces are wrong (Figure 6). In particular, it was observed that the numerical permeability was larger in the case with frictionless interfaces than the case in which friction was considered, whereas, though with a small difference, the Young's modulus was smaller.

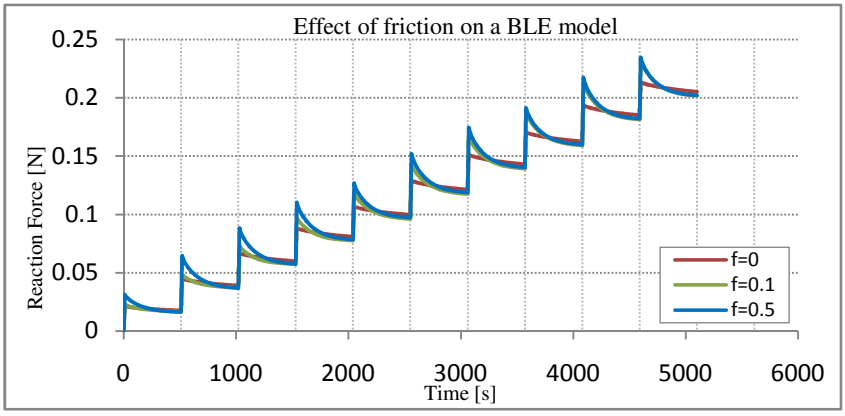

***Figure 6**: Numerical prediction of reaction force versus time obtained from the unconfined compression simulations for different value of the fiction coefficient (f).*

Above was explained the difficulty of biphasic models in reproducing the high ratio from peak to equilibrium typical pattern of the experimental reaction force. Some authors suggest that this lack is because of the assumption of frictionless interfaces. Actually, numerical results showed that friction can help to increase the instantaneous peak of reaction force, hence augmenting the agreement between the numerical and experimental reaction force (Figure 7).

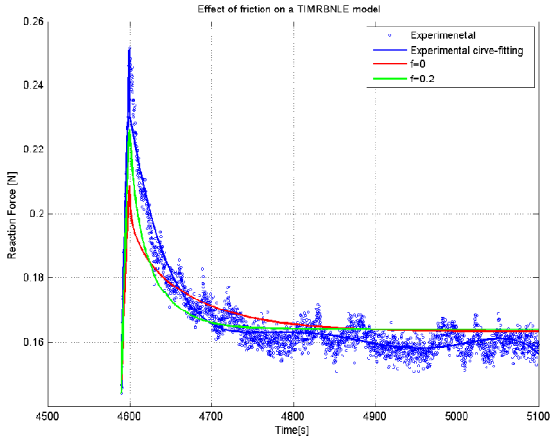

***Figure 7**: In figure is shown how the presence of fiction affect the reaction force predicted with the TIMRBNLE model (in green). Besides, the history of the experimental reaction force (blue) and its curve-fitting with a polynomial of 5^{th} degrees are shown.*

4. Conclusion

From the results showed above it is possible to conclude that is quite hard to find an analytical model that is computationally fast and at the same time accurate in the prediction of AC response. Actually, in order to replicate all the mechanical behavior of cartilage under different experimental test, the description of cartilage as only composed of a linearly elastic solid matrix and a fluid phase is not enough. Also the introduction of anisotropy, through the description of a single family of collagen fibers, is still not enough. In order to reproduce AC response in different mechanical loading more complex model are so needed, but they are also more computationally expensive. An example is the continuum fiber distribution model. However, in order to accurately reproduce the response of cartilage is also necessary to consider the presence of PGs. Thus, the thermal analogy model can be used for this purpose, thanks to the good results obtained.

Finally, results suggested that the presence of friction between sample/platens interfaces, the use of samples that are not flat and the storing method affect the measured mechanical properties of articular cartilage.

Sommario

1. Introduzione

Negli ultimi anni sempre più interesse è stato riposto nell'analisi e comprensione dei meccanismi che provocano la generazione di malattie della cartilagine come l'osteoartrite (OA). OA può essere definita come una perdita graduale della cartilagine che provoca dolore e a volte anche problemi di deambulazione fino a richiedere in alcuni casi l'intervento chirurgico (Wilson, 2005). Alla base di questa malattia ci sono perlopiù fattori meccanici, ma anche fattori genetici e metabolici ne possono essere responsabili. Infatti i carichi meccanici della cartilagine sono essenziali nel regolare l'attività dei condrociti. Questi sono a loro volta responsabili del mantenimento della matrice extracellulare ai valori fisiologici producendo, degradando e organizzando i proteoglicani e la matrice di collagene, affinché la cartilagine possa svolgere le proprie funzioni. E' dimostrato che un carico impulsivo o superiore al valore fisiologico può provocare l'insorgere di osteoartriti. Ne sono esempi il livelli di OA riscontrati nei casi di obesità, in numerosi sportivi praticanti sport in cui le articolazioni sono soggetti a carichi impulsivi, oppure in seguito a traumi riguardanti le articolazioni.

La cartilagine articolare è un tessuto connettivo che ricopre le articolazioni di tutto il corpo. Le sue funzioni fondamentali sono quella di ammortizzare i carichi, distribuendo i picchi di sforzo su una più ampia area di contatto attraverso la deformazione e quella di facilitare il movimento relativo tra le due superfici articolari, al fine di ridurre attrito e usura. Per poter svolgere queste funzioni, la cartilagine articolare possiede una struttura altamente complessa. Principalmente è composta da fibre di collagene, proteoglicani, condrociti, acqua e ioni mobili. E' inoltre aneurale, avascolare e alinfatica. E' soprattutto l'assenza di vasi sanguigni e la bassa concentrazione di cellule che la rendono un tessuto molto difficile da rigenerare e quindi ancora più interessante da studiare. E' dimostrato che OA produce un cambiamento sia nella concentrazione dei proteoglicani e fibre di collagene

sia per quanto riguarda la disposizione spaziale delle fibre di collagene. Studi al riguardo dimostrano come queste ultime in caso di OA passino da un orientamento fisiologico parallelo alla superficie articolare ad uno perpendicolare (Julkunen, 2008).

Accanto a studi sperimentali negli ultimi decenni ha assunto sempre più importanza l'analisi agli elementi finiti, per una maggiore comprensione dei fenomeni che portano alla degradazione della cartilagine. A tal proposito, la modellizzazione della sola cartilagine non è sufficiente, servono infatti modelli di tutta l'articolazione, in cui vengano replicate le interazioni con i tessuti circostanti.

A tal proposito, questo lavoro di tesi si pone all'interno di un più ampio progetto volto alla modelizzazione ad elementi finiti del ginocchio. Tra tutti tessuti presenti in questa articolazione mi sono occupata in particolare della cartilagine. Lo scopo di questo studio è stata l'analisi di numerosi modelli presenti in letteratura, comunemente utilizzati per riprodurre la risposta delle cartilagine in seguito a diversi tipi di sollecitazioni meccaniche. In particolare, il modello richiesto doveva rispondere ai requisiti di accuratezza nella riproduzione della risposta della cartilagine e basso peso computazionale, per poterlo applicare ad un complesso modello ad elementi finiti come l'intera articolazione del ginocchio. Si è partiti pertanto da semplici modelli bifasici, in cui la cartilagine era composta solo da una matrice solida e una fase fluida, fino ad arrivare a modelli più complessi in cui è stata analizzata anche la presenza delle fibre di collagene e dei proteoglicani, per aumentare l'accuratezza nella descrizione della struttura. Sono state poi appositamente svolte prove sperimentali di compressione non confinata, per facilitare la comprensione di quale modello sia più adatto a riprodurre il comportamento della cartilagine.

Un'ulteriore analisi è stata affrontata per analizzare il fenomeno di rigonfiamento della cartilagine dovuto alla presenza dei proteoglicani a seguito di una variazione di concentrazione ai capi del tessuto (chiamato *swelling*). Questa fase del lavoro è una continuazione di un progetto svolto nell'anno 2008/2009 all'Imperial College di Londra da Joanna Li (Li, 2009). Nel suo progetto è stato presentato e validato con dati presenti in letteratura un metodo basato sull'analogia matematica tra le equazioni di diffusione termica e di massa, per lo studio del fenomeno di rigonfiamento della cartilagine. Poiché, i dati necessari non sono sempre facili da reperire dalla letteratura, sono state appositamente

ideate prove di compressione non confinata con variazione di concentrazione della soluzione in cui è stata immersa la cartilagine.

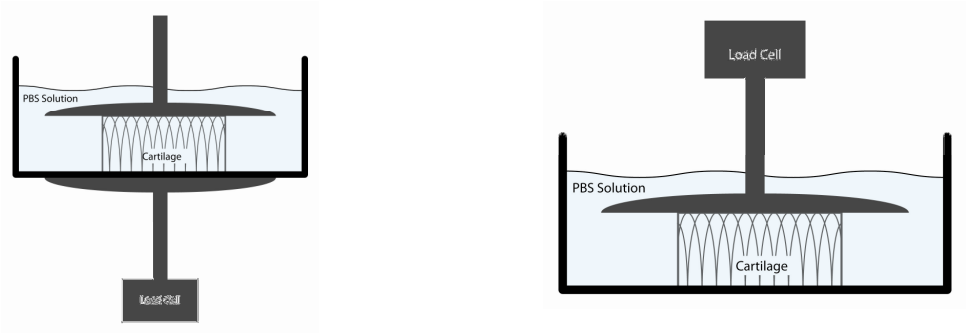

***Figura 1**:Set-up sperimentale utilizzato per la prova di compressione non confinata a 10 step consecutive (sulla sinistra) e per l'analisi dello "swelling" (sulla destra)*

2. Materiali e Metodi

2.1. Test Sperimentali

L'analisi sperimentale è stata basata sullo sviluppo di prove di rilassamento in compressione, in configurazione non confinata su sei provini cilindrici (diametro 3 mm e altezza variabile per ogni provino) estratti dall'articolazione metacarpalphalyngeal di un vitello di 7 giorni. Precisamente, i provini sono stati inizialmente estratti dall'articolazione con l'ausilio di un punch per biopsia cutanea di diametro pari a 6 mm e separati dall'osso sottostante utilizzando un bisturi chirurgico. Per ottenere un provino più piatto possibile il diametro è stato diminuito a 3 mm, tagliando il provino da 6 mm con un punch per biopsia cutanea da 3mm di diametro. I provini sono stati conservati in soluzione PBS 0.154M NaCl (pH 7.4) e a temperatura di 37°C per circa dodici ore prima dell'impiego nella prova meccanica. La macchina di prova (ElectroForce 3200, Bose Corporation, Minnesota, USA) era equipaggiata con un fondo scala da 225N. Il protocollo di prova applicato per lo studio dei modello bifasici consiste nell'applicazione di 10 step consecutivi di spostamento, ciascuno di ampiezza pari a circa l'1% della deformazione con una velocità di deformazione pari a 1μm/s. Ogni livello di deformazione è stato mantenuto per circa 500 s per promuovere il rilassamento della cartilagine. Durante l'intero processo la cartilagine è stata immersa in una soluzione PBS (0.154M NaCl) per mantenerne l'idratazione.

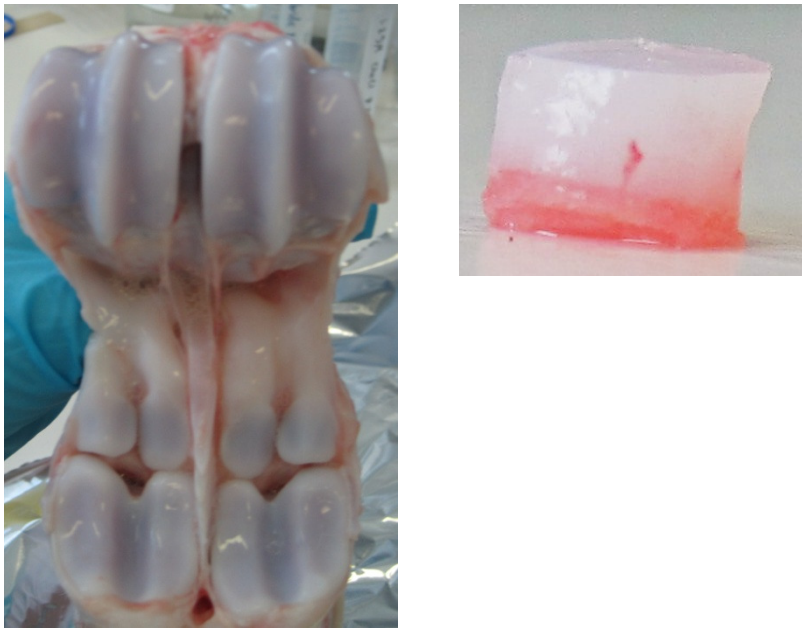

***Figura 2**: Articolazione metacarpalphalyngeal di un vitello di 7 giorni da cui sono stati estratti i provini di cartilagine (sulla destra); provino finale (diametro 3 mm) in cui si nota la presenza dell'osso (sulla destra).*

La prova sperimentale usata per la validazione del modello di analogia termica applicato al fenomeno di swelling, è un test di rilassamento in configurazione non confinata. Ma, in questo caso è stato applicato uno spostamento atto ad indurre una deformazione di circa il 10%, con velocità di deformazione pari a 1mm/s. Una volta terminato il rilassamento (500s) è stata cambiata la soluzione. Inizialmente la cartilagine era immersa in 20 ml di soluzione PBS ad una concentrazione fisiologica pari a 0.154 M NaCl. Da tale volume sono stati estratti 18 ml di soluzione, sostituiti poi da un analogo volume di acqua distillata. In tal modo si è passati da una concentrazione fisiologica di 0.154M ad una ipotonica con concentrazione pari a 0.0154M.

In entrambi i test sperimentali particolare attenzione è stata posta nell'estrazione di provini piatti e nella modalità di conservazione del provino, in modo tale da non alterare la struttura della cartilagine e quindi le sue proprietà meccaniche.

2.2. Analisi Numerica

L'analisi numerica dei modelli bifasici è stata affrontata utilizzando il codice commerciale ad elementi finiti FEBio v.1.2.0 (Musculoskeletal Research Laboratories, University of Utah), in una configurazione tridimensionale. Invece, la validazione del modello di

analogia termica è stato sviluppata utilizzando il software ABAQUS v.6.8.1 (ABAQUS Inc., Providence, USA) in condizioni di assialsimmetria. In entrambi i casi sono state utilizzate geometrie, condizioni al contorno e di contatto analoghe a quelle utilizzate nelle prove sperimentali, per poter attuare un confronto tra risultati sperimentali e quelli numerici.

Dalle prove sperimentali è stato ricavato il modulo di Young a fine rilassamento, punto in cui è possibile considerare la cartilagine come costituita dalla sola matrice elastica, poiché la componente fluida ha già raggiunto l'equilibrio. Gli ulteriori parametri meccanici richiesti da ogni modello sono stati estratti attraverso un *fitting* tra le curve di forza registrate nelle prove sperimentali e quelle predette numericamente.

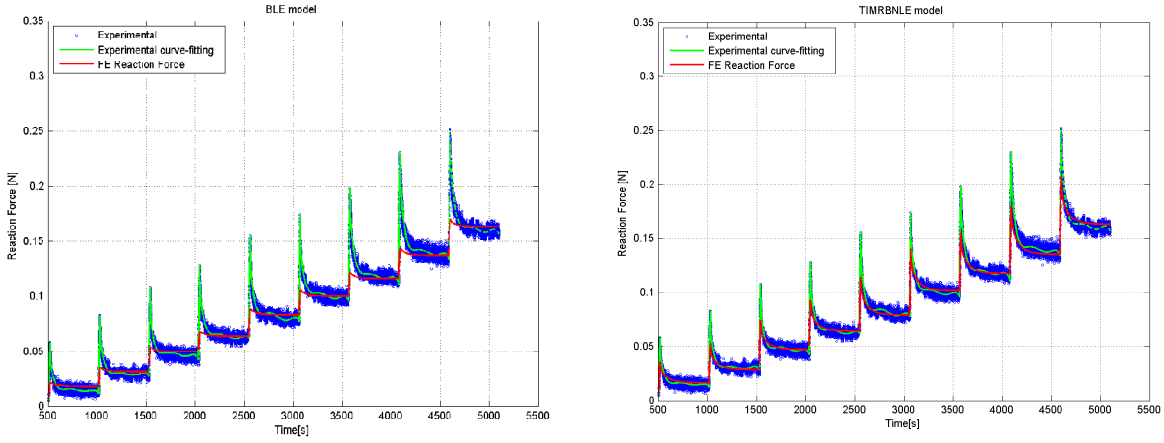

a) *b)*

***Figura 3**: Le curve rappresentano l'andamento della forza ottenuta numericamente (curva rossa) utilizzando un modello BLE (grafico sulla sinistra) e un modello TIMRBNLE (grafico sulla destra). Viene inoltre rappresentato l'andamento della forza misurato sperimentalmente (in blu) e il suo curve-fitting con un polinomio di 5° grado (in verde).*

3. Risultati e Discussione

I più semplici e veloci modelli come quello bifasico lineare (BLE) o la sua generalizzazione al modello bifasico non lineare (BNLE), in cui viene considerata la variazione della permeabilità con la deformazione, non consentono una riproduzione accurata della forza registrata sulla cartilagine (Figura 3a). In particolare il picco di forza risulta essere troppo basso. L'aggiunta della presenza della matrice di collagene attraverso

l'implementazione del modello trasversalmente isotropo con iperelasticità di Mooney-Rivlin (Weiss, et al., 1996) produce un incremento nel picco di forza dovuto

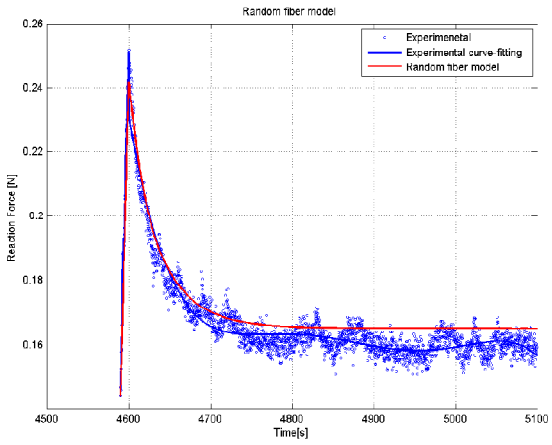

***Figura 4**: In figura è rappresentato l'andamento della forza ottenuta numericamente (curva rossa) utilizzando un modello a fibre continue. Viene inoltre rappresentato l'andamento della forza misurato sperimentalmente e il suo curve-fitting con un polinomio di 5° grado.*

all'introduzione dell'anisotropia (Figura 3b). Tuttavia il picco di forza risulta essere ancora troppo basso. Solamente il modello a fibre continue presentato recentemente da Ateshian (Ateshian, 2007; Ateshian, et al., 2009) ha dimostrato di riprodurre accuratamente la forza misurata sperimentalmente (Figura 4).

La differenza tra i due modelli è insita nella struttura tridimensionale conferita alla matrice di collagene. Nel primo caso, questa è stata rappresentata da una sola famiglia di fibre con un orientamento preferenziale. Invece nel secondo caso le fibre sono state modellizzate come distribuite in tutte le direzioni dello spazio con un modello continuo. Pertanto si ritiene che sia necessario l'utilizzo di numerose famiglie di fibre per poter riprodurre accuratamente la risposta della cartilagine quando sottoposta a diverse sollecitazioni. In conclusione, a causa della complessa struttura della cartilagine, non è possibile trovare un modello accurato e allo stesso tempo veloce nel calcolo dei risultati. Pertanto conviene ricercare un compromesso tra accuratezza e velocità di calcolo nell'applicazione di un modello di cartilagine in un'indagine sull'intera articolazione del ginocchio.

Dall'analisi del fenomeno di rigonfiamento della cartilagine in seguito ad una variazione di concentrazione ai capi del tessuto, è emerso che il modello di analogia termica riesce a riprodurre accuratamente lo *swelling* (Figura 5a). Inoltre, esso si dimostra in grado di poter

analizzare separatamente i fenomeni che provocano il rigonfiamento della cartilagine, osservazioni alquanto difficili da poter fare utilizzando le sole indagini sperimentali (Figura 5b).

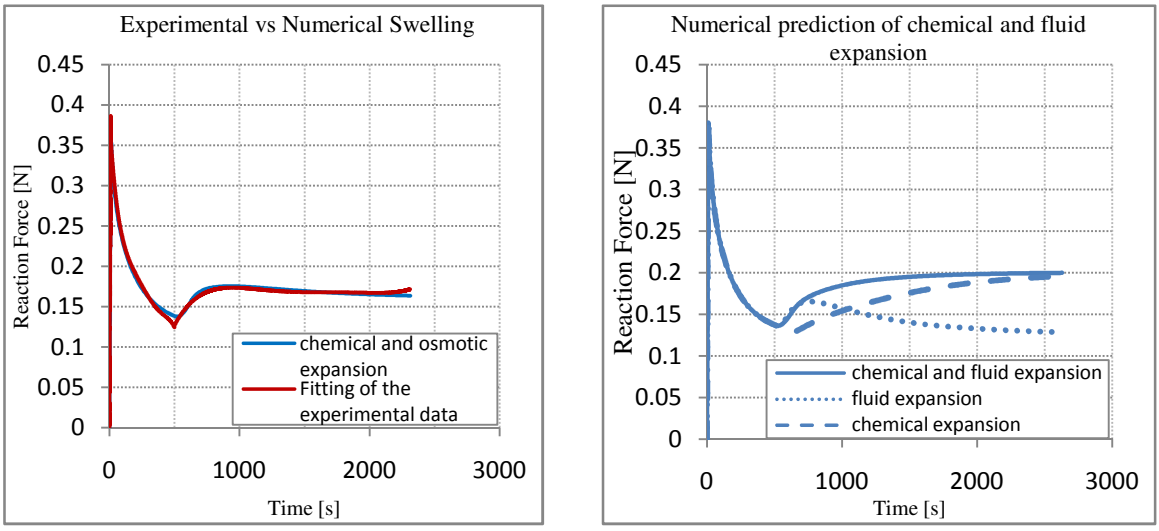

a) *b)*

***Figura 5**: a) confronto tra i risultati ottenuti numericamente implementando il modello di analogia termica sviluppato per studiare il fenomeno di "swelling" e sperimentalmente con le prove descritte precedentemente; b) predizione numerica del rigonfiamento della cartilagine e sua divisione nei meccanismi che lo provocano (espansione dovuta al pressione osmotica e repulsione elettrostatica).*

Accanto a queste analisi, particolare interesse ha suscitato l'effetto che produce la presenza di un provino di cartilagine articolare non perfettamente piatto sulla forza misurata. Infatti, se l'area di contatto è inferiore all'intera superficie del provino, la forza misurata come reazione della cartilagine risulta inferiore a quella che si avrebbe nel caso in cui tutta la superficie del provino fosse sollecitata. Contemporaneamente, anche la forza di picco risulta essere inferiore. Pertanto, potrebbero verificarsi errori nell'estrazione delle proprietà meccaniche.

Infine, una ulteriore analisi è stata condotta per valutare l'effetto dell'attrito tra l'interfaccia provino/piatto di compressione sulla risposta della cartilagine. Generalmente, per l'estrazione delle proprietà meccaniche tramite un *curve-fitting* tra prove sperimentali e analisi numerica, l'attrito viene considerato nullo. Pur utilizzando materiali con elevato grado di raffinatezza superficiale per diminuire l'attrito, questo non può essere trascurato. Pertanto le proprietà meccaniche ricavate considerando che le interfacce siano senza attrito

risultano essere errate (Figura 6). In particolare si è osservato che la permeabilità ricavata attraverso il *fitting* sperimentale risulta essere più elevata rispetto al caso in cui l'attrito sia stato considerato mentre il valore del modulo di Young risulta essere più basso, sebbene di

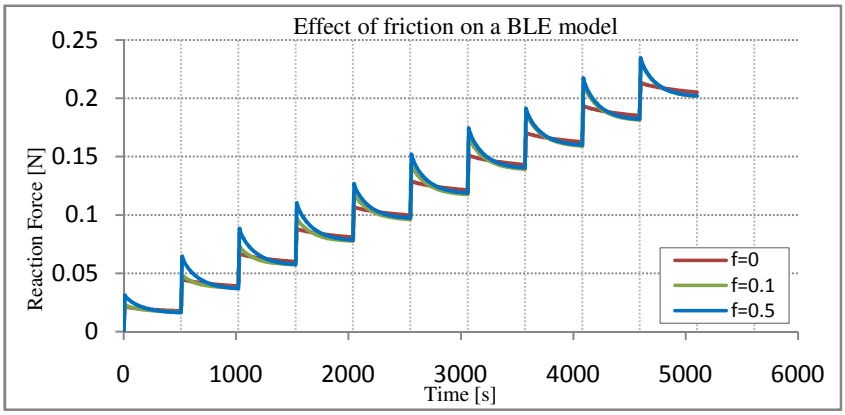

***Figura 6**: Predizione numerica della forza verso tempo ricavata simulando una prova di compressione non confinata al variare del coefficiente d'attrito (f).*

poco. Precedentemente è stata descritta la difficoltà dei modelli numerici nel riprodurre l'elevato picco di forza riscontrato nelle analisi sperimentali. Alcuni autori propongono che questa mancanza sia dovuta al fatto che nel modello non sia stata considerata la presenza dell'attrito. Risultati numerici dimostrano infatti che la considerazione dell'attrito nel modello ad elementi finiti consente di aumentare il picco di forza istantaneo, migliorando così la corrispondenza tra forza ricavata tramite l'analisi numerica e sperimentalmente (Figura 7).

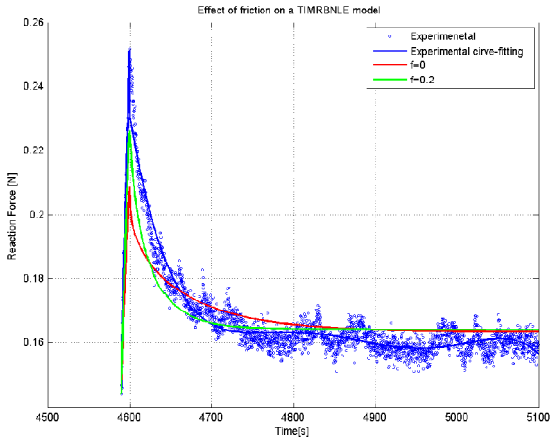

***Figura 7**: In figura è rappresentato l'effetto della presenza dell'attrito (in verde) sull'andamento della forza ottenuto utilizzando un modello TIMRBNLE. Viene inoltre rappresentato l'andamento della forza misurato*

sperimentalmente e il suo curve-fitting con un polinomio di 5° grado.

4. Conclusione

Dai risultati ottenuti si è concluso che è alquanto difficile ottenere un modello analitico che rispecchi contemporaneamente i requisiti di velocità di implementazione e accuratezza dei risultati. Infatti, per poter riprodurre accuratamente la risposta della cartilagine in differenti prove meccaniche, non è sufficiente descrivere la cartilagine come composta solamente dalla fase fluida e dalla matrice elastica. Anche l'introduzione di anisotropia, modellizzando la presenza delle fibre di collagene con un modello ad una sola famiglia di fibre, si è rivelata non sufficiente per riprodurre il comportamento meccanico della cartilagine in compressione confinata. Sono necessari pertanto modelli più complessi, e pertanto più costosi computazionalmente, per riprodurre il comportamento della cartilagine articolare in diverse prove meccaniche. Ne è esempio il modello a fibre continue. Tuttavia, per riprodurre accuratamente la risposta della cartilagine è necessario considerare anche la presenza dei proteoglicani. Può essere utilizzato a tal fine il modello di analogia termica si per descrivere il fenomeno di rigonfiamento della cartilagine a seguito di una variazione di concentrazione, visti gli ottimi risultati ottenuti.

Infine, i risultati raggiunti suggeriscono che le proprietà meccaniche della cartilagine articolare ricavate da una prova di compressione non confinata possono essere influenzate dalla presenza dell'attrito all'interfaccia provino/piatti di confinamento, dall'utilizzo di provini con superfici non piatte e dalla tecnica di conservazione del provino.

List of Abbreviations

AC: Articular Cartilage

BLE: Biphasic Linear Elastic

BNLE: Biphasic Non-Linear Elastic

ECM: Extracellular Matrix

FCD: Fixed Charge Density

FE: Finite Element

GAG: Glycosamminoglycans

OA: Osteoarthritis

PG: Proteoglycan

TI: Transversely Isotropic

TIBLE: Transversely Isotropic Biphasic Linear Elastic

TIBNLE: Transversely Isotropic Biphasic Non-Linear Elastic

TIMRBLE: Transversely Isotropic Mooney-Rivlin Hyperelasticity Biphasic Linear Elastic

TIMRBNLE: Transversely Isotropic Mooney-Rivlin Hyperelasticity Biphasic Non-Linear Elastic

2D: Bi-dimensional

3D: Three-dimensional

Chapter 1
Introduction

The increase in life expectancy as well as the development of quality of life, in recent years has produced the necessity of technological advances in medicine and engineering. In order to study and understand which are the factors that cause diseases inside the human body, as well as to study the forces and stresses that occur in all the biological tissues during daily activities to prevent the onset of injury, *in vivo* and *in vitro* experimental studies have been conducted. Unfortunately, *in vivo* studies are difficult to apply mainly because of their invasiveness. Therefore, the tests that can be executed on patients are limited and usually can be made only during other surgeries. Indeed, *in vitro* studies are easier to develop, but there is the possibility of introducing changes in the internal structure of the biological tissue in the explants. Hence, the mechanical properties obtained from these experiments may be different from natural ones. Moreover, it is difficult to replicate the natural conditions of surrounding tissues and connected structures. In conclusion, it is convenient to combine finite element studies with *in vivo* or *in vitro* experimental tests to study the stresses and deformations occurring within the tissue and fully analyze which are the factors that cause diseases through the variation of some mechanical parameters. Experimental tests are necessary to validate FE models.

This thesis project is placed within a larger project whose goal is the modeling of the knee joint. Since the knee consists of several tissues, for each of these it is necessary to identify the constitutive model which is able to best replicate the behavior of the tissue subjected to various mechanical tests. The biological tissue analyzed in this thesis is the articular cartilage. Thus, the objective of this work is to validate the various models used in the literature through experimental tests starting from previous works based on the analysis of them (Accardi, 2007; Accardi, 2008; Li, 2009).

Cartilage is an extremely complex biological tissue, whose structure is highly specialized. It is mainly composed of: three-dimensional collagen network, negative charged protoeglycans, chondrocytes and water. In order to better comprehend the factors that cause diseases, an accurate description of all the components and an understanding of the interactions between them are required. Unfortunately, the greater precision required and the large the number of components described, the greater the computational cost and number of parameters. Therefore, this thesis started with the analysis of simple models that can be easily implemented in a three-dimensional knee joint model. The simplest model was first proposed by Mow et al. (1980) and describes the articular cartilage as a matrix composed of isotropic elastic solid and a fluid phase (Mow, et al., 1980). Although it is computationally very simple, it cannot fully describe the mechanical behavior of cartilage under different types of mechanical load (Boschetti, et al., 2006; Cohen, et al., 1998; DiSilvestro, et al., 2001; Julkunen, 2008; Li, et al., 1999; Wilson, et al., 2007). Therefore, starting from the poroelastic model other more complex models were studied, in order to obtain the most appropriate model needed to reproduce the mechanical response of cartilage under different loading conditions.

Particular attention was entrusted to study the phenomenon of swelling, produced by the presence of proteoglycans. This phase of the work was a prosecution of Li's project (Li, 2009) on the development of a thermal analogy model used to study this phenomenon. Experimental swelling tests were evaluated to validate the thermal analogy. In the literature there are many useful models for studing swelling, but they are either too computationally expensive, such as electro-mechanical models (Lai, et al., 1991) or not suitable to describe the transient history of reaction force during the swelling (Wilson, 2005; Wilson, et al., 2007). Thus, the thermal analogy model could be useful to overcome both problems.

Particular attention was also paid to the analysis, through the use of FE simulations, of the effects of friction and of the slope of articular cartilage plugs on the mechanical behaviour of cartilage in unconfined compression relaxation tests.

Below is reported a brief description of the structure of this report:

- In **Chapter 2** will be discussed the structure and the composition of articular cartilage, as well as their influence on the mechanical properties of articular cartilage;
- In **Chapter 3** will be described an overview on mechanical models of cartilage currently available in the literature;
- In **Chapter 4** a description of the experimental tests to either analyze the biphasic models and to validate thermal analogy model will be explained. Particular attention will be focused on the description of the extraction of the sample, of the experimental set-up and of loading protocol;
- In **Chapter 5** will be presented the three-dimensional numerical implementation with FE software FEBio v.1.2.0 (Musculoskeletal Research Laboratories, University of Utah) of the biphasic models used in literature and the ones used to study the effect of friction and of the slope of surfaces of articular cartilage plugs. In the same chapter will be also elucidated, the numerical implementation with the FE software ABAQUS v.6.8.1 (ABAQUS Inc., Providence, USA);
- In **Chapter 6** the numerical and experimental results and the comparison between them will be explicated;
- **Chapter 7** will be the end of the thesis. Elucidation on the conclusion deduced from this thesis work and future development will be discussed.

Chapter 2
Structure and Properties of Articular Cartilage

Articular cartilage (AC) is a connective tissue that covers diarthrodial joints, such as tibia, femur or the posterior surface of the patella, as can be seen in Figure 2.1.

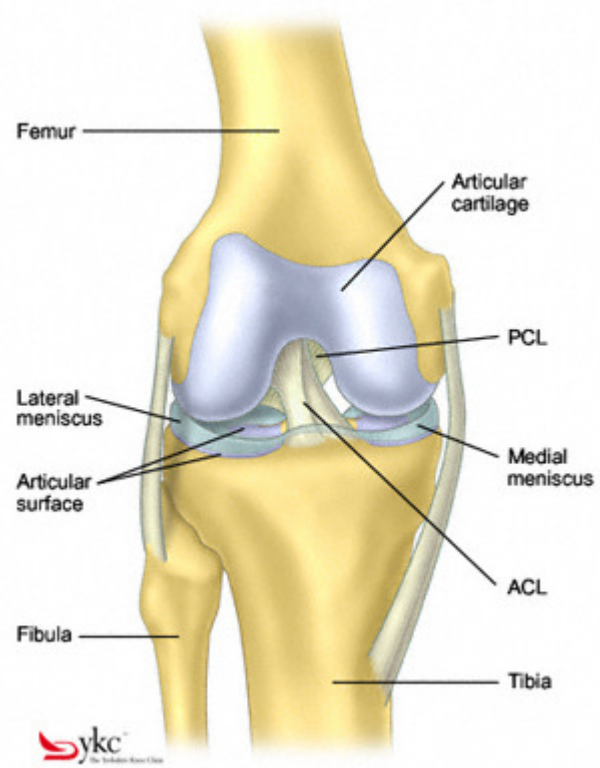

***Figure 2.1**: Knee joint anatomy [yorkshire knee clinic]*

The main functions of AC are to reduce the stresses caused by loading, distributing them on a larger contact area through deformation. Truthfully, this function in knee joint is also performed by other components as the meniscus and the ligaments. Another important

function of articular cartilage in joints is to allow the relative movement of the opposite joints surface, avoiding wear and reducing friction. The last function is provided by the excellent lubrication property of AC due to the elastohydordinamic lubrication (EHL) and the presence of the synovial fluid. Actually, the coefficient of friction of AC is very low, almost two orders of magnitude less than the coefficient of friction obtained by the lubricated metal on metal. For example, the coefficient of friction of the articular cartilage is about 0.001, while the one measure for Teflon sliding on Teflon is 0.04, one order of magnitude bigger than the coefficient calculated for synovial joints (Fung, 1993; Mansour, 2003; Katta, et al., 2008).

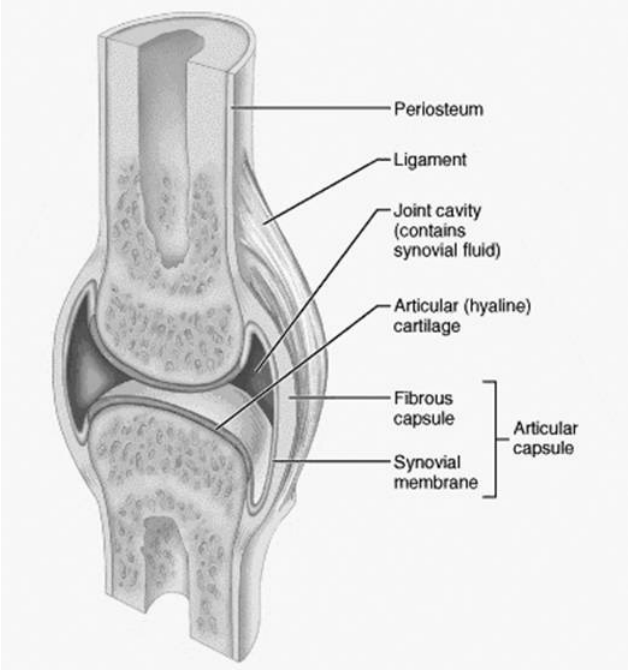

Figure 2.2: *Schematic representation of the synovial joint of the knee. The lubricant synovial fluid is contained by the synovial membrane.*

Articular cartilage has excellent mechanical properties. These arise from the complexity of its structure. Actually, AC consists of two phases: a solid matrix phase and a fluid phase. The first comprise chondrocytes (cartilage cells), collagen network, proteoglycans (PG) and a small amount of proteins, glycoproteins and lipid. The interstitial fluid phase consists of water and free mobile ions (Na+, K+, Ca2+, etc.) (Julkunen, 2008; Wilson, 2005). Physiologically, it is an avascular, aneural, alymphatic tissue; thus, the nutrients needed by

the tissue are transported by the synovial fluid. Its cellular density is less than in every other tissue, less than 10% of the tissue's wet volume and their mitogenic potency is very low, which means that AC has a very low regenerative capacities (Mow, et al., 2000). This is the main reason why osteoarthritis and damaged tissue presents a real problem to the correct functioning of the joint and this explains why artificial replacements are sometimes the only efficient solution.

2.1 Structure and Composition of Articular Cartilage

2.1.1 Collagen

The collagen network form approximately 15%-22% of the AC wet weight (Mow, et al., 2000). In the human body exist almost 28 type of collagen. Articular cartilage is mainly composed of type II, with a minor amounts of type V, VI, IX and XI (Wilson, et al., 2007).

Collagen (Figure 2) is a protein, whose basic structure is tropocollagen, composed by three procollagen polypeptide chains, called α chains. Each α chain is composed of a repeating GLY-X-Y triplets of amino acids and arranged as a left-handed helix with three amino acids per turn. GLY is the amino acid Glicyne, whereas X and Y represent other two amino acids (commonly, Proline and Hydroxyproline but them may be any other amino acids). These three α chains are then further coiled into a right-handed triple helix, called α helix, reported as collagen microfiblils. Each microfibril is overlapped with its neighbouring microfibrils for about one quarter of its length, giving rise to a repeated banded pattern of the collagen (Figure 2.3 on the right) that can be seen with a electron microscopy (Mow, et al., 2000).

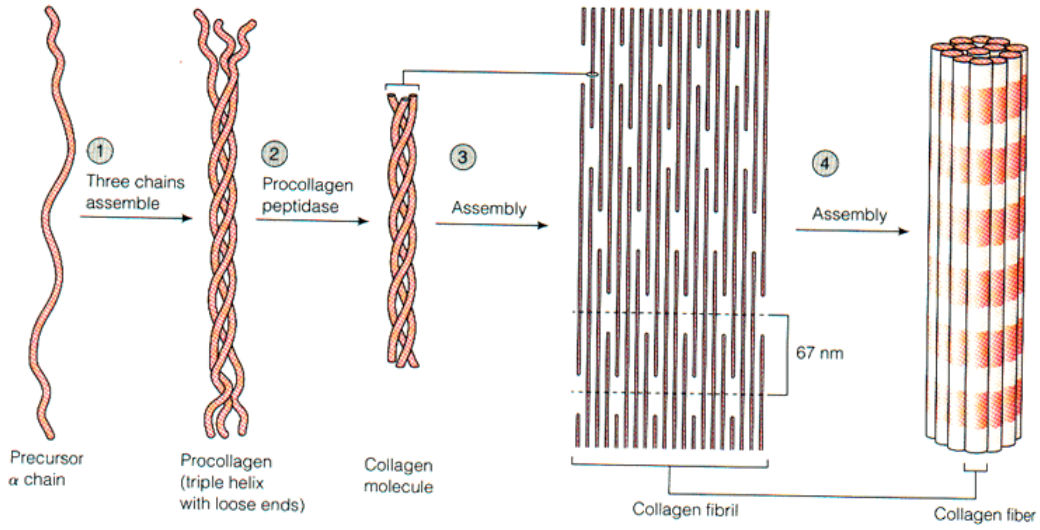

***Figure 2.3**:Development of a collagen fiber, from the α chain (on the left) to the final collage fiber (right). A typical electron microscopy made on collagen fiber shows a repeated banded pattern as drawn on the right of this figure. The red rows suggest the presence of hole zone in the fiber, while the white one represents that all the collagen fibers are overlapped.*

The collagen in articular cartilage is inhomogeneously distributed and its orientation varies throughout the depth of the tissue, giving to the AC a layered character (Figure 2.5c). In the superficial zone (10%-20% of the total thickness) collagen fibers are densely packed in planes parallel to the articular surface, with a small diameter. The middle zone is the biggest one, actually it represents between 40% and 60% of the total thickness. In this layer the collagen fibers are randomly oriented and homogeneously dispersed, with more distance between the fibers compared to the others layers and a bigger diameter then in the upper one. In the deepest layer (about 30% of the total thickness) these fibers have the biggest diameter and they are oriented perpendicularly to the subchondral bone, in order to anchor the cartilage to the underlying bone (Mow, et al., 2000; Wilson, et al., 2007). The complex tridimensional structure of collagen network is stabilized by the presence of cross-links between the fibers.

Like all the body tissues, also cartilage is not composed of only one type of collagen. Actually, the most abundant one is type II (85-90%), but also type XI and IX are very important to maintain the functionality and integrity of the tissue, though these types of collagen represent only 3% of the total content of collagen. In particular, type IX collagen

seems to play this important role for the maintenance of AC integrity, interacting with other fibers. Thus, it contributes to the ability of collagen to resist the swelling pressure caused by the presence of GAG inside the cartilage (see chapter 2.2.3) and the tensile stress arising in the tissue when loaded (Wilson, et al., 2007). Whereas type XI collagen is essential for assembly, organization and development of cartilage.

Collagen is essential for mechanical strength. Due to the structure of tropocollagen (triple helix) and the presence of numerous cross-link between the fiber, collagen presents a high tensile stress. Despite being strong in tension, collagen fibers presents a little resistance in compression, because they tend to buckle under a compressive loading. In particular, type II collagen determine the mechanical strength of the tissue, whereas the minor collagen components, through the interaction with other matrix components influence tissue integrity.

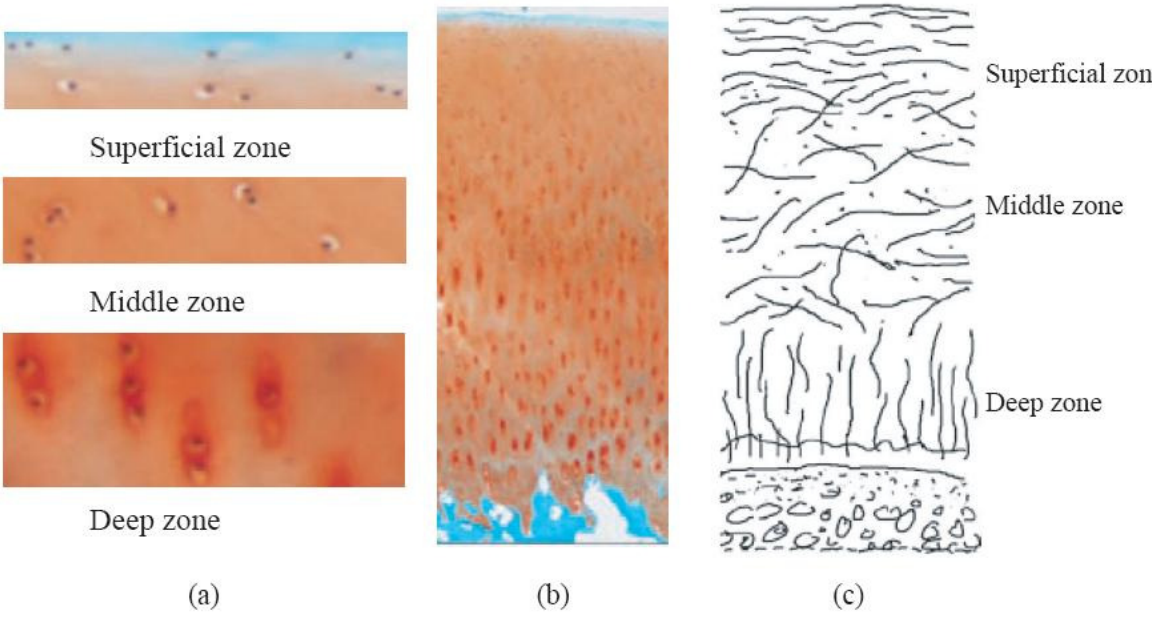

***Figure 2.4**: (a–b) Histology of articular cartilage stained with Safranin O and fast green; (a) shows the different layers; (b) the total thickness cartilage; (c) schematic representation of the layered structure of collagen network [reproduced from Wang and Zheng 2007]*

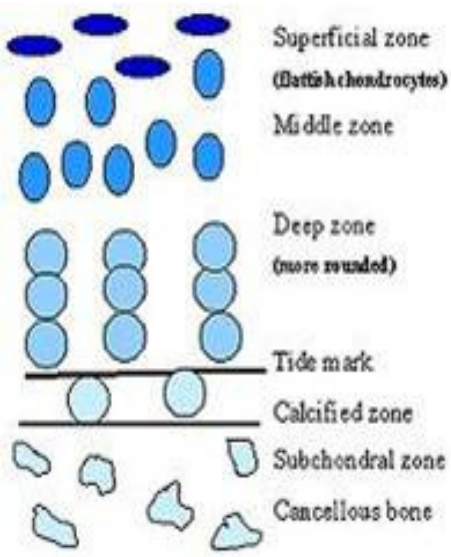

Figure 2.5: *schematic representation of the change in shape and distribution of condrocytes through depth*

2.1.2 Chondrocytes

Cartilage is one of the tissues with a low density of cells, actually chondrocytes amount for less than 10% of the AC wet weight (Mow, et al., 2000). Their function is to secrete, organize and degrade PGs and collagen fibers in order to enable the cartilage to perform its main functions.

Like the collagen fibers, also chondrocytes vary in shape and distribution with depth (Figure 2.5 and 2.6). In the superficial layer they have an ovoid shape, they are oriented parallel to the surface and they are relatively inactive. In the middle zone their shape is more spherical, their diameter is bigger and they are more active than in the upper layer. In the deepest layer the shape is almost spherical and they have a high synthetic activity (Wilson, et al., 2007).

2.1.3 Proteoglycans

In normal articular cartilage proteoglycan content ranges from 4% to 7% by wet weight (Mow, et al., 2000). PGs are large protein-polysaccharide molecules composed of a core

protein, hyaluronan (HA), to which are covalently attached molecules of aggrecan, through a link protein (Figure 2.7).

Aggrecans are composed of two types of glycosamminoglycans (GAGs): chondroitin sulfate (CS) and keratin sulfate (KS). At physiological pH GAGs show their negative charge (SO^{3-} and $C00^{-}$) producing high concentration of the so called fixed charge density (FCD). Since AC is not permeable to PGs (because PGs are too large to diffuse out from the tissue), the anion concentration within the tissue is higher than in the synovial fluid, causing an osmotic pressure difference that leads to swelling of the AC. Thus, PGs are essential to describe cartilage resistance in compression. Actually, without PGs and the negatively charged GAGs, water is not blinded inside the tissue and so collagen network is stressed only in compression (not in tension). Due to the fibrillar shape of collagen network, it can resist only in tension, because it burkes under compressive loading. In conclusion, collagen network has an optimal structure, but the interactions between PGs ang GAGs are essential for tissue integrity.

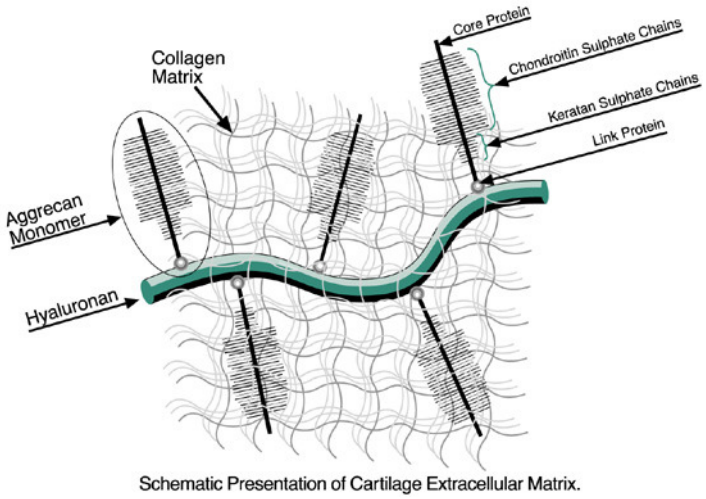

Figure 2.6: *schematic representation of PG structure and all its component.*

As well as for the other components also the content of PGs varies with depth, in particular their concentration increases with depth (Wilson, et al., 2007).

2.1.4 Interstitial Fluid

The interstitial fluid is composed of water and mobile ions (Na^+, K^+, Ca^{2+}), free to diffuse through it. Water is the most abundant component of AC, its content varies between 65% to 80% depending on the layer considered, indeed, in the upper layer the concentration of water is very high (almost 80% by wet weight) and it decreases with increasing depth to a concentration of approximately 65% in the deep zone.

Water occupies the interfibrillar space of ECM and it is free to move under loading. This movement is very important in ensuring nutrition (in fact AC is avascular), joint lubrication and in controlling mechanical behaviour (for example creep and stress relaxation (Mow, et al., 1980)). The presence of mobile ions influences the mechanical and physiochemical behaviour of cartilage and is one of the causes of swelling or shrinkage (Lai, et al., 1991).

2.2 Mechanical Properties of Articular Cartilage

The mechanical behaviour is influenced by the complex structure, in particular there are three components that most affect it: collagen, PG and the interstitial fluid. Below is discussed the relation between each component and the mechanical properties of AC.

2.2.1 Compressive Behaviour

Due to its biphasic composition, and in particular the *fluid dependent* viscoelasticity (see Chapter 2.2.4), under compression AC presents time dependent and strain dependent mechanical properties. The quantity of water present in the tissue at a given time is one of the major determinants for the mechanical properties of cartilage in compression, together with PGs and collagen. Basically, the change of the fluid component due to compressive loading produces an increase in the FCD (relate to PG content), inducing an increase in the osmotic pressure and chemical expansion. As a result the effective stiffness of the tissue in compression increases. Although collagen fibers present a poor behaviour in compression, i.e. they buckle under a compressive loading, they prevent the tissue swelling. Thus, due to the presence of a high swelling pressure, the collagen network also contributes to increase the compressive stiffness of the AC (Wilson, 2005).

2.2.2 Tensile Behaviour

In traction AC has strain dependent mechanical properties (Figure 2.8): stress increase with tensile strain because of the progressive arrangement of the collagen fibers along the direction of stress. When the cartilage is subjected to uniaxial tensile loading, for small strain the stress-strain curve presents a non-linear toe region due to the realignment of the fibers, with a very poor stiffness (5-10 MPa), because the collagen fibers have not been elongated and stretched yet. For larger deformations these fibers start to resist in traction, up to a real linear region where the fibers are aligned and stretched along the direction of stress, thus presenting a high stress because of intrinsic collagen high stiffness in traction (5-100MPa) (Mow, et al., 2000; Wilson, 2005).

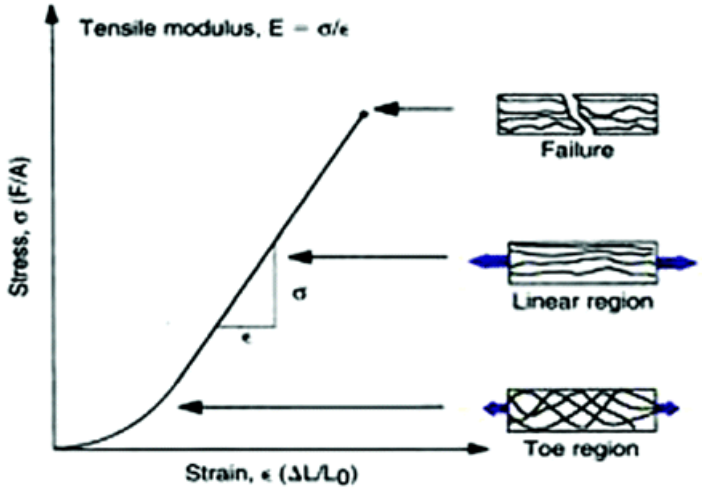

Figure 2.7: *tensile behaviour of articular cartilage. Reproduced from Mow et al. , 2000*

2.2.3 Swelling Behaviour

Swelling is defined as "the ability of articular cartilage to gain or lose weight and water when an osmotic load is applied on the tissue" (Wang, et al., 2007). In physiologic pH GAGs show a repetition of sulphate and carboxyl groups that are negatively charged, producing an increment in the FCD. There are two forces that produce cartilage swelling due the presence of these negative charges: (1) a charge-to-charge repulson called chemical expansion; (2) Donnan osmotic pressure. The latter arises from the presence of a difference

in concentration between the interstitial fluid and the synovial fluid. Precisely, the anion concentration inside the cartilage is higher than outside the AC, causing the diffusion of cations (predominantly Na^+ and Ca^{2+}) inside the cartilage to reduce the repulsive force, hence to obey the electro-neutrality law. As a result, within the ECM the total ion concentration is higher than outside the cartilage, producing an increase of Donnan osmotic pressure, which in turn causes fluid to flow into the tissue and hence swelling to occur.

In normal cartilage swelling is important for a complete deformation recovery. According to Mow (1980) and Fung (1993) this is possible only if the tissue is submerged in a bath of fluid. So, experimentally it is possible to see cartilage swelling by submerging the sample in a fluid bath that mimics the synovial fluid. Actually, fluid flow into the cartilage due to the Donnan osmotic pressure depends on FCD and the external ion concentration. If cartilage is placed in a hypertonic solution (i.e a solution with high concentration of ions), the difference between the ion concentration in the cartilage and in the bath will decrease, causing a decreasing of Donnan osmotic pressure and hence cartilage shrinking. Otherwise if the sample is submerged in a hypotonic solutions (i.e. a solution with low ion concentration) the difference between the ion concentration inside and outside the cartilage will increase, producing an increment in the Donnan osmotic pressure and thus cartilage swelling.

In the physiological state cartilage is subjected to a cyclic loading in compression. In this case, swelling automatically takes place. In fact, when cartilage is subjected to compression, the hydraulic pressure inside the cartilage increases, causing fluid exudation. Thus, the increase of FCD inside the cartilage generates both an increase in chemical expansion and in Donnan osmotic pressure, causing cartilage swelling and a complete deformation recovery.

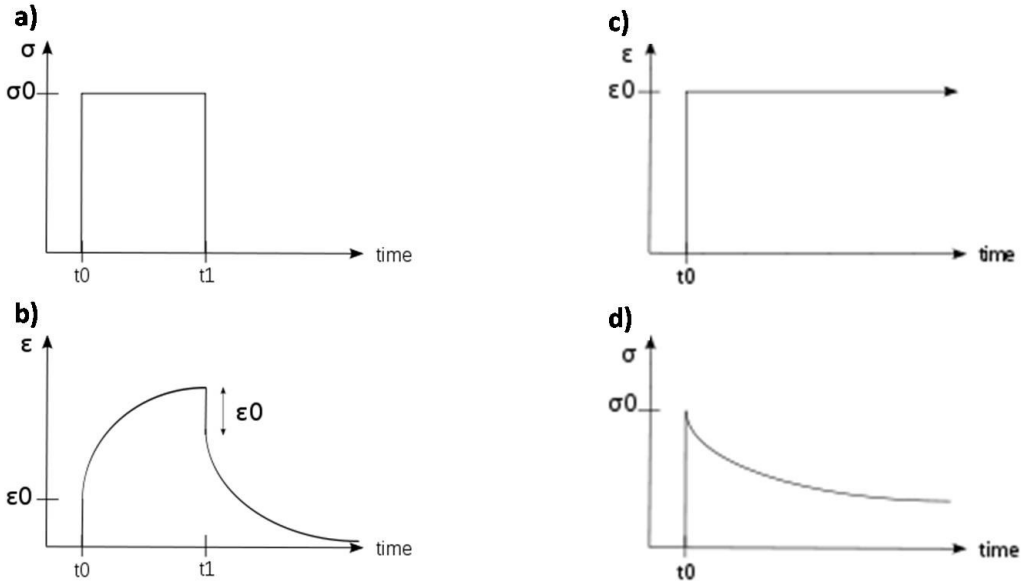

***Figure 2.8**: a), b) Creep test for a viscoelastic material; a) Applied stress; b) induced strain as functions of time over a short period; c),d) Stress relaxation test; c) Applied strain d)induced stress.*

2.2.4 Viscoelasticity

Like all the tissues, also cartilage is not an elastic material, but it is actually viscoelastic. This means that the relation between stress and strain changes with time (Fung, 1993).

To study viscoelasticity three different tests exist: creep test, relaxation test and cyclic test. In a compression creep test the sample is subjected to an instantaneous stress, that is then maintained constant (Figure 2.9a). The resulting strain increases more and more although the force applied to the sample is maintained constant (Figure 2.9b). In the second test, an instantaneous compressive strain is applied to the cartilage that is then kept constant (Figure 2.9c). The resulting internal stress increase during the compressive phase and then decrease in time until the tissue reaches a complete relaxation (Figure 2.9d). In a cyclic test stress and strain in the loading phase do not match with the unloading phase. Due to the frictional internal energy dissipation the stress-strain curve presents a hysteresis, typical for viscoelastic materials. Furthermore, stress and strain are not in phase with each other.

Cartilage presents these three features demonstrating that cartilage is a viscoelastic material (Fung, 1993; Mow, et al., 1980).

In AC viscoelasticity is primarily caused by the flow of interstitial fluid through the matrix pores and its frictional drag; this mechanism is referred as *fluid dependent* viscoelasticity. Cartilage also presents *fluid independent* viscoelasticity, due to the viscoelastic properties of the ECM matrix, in particular of PGs and collagen fibers.

Mow (1980) demonstrated that the main cause of creep and relaxation is *fluid dependent* viscoelasticity. In particular, in a stress relaxation test, during the loading phase fluid exudes out of the cartilage (Figure 2.10b, phase OAB). When strain is maintained constant, no fluid exudation in and out of the cartilage occurs and fluid redistributes within the ECM matrix, from the deeper layers full of fluid and less strained to the upper layers more deformed and poor in fluid (Figure 2.10b, phase BCDE). This fluid distribution ends when all the layers of AC are equally deformed and cartilage reach an equilibrium state(point E) (Mow, et al., 1980). The presence of water is hence very important under physiological conditions, because it will permit to attenuate rapidly the internal stress if an excessive stress levels are applied to the tissue during loading.

The ease with which the fluid flows through the porous matrix, i.e. permeability, is strain dependent. In particular, according to Mow (Mow, et al., 1980), the relationship between permeability and compressive strain decreases exponentially (Figure 2.11). Actually, when the cartilage is compressed the ECM compacts restricting the pores and thus the flow of fluid through the ECM becomes more difficult.

2.2.5 Anisotropy

As previously described AC presents a very complex structure. Due to the presence of collagen fibers this tissue exhibits anisotropic behaviour. It means that cartilage presents different mechanical properties depending on the direction in which the load is applied, both in compression (Jurvelin, et al., 2003) and in tension (Chahine, et al., 2004). Furthermore, the variation with depth of PGs, water and collagen concentration, shape of condrocytes and collagen fibers orientation, cause the mechanical properties to vary through the depth of the tissue, in particular cartilage changes stiffness through depth

(Chen, et al., 2001; Federico, et al., 2005). The variation of PG content with depth also produces a variation in the osmotic pressure and so in the swelling behaviour.

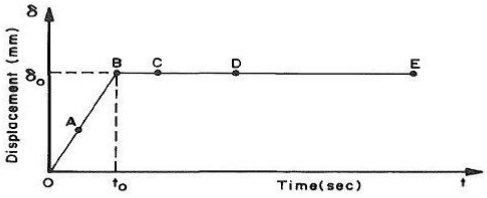

a)

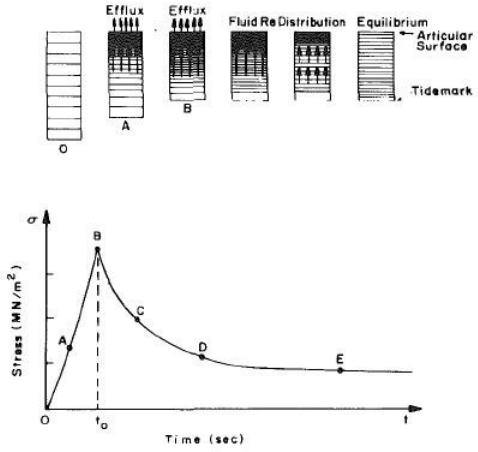

b)

Figure 2.9: a)*Prescribed displacement in a free-draining stress relaxation experiment. OAB defines the compressive phase and BCDE the relaxation one.* ***b)*** *Stress history and schematic representation of the fluid flow during a stress relaxation test. Reproduced from Mow et al. 1980.*

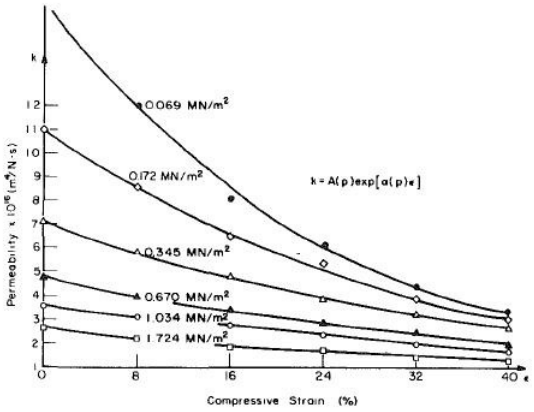

Figure 2.10: *Experimental curves of permeability versus strain obtained at various pressure from a sample of bovine articular cartilage. Reproduced from Mow et al. 1980.*

Chapter 3
Finite Element Models of Articular Cartilage: Description and Theory

3.1 Introduction

Finite element models (FE) are essential to investigate AC mechanical properties and the interaction, structure and function of each component of this tissue, for a better comprehension of diseases. However, particular attention has to be made on the contact and geometric assumption in order to obtain realistic results.

As described in the previous section articular cartilage has a very complex structure that made this tissue inhomogeneous, anisotropic and poroviscoelastic. The first numerical model proposed, reproduced this tissue as a linear elastic material. Although this model is very simple, it does not take into account one of the most important component in AC: the fluid phase. The need of more accurate models for a better characterization of cartilage leads to the development of more complex models. In the literature exist and are well validated a lot of them, from the simple homogeneous biphasic model (Mow, et al., 1980), through the transversely isotropic biphasic model (Cohen, et al., 1998) and poroviscoelastic (DiSilvestro, et al., 2001; DiSilvestro, et al., 2001) to the poroviscoelastic fibril-reinforced with swelling (Wilson, 2005).

Below, the models used during this study will be described. The fibril-reinforced (FR) models as well as proroviscoelastic models were not considered in this study, although them are well validated. The former model showed to be time-consuming because the spring elements must be insert by the user connecting each node, instead the

poroviscoelastic model requires further experimental test to investigate viscoelasticity properties.

3.2 Biphasic Models

3.2.1 Biphasic Linear Elastic (BLE) Model

The most simple and widely employed model to describe articular cartilage is the biphasic linear elastic model. According to the biphasic theory (Mow, et al., 1980), AC consists of two phases: an incompressible solid matrix (made up of collagen network and PGs) and an incompressible fluid phase. The total stress of the tissue is, thus, given by the sum of the stress (σ) of the solid and fluid phases (Wilson, 2005):

$$\boldsymbol{\sigma}_{tot} = \boldsymbol{\sigma}_s - p\mathbf{I}\,, \tag{3.1}$$

where σ_s is the effective stress of the solid matrix, whereas p is the hydrostatic fluid pressure. In most widely used biphasic models the solid matrix is modelled as linear elastic and isotropic, in order to simplify the model. Therefore, the Chauchy stress depends only on two independent parameters: the two Lame's constant λ and μ. The stress-strain relationship is the following (Maas, et al., 2010):

$$\boldsymbol{\sigma}_s = \lambda\,(tr\varepsilon)\mathbf{I} + 2\mu\boldsymbol{\varepsilon}\,, \tag{3.2}$$

where ε is the strain tensor. The two Lame's constant can be expressed in function of the Young's modulus (E) and Poisson's ratio (ν) :

$$\lambda = \frac{\nu\,E}{(1+\nu)(1-2\,\nu)}\,, \tag{3.3}$$

$$\mu = \frac{E}{2\,(1+\nu)}\,. \tag{3.4}$$

Besides, the fluid flow (**w**) is calculated with Darcy's law. According to this equation (3.5) the fluid flow relative to the solid is proportional to the fluid pressure gradient and the costant of proportionality is permeability (k):

$$\boldsymbol{w} = \boldsymbol{k}\nabla p, \tag{3.5}$$

where **k** in three-dimensional cases is the spatial permeability tensor. For an anisotropic material it varies with direction and also it depends on deformation as discussed in Chapter 2. However, to simplify the numerical solution, in a BLE model k is considered constant, i.e. independent from the deformation of the tissue.

Although the oversimplifications of this model, it is widely used because it describes one of the most important characteristic of cartilage: *fluid-dependent* viscoelasticity. Even though this model can satisfactory explain the creep and stress relaxation response of cartilage during confined compression (Mow, et al., 1980; Cohen, et al., 1998; Li, et al., 1999), it cannot describe cartilage response in unconfined compression. Principally, this theory has failed to reproduce the high ratio from peak to equilibrium in unconfined compression stress relaxation (Cohen, et al., 1998), mainly because the anisotropic structure of the tissue is not taken into account. Actually, during unconfined compression test collagen fibrils are put in tension (Boschetti, et al., 2006; Li, et al., 1999). The ratio from peak to equilibrium can be increased considering the specimen/platen friction. Really, without friction the specimen is deformed in a uniform way, whereas with friction the specimens are deformed non uniformly because of the frictional restraints at the ends of them (Spilker, et al., 1990; Wu, et al., 2003; Wu, et al., 2004). However, the relaxation is still less than the one observed experimentally.

Moreover, this model is so widely employed thanks to the ease of use and implementation in FEM software, the need of only three parameters (E, ν and k) to describe the mechanical properties of the tissue and because is not very expensive computationally, compared with all the other more complex biphasic models.

However, this model cannot describe thoroughly the complex response of cartilage in compression, because a lot of oversimplifications are done. In fact, as studied by Mow et al. (Mow, et al., 1980), permeability decrease exponentially with increasing deformation (Figure 2.10), due to the reduction of pores dimensions. Furthermore, the solid matrix is modelled like linear elastic and isotropic, thus, the model cannot describe the effect of anisotropy, inhomogeneity and viscoelasticity of the cartilage on the response of the tissue. Besides, solid matrix is described like a single material made up of cartilage network and PGs, thus, the role of each component in compression is not considered. The latter question

might be overcome for a better prediction of cartilage behaviour in compression and then for a greater understanding of the development of diseases.

3.2.2 Biphasic non Linear Elastic (BNLE) Model

As discussed above and in Chapter 2, permeability of cartilage is strain-dependent. In particular, the parameter k decreases exponentially with strain, following the expression derived by Mow (Mow, et al., 1980):

$$k = k_0 e^{-M\varepsilon} , \tag{3.6}$$

where k_0 is the permeability when the tissue is unloaded and M is a material constant that describe the sensitivity of the permeability to strain.

In the FE software FEBio (Musculoskeletal Research Laboratories, University of Utah) expression 3.6 is implemented in terms of the Jacobian J, that is the determinant of the deformation gradient **F**, to consider the decrease of permeability with strain (Maas, et al., 2010), as follows:

$$\boldsymbol{k} = k\,(J)\boldsymbol{I} , \tag{3.7}$$

$$k(J) = k_0 \left(\frac{J-\varphi_0}{1-\varphi_0}\right)^{\alpha} e^{1/2M(J^2-1)}, \tag{3.8}$$

where α is a material constant that approaches how fast the permeability decreases to zero when cartilage consists only of solid phase, and φ_0 is the porosity in the reference state (Holmes, et al., 1990) and k_0 and M are the same constant used in equation 3.6.

Another widely used implementation of equation 3.6 is in term of void ratio (e) and is given by (Wilson, 2005):

$$k = k_0 \left(\frac{1+e}{1+e_0}\right)^{M}, \tag{3.9}$$

$$e = \left(\frac{V_f}{V_s}\right), \tag{3.10}$$

where V_f and V_s represent the volume of the fluid phase and solid phase, respectively; e and e_0 are the current and initial void ratio, respectively; all the other constant are the same used in the equations above.

3.2.3 Transversely Isotropic Models

Cartilage is a fully anisotropic material, i.e. the tissue mechanical properties change with direction. According to linear elasticity theory, the relation between the Cauchy stress and strain tensors is the following:

$$\boldsymbol{\sigma} = \boldsymbol{C}\,\boldsymbol{\varepsilon}\,, \tag{3.11}$$

where **C** is the stiffness tensor. For highly isotropic material **C** has 21 independent parameters. However, the presence of symmetry can reduce the number of them. Actually, in the case of a transversely isotropic material (TI) only five coefficients are needed.

In the TI model for articular cartilage, it is assumed that all the fibers of the tissue are aligned in the same direction, called longitudinal direction (Wilson, 2005; Cohen, et al., 1998), whereas in the perpendicular direction is there is an isotropic plane. However, this assumption is far from the real structure of collagen fibers, as discussed in the previous chapter. When assuming that the fibers lie in the third direction, the stresses of the solids are given by:

$$\begin{bmatrix}\sigma_{11}\\ \sigma_{22}\\ \sigma_{33}\\ \sigma_{12}\\ \sigma_{13}\\ \sigma_{23}\end{bmatrix} = \begin{bmatrix} \frac{1}{E_T} & -\frac{\upsilon_{TT}}{E_T} & -\frac{\upsilon_{LT}}{E_L} & 0 & 0 & 0\\ -\frac{\upsilon_{TT}}{E_T} & \frac{1}{E_T} & -\frac{\upsilon_{LT}}{E_L} & 0 & 0 & 0\\ -\frac{\upsilon_{TL}}{E_T} & -\frac{\upsilon_{TL}}{E_T} & \frac{1}{E_L} & 0 & 0 & 0\\ 0 & 0 & 0 & \frac{1}{G_T} & 0 & 0\\ 0 & 0 & 0 & 0 & \frac{1}{G_T} & 0\\ 0 & 0 & 0 & 0 & 0 & \frac{1}{G_L} \end{bmatrix}^{-1} \begin{bmatrix}\varepsilon_{11}\\ \varepsilon_{22}\\ \varepsilon_{33}\\ \gamma_{12}\\ \gamma_{13}\\ \gamma_{23}\end{bmatrix}, \tag{3.12}$$

where E_L and E_T are the longitudinal and transversal Young moduli, respectively; G_L is the longitudinal shear modulus; ν_{TL}, ν_{LT} and ν_{TT} are the Poisson's ratio. Knowing the value for E_T and ν_{TT} is possible to obtaine the value for the transversal shear modulus (G_T), that is given by:

$$G_T = \frac{E_T}{2(1+\nu_{TT})}. \tag{3.13}$$

Because of the symmetry:

$$\frac{\nu_{LT}}{E_L} = \frac{\nu_{TL}}{E_T}\,. \tag{3.14}$$

Therefore only five independent parameters (E_L, E_T, G_L, ν_{LT} and ν_{TT}) must be defined for the transversely isotropic materials.

Instead of the BLE model, a transversely isotropic biphasic model (TIBLE) can well reproduce the typical mechanical test on cartilage: indentation test, confined compression test and unconfined compression test. In particular, it is able to describe the high ratio from peak to equilibrium of reaction force under unconfined compression stress relaxation (Cohen, et al., 1998), lack of the BLE model (Donzelli, et al., 1999). Actually, in this type of test, due to the radial expansion of the tissue under unconfined compression, the collagen fibers are in tension. Thus, the solid matrix in this direction results to be stiffer than in the transversal one. Thus, a high peak load intensity together with a faster stress relaxation can be attained. However, Di Silvestro et al. (DiSilvestro, et al., 2001) provided that although TIBLE model can either reproduce the measured reaction force and lateral displacement, it is not able to account for both the variable simultaneously. Besides, this model has other disadvantages: the fibers are considered parallel to the articular surface and changes in orientation with depth are not taken into account; it is not assumed collagen fibers tension-compression non linearity; the TIBLE model requires seven independent parameters (five elastic constants and two permeability coefficients) that are uneasy to find experimentally. However, this model can be seen as a simplification of the well validated FR model or of the transversely isotropic Mooney-Rivlin model that will be describe in section 3.2.5.

3.2.4 Mooney-Rivlin Hyperelasticity

All the elastic material models described above are characterized by a constitutive equation which specifies that stress is a function of strain only. It is also possible to express an elastic material by a constitutive equation that denotes stress as a function of the deformation gradient, **F**. This is the case of hyperelastic material, where the stress are denoted in term of strain energy potential (W).

In the Mooney-Rivlin constitutive equation, strain energy potential is defined dividing the deviatoric and volumetric behaviors:

$$W = W_{dev}(I_1, I_2) + W_{vol}(\mathrm{J}). \tag{3.15}$$

The extended form is given by (Maas, et al., 2010):

$$W = C_1(I_1 - 3) + C_2(I_2 - 3) + \frac{1}{2}K(\ln J)^2, \quad (3.16)$$

where C_1 and C_2 are material coefficients, K is the bulk modulus of the material. The relation with the deformation gradient F is expressed through the first (I_1) and second deviatoric strain invariant (I_2) and the Jacobian J, defined as follows (Maas, et al., 2010):

$$I_1 = tr(\boldsymbol{F}\boldsymbol{F}^T), \quad (3.17)$$

$$I_2 = \frac{1}{2}I_1^2 - tr(\boldsymbol{F}\boldsymbol{F}^T), \quad (3.18)$$

$$J = \det(\boldsymbol{F}), \quad (3.19)$$

where *tr* indicates the trace of a matrix.

Brown et al. (Brown, et al., 2009) showed in their work that Mooney-Rivlin hyperelastic constitutive equation can provide a good fit with experimental data from indentation test, either for normal articular and osteoarthritic articular cartilage. This hyperelastic model can be easily used due to the need of only three parameters to reproduce the response of the material. However, Brown and his co-worker had not considered cartilage *fluid-dependent* viscoelasticity, as well as anisotropy, intrinsic viscoelasticity and tension-compression non linearity. Thus, this model cannot accurately reproduce AC response under all experimental loading.

To overcome the last two incoherence between the model and the real mechanical properties of cartilage, a biphasic transversely isotropic hyperelastic Mooney-Rivlin (TIMRBLE) constitutive equation is implemented in FEBio (Maas, et al., 2010). This model will be described in the following chapters.

3.2.5 Transversely Isotropic Mooney-Rivlin Hyperelasticity

TIMR constitutive model was developed for material that can be represented with a single preferred fiber direction. Thus, it should be useful for biological soft tissue like tendons, ligaments and muscle (Weiss, et al., 1996). A similar model is used by Boschetti at al. (Boschetti, et al., 2006) to predict the mechanical response of articular cartilage in confined and unconfined compression with a good fit between the numerical implementation and experimental tests.

The solid phase of AC is modeled as a composite material consisting of two components: an isotropic matrix representing PGs and the fiber family corresponding to the collagen network. As in the Mooney-Rivlin model the strain energy potential is divided into a deviatoric and a volumetric part, but in the TI case, the former depends also on the pseudo invariant (I_4) that account the fiber preferred direction. Actually the relation between the pseudo invariant and the initial fibers direction is (Weiss, et al., 1996):

$$I_4 = \boldsymbol{a_0 C a_0} = \lambda^2, \tag{3.20}$$

λ represents the deviatoric part of the stretch along the fiber direction and **C** is the Cauchy-Green deformation tensor ($\boldsymbol{C=FF}^T$).

Thus, the strain energy function can be written as follows:

$$W = W_{dev}(I_1, I_2, I_4) + W_{vol}(\mathrm{J}). \tag{3.21}$$

The volumetric stain energy potential is assumed as (Weiss, et al., 1996):

$$W_{vol}(J) = \frac{1}{2} K\ (lnJ)^2, \tag{3.22}$$

where K is the bulk modulus and J the Jacobian.

Instead the deviatoric part is assumed to be the sum of the strain energy that depends on the fibers and on the solid matrix:

$$W = W_{dev}^{m}(I_1, I_2) + W_{\mathrm{dev}}^{\mathrm{f}}(I_4)\ . \tag{3.23}$$

The strain energy of the isotropic matrix has the same expression of the Mooney-Rivlin material, as specified above, whereas the deviatoric part that depends on collagen network is as follows (Weiss, et al., 1996):

$$\lambda \frac{\partial W_{dev}^{f}}{\partial \lambda} = 0, \quad \lambda \leq 1$$

$$\lambda \frac{\partial W_{dev}^{f}}{\partial \lambda} = \mathrm{C}_3\left(\mathrm{e}^{\mathrm{C}_4(\lambda-1)} - 1\right), \quad 1 < \lambda < \lambda_{\mathrm{m}}$$

$$\lambda \frac{\partial W_{dev}^{f}}{\partial \lambda} = \mathrm{C}_5 + \mathrm{C}_6\lambda, \quad \lambda > \lambda_{\mathrm{m}}, \tag{3.24}$$

where λ_{m} is the stretch at which the fiber are strengthened, C_3 scales the exponential stress, C_4 is the rate of uncrimping of the fibers and C_5 is the modulus of strengthened fibers. C_6 is

a parameter that allows to enforce the continuity of $\partial W_{dev}^{f}/\partial\lambda$ and $\partial^2 W_{dev}^{f}/\partial\lambda^2$ at $\lambda = \lambda_m$ (Boschetti, et al., 2006; Maas, et al., 2010).

3.3 Swelling Model

As described in the previous chapter there are two mechanisms that cause swelling in cartilage: (1) the excess of mobile ions that produce an increase in the osmotic pressure inside the tissue; (2) repulsive forces between negative charges of GAGs, bounded to PGs, that produce a chemical expansion. Different theoretical models exist to describe swelling: mechano-electrochemical model and triphasic model (Lai, et al., 1991). Nowadays, these models are still computationally expensive, thus they can be used only for simple geometry. In order to simplify them, Wilson et al (Wilson, et al., 2005) introduced the hypothesis that electrolyte flux can be neglected, so that the ion concentration must be calculated only at equilibrium. Obviously this model can not to be used to investigate the events that take place inside the tissue before a new equilibrium state is reached. To enable this investigation a thermal analogy may be useful. Actually, because of the mathematical identity between thermal and mass diffusion processes the mechano-electrochemical model and triphasic models can be converted in a biphasic thermal diffusion models (Wu, et al., 2002; Myers, et al., 1984). These models and the numerical implementations will be briefly described below.

3.3.1 Osmotic Swelling

3.3.1.1 Triphasic Models

A triphasic model for cartilage is an extension of the biphasic models, but in the former the tissue is modelled as composed by three phases: a solid phase (PGs and collagen network); an interstitial fluid phase and a ionic phase (predominantly Na^+ and Cl^-). As in the biphasic model, the total stress within the tissue is given by the sum of the solid and fluid stress, as presented in equation 3.1. But in this case the hydrostatic pressure does not depend only on the load, but also on the osmotic pressure (π) and to the electrochemical potential μ^f, both produced by the presence of the mobile ions:

$$p = \mu^f + \Delta\pi. \tag{3.25}$$

Equation 3.1 for the biphasic materials is so developed in the following expression:

$$\boldsymbol{\sigma}_{tot} = \boldsymbol{\sigma}_s - (\mu^w + \Delta\pi)\mathbf{I}, \tag{3.26}$$

where the osmotic pressure gradient is given by:

$$\Delta\pi = \pi_{int} - \pi_{ext}, \tag{3.27}$$

and the internal and external osmotic pressure are respectively:

$$\pi_{int} = \Phi_{int} RT(c^+ + c^-), \tag{3.28}$$

$$\pi_{ext} = \Phi_{ext} RT c_{ext}. \tag{3.29}$$

In the above equation Φ_{int} and Φ_{ext} represent respectively the internal and external osmotic coefficient, R is the universal gas constant, T the absolute temperature and c^+ and c^- are the internal concentration of the mobile cations (Na^+) and anions (Cl^-), respectively.

The electro neutrality law has to be respected in all the points of the tissue at every, thus the concentration of cations has to be equal to concentration of anions (Cl^- and GAGs):

$$c^+ = c^- + c^F, \tag{3.30}$$

where c^F represents FCD.

The chemical potential outside and inside the cartilage is, respectively (Lai, et al., 1991):

$$\mu_{ext} = \mu_{0,ext} + RTln(\gamma^+_{ext} c^+_{ext}) + RTln(\gamma^-_{ext} c^-_{ext}) = \mu_{0,ext} + RTln\left(\gamma^{\pm}_{ext}{}^2 c_{ext}{}^2\right), \tag{3.31}$$

$$\mu_{int} = \mu_{0,int} + RTln(\gamma^+_{int} c^+) + RTln(\gamma^-_{ext} c^-) = \mu_{0,ext} + RTln\left(\gamma^{\pm}_{int}{}^2 c^-(c^- + c^F)\right), \tag{3.32}$$

where $\gamma^{\pm}_{int}$ and $\gamma^{\pm}_{ext}$ are the mean activity coefficients and μ_0 represents the concentration independent chemical potential.

At equilibrium the mobile ion concentrations are given by (Wilson, et al., 2007):

$$c^{\pm} = \frac{-c^F \pm \sqrt{{c^F}^2 + 4\frac{\left(\gamma^{\pm}_{ext}\right)^2}{\left(\gamma^{\pm}_{int}\right)^2} c^2_{ext}}}{2}. \tag{3.33}$$

Thus, the internal osmotic pressure at the equilibrium can be given by:

$$\pi = \Phi_{int} RT(c^+ + c^-) = \Phi_{int} RT \sqrt{{c^F}^2 + 4\frac{\left(\gamma_{ext}^{\pm}\right)^2}{\left(\gamma_{int}^{\pm}\right)^2} c_{ext}^2}. \quad (3.34)$$

3.3.1.2 Biphasic Swelling Model

Since the FE implementation of the fully mechano-electrochemical and triphasic models are computationally expensive and still not implemented in a FE software, the biphasic swelling model was introduced by Wilson et al. (Wilson, et al., 2005). Their model is based on the hypothesis that changes in the chemical potential are one order of magnitude less than permeability and variations due to mechanical loading. Thus, ions flux can be neglected and the ionic concentrations can be considered at equilibrium at each time, reducing the computational burden required to compute the solutions.

The total stress is given by the same expression of the triphasic theory (Equation 3.26) and the concentration has to be determined only at equilibrium with equation 3.33.

At equilibrium the osmotic pressure gradient measured between the external bath and within the tissue, depends only on the external bath concentration and the fixed charge density:

$$\Delta\pi = \Phi_{int} RT \sqrt{{c^F}^2 + 4\frac{\left(\gamma_{ext}^{\pm}\right)^2}{\left(\gamma_{int}^{\pm}\right)^2} c_{ext}^2} - 2\Phi_{ext} RT c_{ext}. \quad (3.35)$$

Wilson et al. (Wilson, et al., 2005) demonstrated that a biphasic swelling model is equivalent to a mechano-electrical one, with the advantage to be computationally less expensive. However, this simplification introduces the unreal hypothesis that ions velocity is infinite in order to maintain the chemical equilibrium. Besides, this model cannot be useful to investigate the ions flux inside the tissue and should be used with care in interpreting the transient swelling (Wilson, et al., 2005).

3.3.1.3 Thermal Analogy

To overcome the computational need of the thriphasic model and the inaccuracy of the biphasic swelling model to describe the transient swelling, a biphasic thermal diffusion models can be used. This model is based on the mathematical analogy between the mass

and thermal diffusion processes. Wu (Wu, et al., 2002) demonstrated that it could be fully implemented in a FE code to investigate swelling and that it is equivalent to the mechano-elechrochemical model.

AC is assumed to be a triphasic material composed, as in the triphasic models, by a solid matrix (representing collagen and PGs), a fluid phase and the mobile ions (prevalently Na^+ and Cl^-). The total stress is calculated as the sum of the solid stress and fluid stress as in the biphasic model (equation 3.1). The difference between the thermal analogy and the triphasic model resides in the equations of motion of the fluid phase and ions (Wu, et al., 2002). Actually, if friction between fluid phase and ions, friction between anions and cations and the electrical potential is not considered, it is possible to reduce the equations of motions used in the triphasic theory (Lai, et al., 1991) into Darcy's law (equation 3.5) and Fick's law, that is the follow:

$$\boldsymbol{J} = -\boldsymbol{D}^{\pm}\nabla c^{\pm}\,, \tag{3.36}$$

where $\boldsymbol{J}$ represent the ions flow, while $\boldsymbol{D}^{\pm}$ is the diffusion coefficient of anions and cations. For an anisotropic material **D** is a three-dimensional tensor and it varies with direction.

The mass conservation for the electrolyte is the follow:

$$\frac{\partial c^{\pm}}{\partial t} + \nabla(c^{\pm}\boldsymbol{v}^{\pm}) = 0, \tag{3.37}$$

From the mass conservation (3.37) and Fick's law (3.36) is possible to obtain the governing equation of the convective-diffusion process:

$$\frac{\partial c^{\pm}}{\partial t} + \boldsymbol{v}^{s}\nabla c^{\pm} = D^{\pm}\Delta c^{\pm}, \tag{3.38}$$

Where the convection-diffusion problem is solved in terms of temperature instead of concentration.

3.3.2 Chemical Expansion

In the literature is possible to find two way to define the chemical expansion. Lai et al. (Lai, et al., 1991) suggested:

$$T_c = a_0 c_F e^{-k\frac{\gamma^{\pm}_{ext}}{\gamma^{\pm}_{int}}\sqrt{c^-(c^-+c^F)}}, \tag{3.39}$$

where a_0 and k are material constants.

Another form of chemical expansion was formulated by Eisemberg and Grodzisky to implement it in their finite element analysis (Eisemberg, et al., 1987):

$$T_c = \beta_o e^{c/c_\beta}, \tag{3.40}$$

where β_0 and c_β are material constants, while c is the effective NaCl concentration given by:

$$c = c^{\pm}\sqrt{1 + c^F/c^{\pm}}\,. \tag{3.41}$$

In the biphasic swelling model the effective concentration c is given by equation (3.33). Instead for the thermal analogy the two equation for the chemical expansion are solved in terms of temperature.

Chapter 4
Experimental Tests

4.1 Sample Preparation

Articular cartilage plugs were harvested from metacarpalphalyngeal joint of 7-day-old bovine calves. Full thickness AC plugs were first punched with a dermal biopsy punch (diameter of 6 mm) and then separated from the subchondral bone using a razor blade. Particularly attention was made to obtain AC samples as flat as possible. Unfortunately, due to the shape of the joint it was quite hard to obtain parallel surfaces, thus each AC plug was then drilled with a dermal biopsy punch of 3 mm in diameter to obtain flatter surfaces.

All samples were then equilibrated in a phosphate-buffered saline (PBS) with a sodium chloride concentration of 0.154M. The solution pH was 7.4. The samples were stored in these conditions for approximately twelve hours before the mechanical tests at the physiological temperature of 37°C.

The main problem observed in the sample preparation is the necessity of flat samples. Although the great care required to in obtain flat specimens, this technique can be affected by the ability of the user. In some studies to get flat samples, AC plugs were placed in a sledge microtome and the upper surface was trimmed until it was parallel to the osteochondral surface. To facilitate the trimming, AC plugs could be covered with wax or frozen. A big disadvantage of the further arise during wax removal: AC plugs have to be exposed to high temperature and this procedure could ruin the ECM matrix. Similarly, the freezing of AC plugs lead to ECM matrix disruption. Actually, the formation of ice-crystals inside the tissue fractures the ECM matrix and disrupts the membranes of chondrocytes (Willett, et al., 2005; Muldrew, et al., 2000).

In numerous studies the samples were stored at -20° C (Boschetti, et al., 2006; Chen, et al., 2001; Cohen, et al., 1998) or at -80° C (Chahine, et al., 2004). Many studies on

cryopreservation demonstrated that it should lead to a significant change in the mechanical properties in compression. In particular, the aggregate modulus and the compressive stiffness decrease when the cartilage is frozen (Kennedy, et al., 2007; Willett, et al., 2005).

***Figure 4.1**: Instrument used to harvest the AC plugs from the metacarpalphalyngeal joint. a) razor blade; b) 3 mm dermal biopsy punch c) 6 mm dermal biopsy punch.*

***Figure 4.2**: The photo shows the metacarpalphalyngeal joint of the 7-days-oldbovine calves, from which the samples were harvested.*

The decrease of the aggregate modulus in compression suggests a change in the PG content, responsible of the mechanical properties in compression. Zheng et al. (Zheng, et al., 2009) recently using microscopic MRI discovered that freezing AC plugs at -20°C and -80°C produces a significant loss of GAGs (till 56,5%) and that this loss increases within the time scale of hours. The results confirm that the formation of ice-crystals can disrupt the ECM matrix in AC and the bound between the latter and PGs. As a consequent small pieces of PGs and GAGs can diffuse out from the tissue due to the presence of charge-to-charge repulsive forces. At the same time also the fluid-dependent properties are altered: the stress decay to half the peak stress decreased, suggesting a change in the permeability of the tissue (Willett, et al., 2005). Even so, in numerous investigation on mechanical properties of cartilage, samples preparation included freezing of AC plugs at -20° C (Boschetti, et al., 2006; Chen, et al., 2001; Cohen, et al., 1998) or at -80° C (Chahine, et al., 2004). In this study AC plugs were not frozen to preserve the ECM matrix and the presence of GAGs, fundamental to analyze swelling and the biphasic behavior of cartilage in unconfined compression.

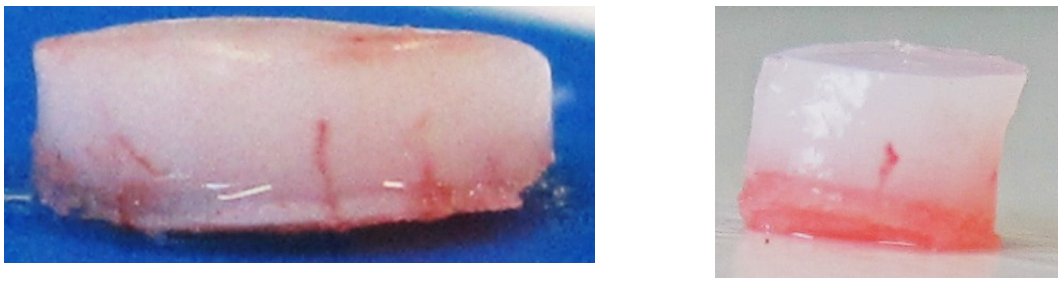

a) *b)*

***Figure 4.3**: Full thickness AC plugs. a) in the photo the 6 mm sample is shown ; b) 3mm sample. As can be seen from these photos, the specimens are not completely flat, but with the 3 mm one is possible to improve it.*

4.2 Mechanical Testing

Compressive mechanical testing on articular cartilage to investigate the mechanical properties is commonly performed with three type of tests: confined compression test, unconfined compression test and indentation. Confined compression and unconfined compression are generally performed *in vitro*. Stress relaxation tests performed in both configurations demonstrated a similar equilibrium reaction force (Cohen, et al., 1998; Korhonen, et al., 2002). That means that both unconfined compression and confined compression could be used to study AC plugs properties at equilibrium. The third type of mechanical tests, i.e. indentation, may also be applied *in vivo* during athroscopy (Julkunen, 2008). However, the Young modulus at equilibrium obtained in an indentation test is bigger than the one obtained with the unconfined compression (Korhonen, et al., 2002). As suggested by the same author this lack could be due to the damaging of the collagen network during the preparation of the sample for the *in vitro* unconfined compression, whereas for the *in vivo* indentation test intact articular cartilage was used. Anyway, in this work to analyze the mechanical properties of AC we performed unconfined compression stress relaxation test.

Mechanical testing to investigate AC cartilage swelling were always performed *in vitro*. There are two kinds of compressive tests that are commonly performed: free-swelling (Lai, et al., 1991; Myers, et al., 1984) and isometric swelling (Lai, et al., 1991; Myers, et al., 1984; Wilson, 2005; Wilson, et al., 2005; Wilson, 2005). In the former one AC plugs

are free to swell or shrink under a sudden change of concentration, no force is applied to the sample and the change in thickness is measured (Figure 4.4a). The second type of experiment (Figure 4.4.b) is generally used to measure the isometric reaction force needed to maintain the sample at a fixed thickness. In this experiment generally a pressure or a displacement is applied to the sample until the equilibrium is reached. When equilibrium is reached the external salt concentration is suddenly changed to measure the change in reaction force due to swelling or shrink. Commonly both tests are performed in confined compression to simplify numerical and analytical model. However, in this thesis works an unconfined compression test is performed to study the transient behavior of articular cartilage during swelling.

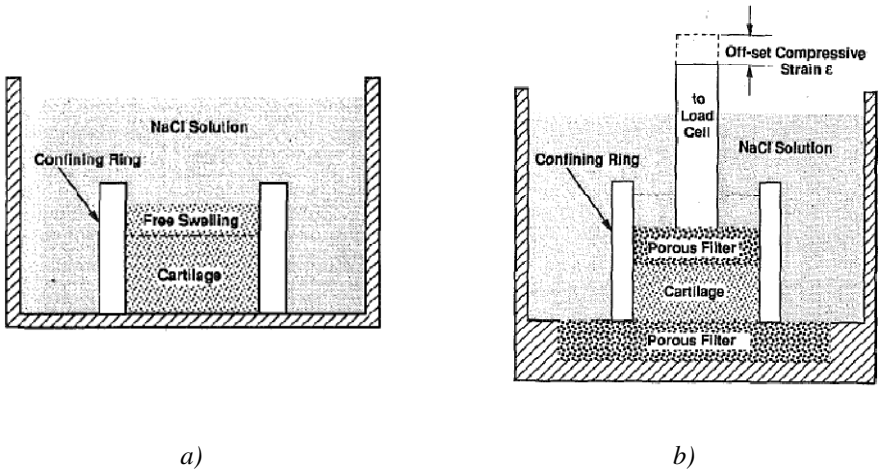

Figure 4.4*: Schematic representation of the typical set-up of mechanical tests that are commonly performed on cartilage to investigate swelling: a) free-swelling; b) confined compression free-swelling.*

4.2.1 Investigation of the Biphasic Behavior

Unconfined compression tests on cartilage were performed using a testing machine (ElectroForce 3200, Bose Corporation, Minnesota, USA) equipped with a stainless steel 225 N load cell. This load cell allows to minimize the effect of off-axis forces and the structures provide a submersible capability. The extracted data were corrected taking into account the machine stiffness in order to consider only the real displacement.

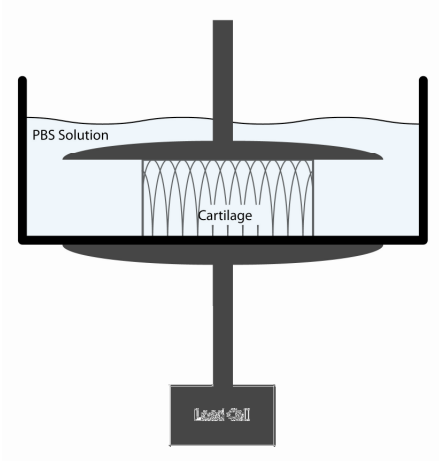

Figure 4.5: *Schematic representation of the set-up used to perform the unconfined compression test on AC plugs. The load cell was below the sustaining dish to decrease the noise in the measurement. Cartilage was submerged in PBS 0.154M during the test.*

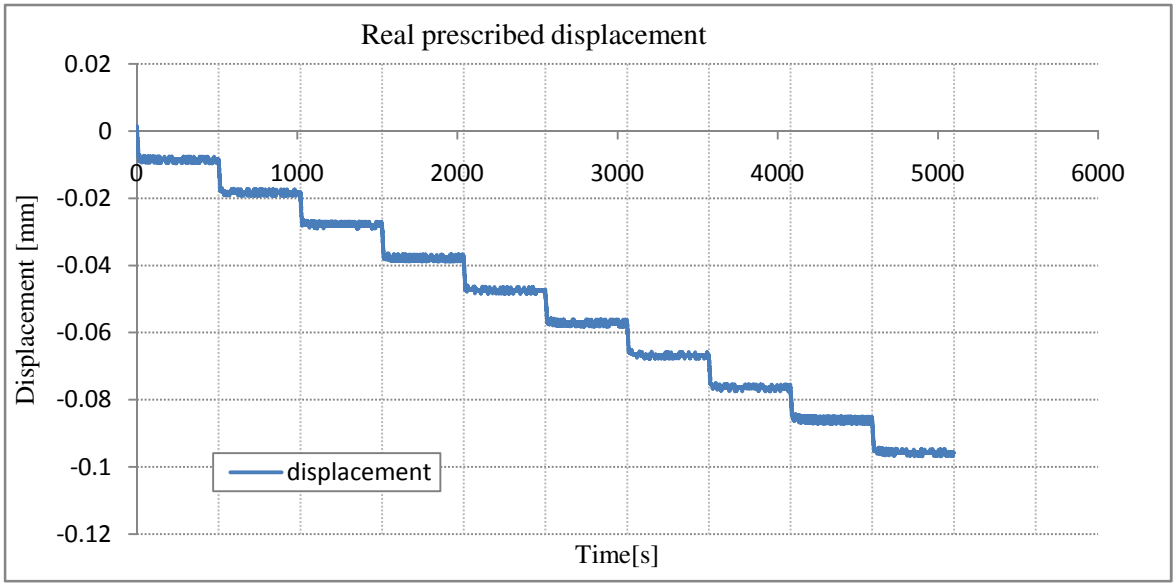

Figure 4.6*: Prescribed displacement in the unconfined compression relaxation tests. The displacement was adjusted to takes into account the stiffness of the loading machine.*

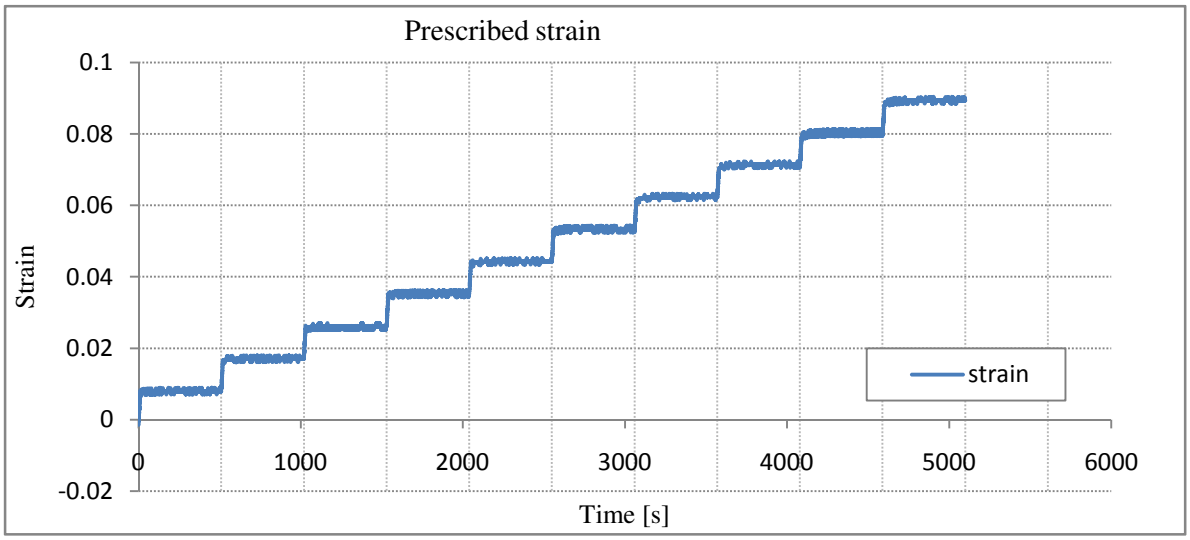

***Figure 4.7**: Prescribed strain on one articular cartilage plug in the unconfined compression relaxation tests. The dimension of the sample considered are: diameter=3mm and thickness=1.07 mm.*

Each samples underwent stress relaxation during the unconfined compression test, through a step-wise compression (Figure 4.6) defined by 10 ramps, each of 1% strain at a velocity of 1μm/s until the equilibrium was reached. From previous tests were observed that AC plugs with the same dimensions and from the same joint reached the equilibrium before 500s. Therefore, the relaxation time between each step was considered to be 500s.

Each plug was placed between a smooth non-porous loading indenter and a non porous plate. The compressive displacement was applied to the indenter and the reaction force was registered through the sustaining plate. Actually, the load cell was placed below the dish to decrease the noise produced by the motor of the loading machine to apply the displacement. During all the experiment the AC plugs were bathed in PBS 0.154 M NaCl to maintain the hydration.

Before each test a preload of 0.1 N was applied to ensure contact between the sample and the indenter. This value corresponded to a strain of about 0.05% during an unconfined compression test on cartilage sample with radius of 1.40 mm and thickness of 1.11 mm (Li, et al., 1999). The initial force of contact was considered non influential to the recorded force, due to its small value. However, during the comparison between experimental and numerical tests, the first step has not been considered so as to ensure that initial stresses and deformations due to contact can be neglected.

Thickness of AC in the joint is irregular, so for each AC plug it depends on the region of belonging. Besides, during the separation of the sample from the subchondral bone, the user introduces an unpredictable change in thickness. The resulting thickness for each sample was hence measured as the difference between the position of the indenter when in touch with the superior surface of the sample and the supporting plate.

4.2.2 Investigation of the Swelling

Unconfined compression tests on cartilage to investigate swelling were performed using the same testing machine and the same experimental set–up used for the investigation of AC biphasic properties. The only difference in the experimental configuration was that the load cell was placed under the supporting plate, to facilitate the change of solution. Each plug was placed between a smooth non-porous loading indenter and a non porous plate. The compressive displacement was applied to the indenter and the reaction force was registered through the sustaining plate.

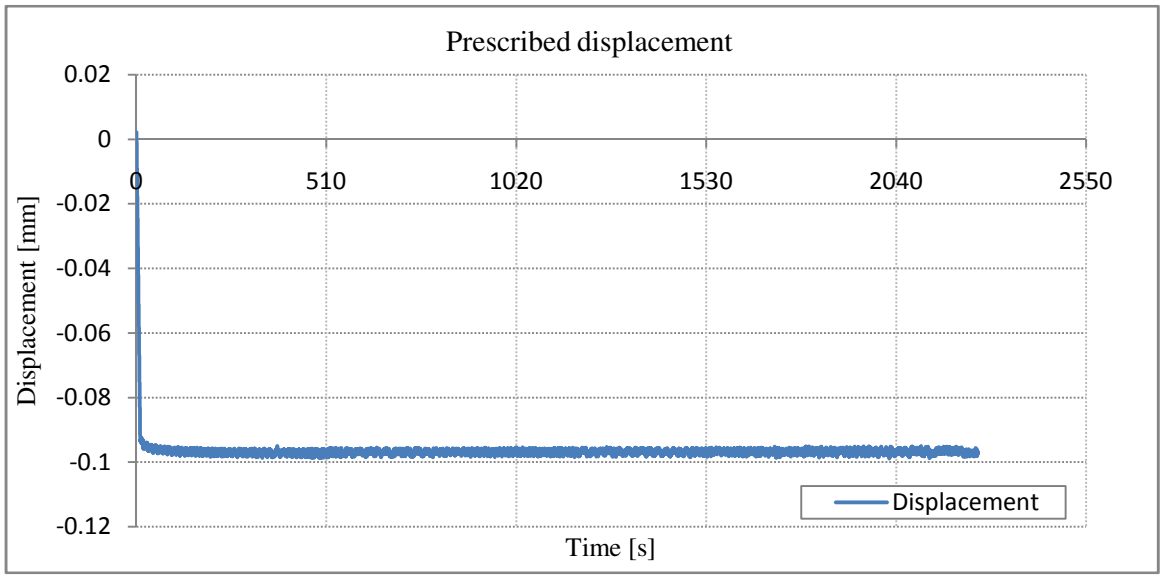

***Figure 4.8**: : Prescribed displacement in the unconfined compression swelling tests. The displacement was adjusted to takes into account the stiffness of the loading machine*

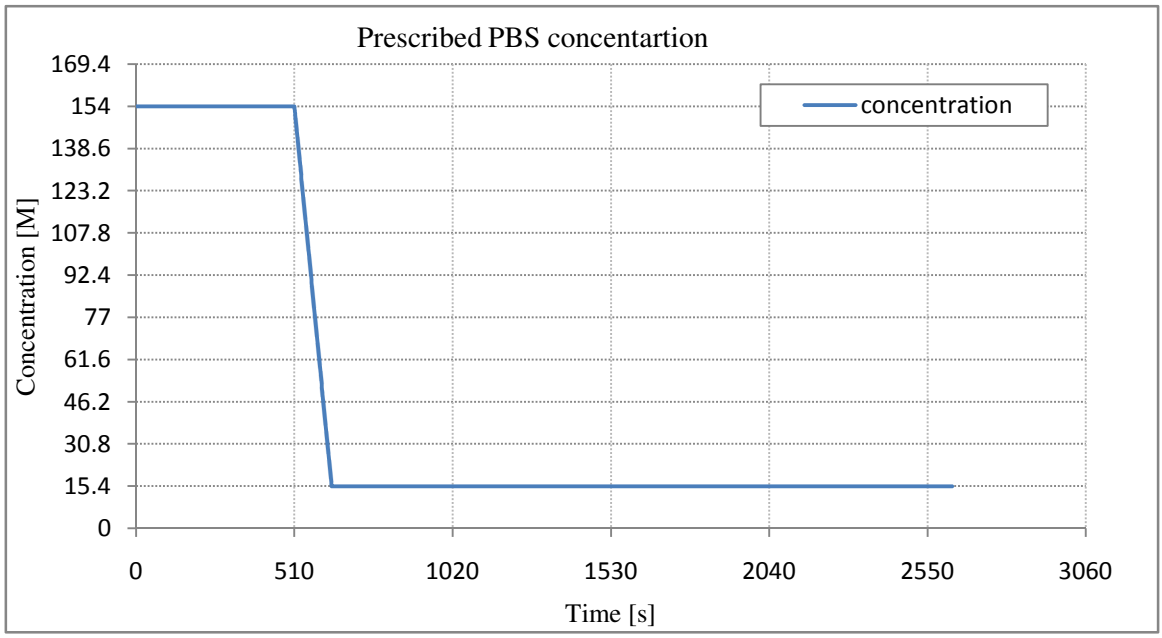

***Figure 4.9**: Prescribed change of concentration of the PBS solution. The solution was changed from 0.154 M to 0.0154M in about 120s.*

Prior the testing the samples were stored in PBS 0.154 M NaCl (concentration considered physiological). At the moment of testing all the samples were, so, at equilibrium with the storing solution. Each sample was then placed between the non porous indenter and the supporting plate, bathed in 20 ml PBS at physiological concentration (0.154M). During the mechanical test, each sample was first subjected to stress relaxation compression of 10% strain at a velocity of 1mm/s until the equilibrium was reached, to quantify the mechanical properties of each sample (Figure 4.8). As well as the test described above, the relaxation time was considered 500s. At the end of this step, a rapidly change in concentration was applied (Figure 4.9), while the displacement was maintained at the constant value of 10% strain. In this way the thickness was fixed at a constant value while the cartilage was free to expand in the radial direction due to swelling. The use of a confined compression configuration allow the change of the bathing solution in an easy and fast way. In particular, the concentration was changed from a physiological value to a hypotonic one (0.0154 M) to allow AC to swell. To decrease the concentration of one tenth, 18 ml of solution were removed from the total PBS volume equal to 20 ml that there were in the dish. The same quantity of distilled water was then added to obtain a solution of 0.0154M NaCl. To remove and add the two liquid a volumetric pipette with a maximum volume of 3

ml was used. This type of pipette allows the transport of the same quantity of fluid. Particular attention was made during each step in order to avoid to affect the reaction force during the change of solution.

Before testing, each AC plugs was subjected to a preload of 0.1 N to ensure contact between the sample and the indenter, as in the unconfined compression tests presented above. Again, the thickness was measured as the difference between the position of the indenter in contact with the sample and when in contact with the supporting plate.

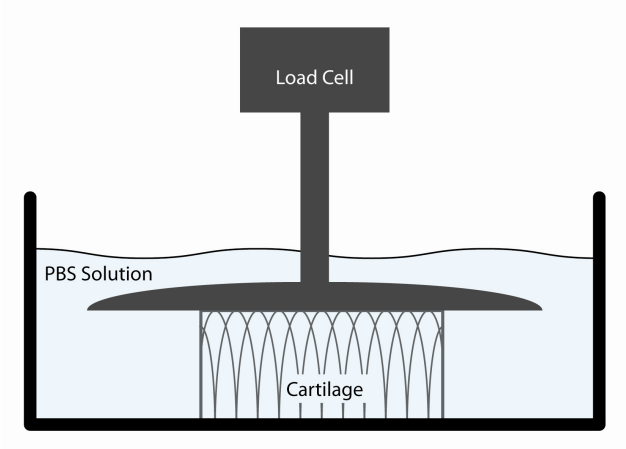

Figure 4.: *Schematic representation of the set-up used to perform the unconfined compression test on AC plugs. The reaction force during swelling was measured at the loading platens. Cartilage was submerged in PBS 0.154M for 500s, after that time concentration was changed to 0.0154M NaCl to induce swelling.*

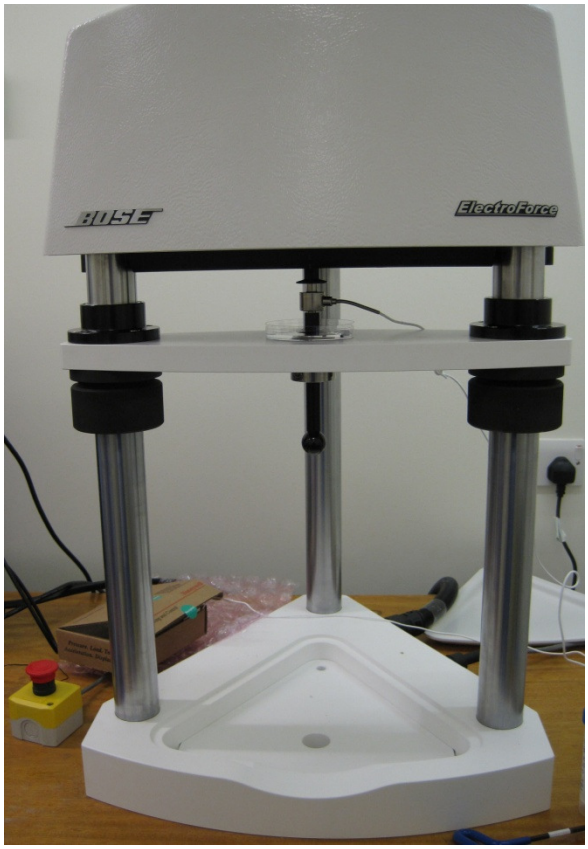

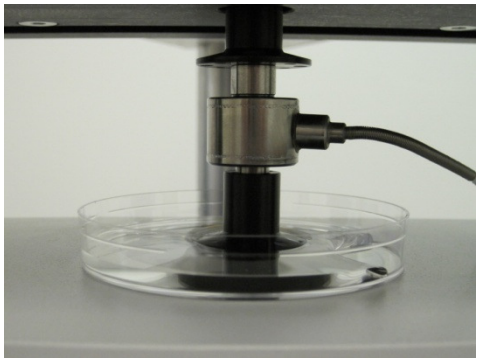

a) *b)*

***Figure 4.7**: a) Testing machine; b) experimental set-up of the unconfined compression test with change of solution concentration to analyze swelling.*

Chapter 5
Finite Element Analysis

5.1 FE Implementation of the Biphasic Models

Three-dimensional FE implementation in the free FE software FEBio was used to validate the biphasic models used in the literature. The objective of this study was to evaluate which model would be more truthful to predict the history of AC reaction force registered under unconfined compression test. The model required must be accurate and simple, but at the same time efficient in term of time required to compute the solution. Thus, some features during FE analysis were maintained constant to compare the biphasic models. In particular, only the definition of material properties was changed depending on the type of model.

Geometry, mesh, material definition, boundary condition and contacts were defined using the software Preview v.1.2.3 (Musculoskeletal Research Laboratories, University of Utah). Whereas the force measured on the loading platen were recorded in a text file and then read with the software MATLAB (MathWorks Inc Cary, NC).

5.1.1 Geometry

In this part of the work the materials to be examined are two: the loading platen and articular cartilage (Figure 5.1). The supporting plate cartilage is not represented to decrease the number of materials and thus, the number of nodes used in the model, in order to have a low computational burden. This assumption is true, if the interfaces are frictionless, in order to decrease the time required to compute the solution. Furthermore, the value of stress and strain within the dish are not part of this study.

Cartilage was modeled as a cylinder with the same dimensions as the articular cartilage plugs used for the experimental tests. Thus, the diameter in each simulations was of 3 mm

while the thickness of cartilage changed in each simulation, with a value between 0.656 mm and 1.207 mm. The thickness in each simulation was measured as described in Section 4.2.1.

The loading platen was modelled as a cylinder too. Stress and strain within this material are not interesting for this study, thus the dimensions considered are different from the real ones. A diameter of 5 mm and a thickness of 0.3 mm were considered.

In order to decrease the computational time and the resources that are needed to compute the solutions, only a quarter of the total geometry was considered due to the symmetry.

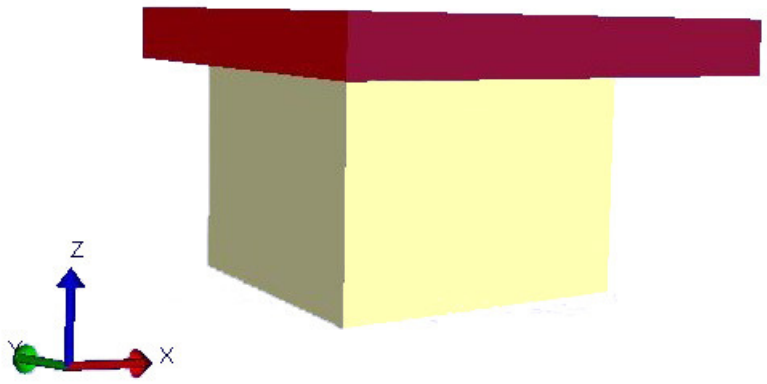

***Figure 5.1**: Simple three-dimensional geometry used in the FE implementation for the analysis of the biphasic materials. In this simulation only the indenter (red) and cartilage (white) where represented. The dimensions are in [mm].*

5.1.2 Mesh

Cartilage was meshed with a *butterfly centre* meshing method, one of the two methods implemented in the Preview software. Unfortunately, this type of meshing method does not allow the user to refine the mesh radially, so as the mesh will be finer where the pressure of the fluid phase changes more rapidly. The fluid flux is only in the radial direction because the fluid phase cannot flow through the surface in contact with the loading platen and the sustaining dish, because of the imposed boundary conditions on the bottom surface of the cartilage and due to the presence of the non porous loading platen. Therefore, a refinement of the mesh in the axial direction is not needed. Thus, different refinements of

the mesh in the radial direction were prepared. In particular, mesh with 640, 1848 and 12696 elements were compared. An analysis on the refinement of the mesh with the three types of meshes was done, so as to choose the mesh with the best compromise between accuracy and computational burden. Mesh with a bigger number of elements than the ones used, were considered too computationally expensive, thus, them were not considered. This mesh evaluation was performed on a relatively simple model (a BNLE model) with a short associated processing time. For more complex models including anisotropy of the material, the processing time drastically increases. Considering the results presented in Table 5.1 mesh with 1848 elements was chosen because it was considered the best compromise between required computational time and accuracy of the results. Cartilage was discretised with 3D hexahedral brick elements. These type of elements were selected by default by the software to implement the poroelastic theory. FEBio implements them with 8-node trilinear hexahedral element (Maas, et al., 2010).

Number of elements	**Reaction Force at equilibrium [N]**	**Reaction Force at peak [N]**	**Computational time [s]**
640	0.1628	0.1699	60
1848	0.1635	0.1707	1200
12696	0.1639	0.1714	7200

Table 5.1*: Comparison between the reaction force at equilibrium (end of relaxation) and the peak reaction force obtained for different meshes. The value were obtained with the same dimensions, material properties, boundary conditions and contact to implement cartilage, whereas the mesh was changed. Cartilage has a diameter of 3 mm and thickness of 1.07 mm. A BNLE model was used with the following material properties: E=0.3 MPa; v=0.1;* φ_0*=0.8;* α*=0.0848; M=9.276; k=0.04* mm^4/Ns*. All the values were measured at the last step corresponding to a strain of about 10%. The Boundary conditions and contact that were used were the same illustrated below.*

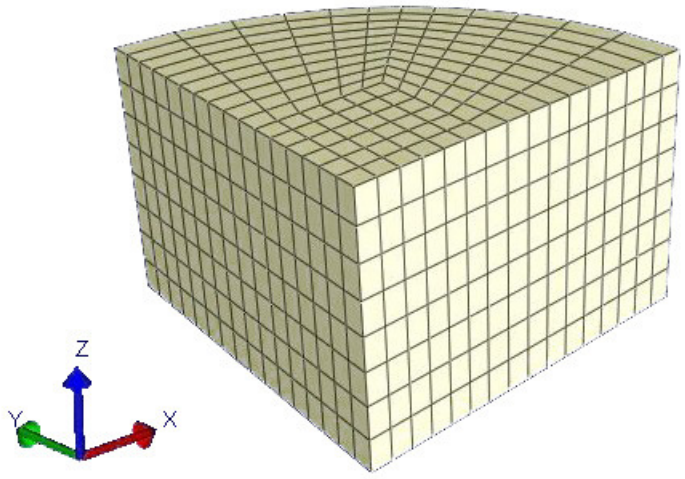

***Figure 5.2**: Representation of the three-dimensional mesh used in the FE implementation for the analysis of the biphasic materials. The total number of element is 1848.*

5.1.3 Material Properties

The AC material properties for each biphasic model were appropriately changed in order to allow a comparison between the predicted AC response and the experimental data. In particular, it is necessary that the material properties are obtained directly from the unconfined compression relaxation tests specially performed.

Actually, through the unconfined compression relaxation test, it is possible to measure the Young's modulus at the end of relaxation. At this time the fluid phase can be considered at equilibrium, thus, the mechanical properties of cartilage depends only on the solid matrix and collagen fibers. The measured Young's modulus takes into account the response of either the collagen fibers and PGs, because is not possible to discriminate the contribute of each component in compression. Luckily, for the BLE and BNLE models, it is easy to find the mechanical parameters that define the response of bovine articular cartilage in compression because considering their definition (Section 3.2.1 and 3.2.2 respectively), there is no differentiation between the contribute of collagen network and proteoglycans. Instead, TIMRBLE model (and its extension with the consideration of the strain-dependent permeability) and random fiber models implemented by Ateshian et al. (Ateshian, 2007; Ateshian, et al., 2009), consider the discrimination between the response of collagen

network and the solid matrix representing PGs contribute in compression. Thus, it is not possible to directly use the material parameter (E) measured through the experimental test, but is needed a curve-fit between the experimental test and the numerical model.

Referring to the theory described in Chapter 3 on the different biphasic models used in the literature, below follows a brief description of the mechanical parameters used and any assumption considered. The BLE models requires only three parameters (described in Section 3.2.1): E, ν and k. As described above, E is easily obtained from the experimental test. Whereas ν and k can be calculated from a comparison between the reaction force measured from the experimental test and the numerical prediction of the force. Introducing the strain-dependent permeability in the BLE model (BNLE model), other three parameters must be defined (see Section 3.2.2 for details): φ_0, α and M. These parameters were chosen from the value presented in literature (Accardi, 2008; Holmes, et al., 1990), observing that a good correlation between the experimental data and the numerical prediction of the reaction force can be achieved. A porosity 80% were considered; α was taken from Holmes' work (Holmes, et al., 1990) and was considered equal to 0.0848 and M was considered 9.276 (Accardi, 2008; Holmes, et al., 1990). Increasing the accuracy in the description of the structure of articular cartilage, also the number of parameters that must be used increase. Actually, the TIMRBLE requires the definition of seven parameters as described in Sections 3.2.4 and 3.2.5: C_1, C_2, K, C_3, C_4, C_5, k. Furthermore, also the preferred fiber orientation has to be defined (see FEBio User's Manual for details). The coefficient C_2 was set equal to zero, thus Mooney-Rivlin's coefficient C_1 is given by:

$$C_1 = \frac{G}{2}. \tag{5.1}$$

In addition, due to the hypothesis that the solid matrix is isotropic, the shear modulus and the bulk modulus are calculated from the isotropic parameters E and ν , as follows:

$$G = \frac{E}{2(1+\nu)}, \tag{5.2}$$

$$K = \frac{E}{2(1-2\nu)}. \tag{5.3}$$

In conclusion , the independent parameters necessary to use the TIMRBLE are: E, ν, k , C_3, C_4, C_5. The material constants, requested by the constitutive equation of the fiber (equation 3.19) can be obtained from literature (Boschetti, et al., 2006; Julkunen, 2008; Li, et al.,

1999; Li, et al., 2009; Maas, et al., 2010; Weiss, et al., 1996). In particular, the values presented in Weiss's work (Weiss, et al., 1996) were considered because of the best agreement between the numerical prediction and experimental reaction force. C_3 was considered 0.6 MPa (Boschetti, et al., 2006), C_4 equal to 64 and C_5 640 MPa (Weiss, et al., 1996). Thus only three parameters (E, ν and k) were obtained from a comparison between the numerical prediction of reaction force and the measured one. The introduction of the strain-dependent permeability in the TIMRBLE model requires the definition of other three parameters, as described above for the BNLE model. The random fiber model contrived by Ateshian et al. (Ateshian, et al., 2009; Ateshian, 2007) was also implemented to analyze the effect of the presence of a continuum distribution of fiber. The search for exacts value of the mechanical parameters required by this model is not part of this project. I believe that the accuracy of this constitutive model in predicting the behaviour under different mechanical load, is not enough to justify its implementation in a knee joint model, due to the computational burden and the large number of parameters required.

For a better correlation between the numerical reaction force and the experimental data, in each step appropriate parameters were used. I believe that this measure is due to the fact that the AC plugs, used for the unconfined compression relaxation tests, were not completely flat (for more detail see Chapter 6).

Instead, the loading platen was modeled as a *rigid body*, because its deformation can be considered negligible compared to articular cartilage. Thus, any material property was not required (Maas, et al., 2010).

5.1.4 Boundary Conditions

All the displacements and rotations of the loading platen were set to zero, due to the symmetry of the material, except the displacement in the axial direction (z). In particular was imposed the same displacement applied in the step-wise unconfined compression relaxation test (see Chapter 4).

Instead, on cartilage due to symmetry conditions, displacements in the direction perpendicular to each the constrained surface were fixed. On the bottom surface of articular cartilage, displacement in the same direction of compression (z) were set to zero, to represent the presence of the sustaining dish. Displacements in x and y directions (radial

direction) were not constrained in order to allow the sample to expand radially, as in a frictionless interface. The unconfined compression model has impermeable boundary conditions at the top and bottom surfaces of the tissue sample as no fluid exudation can occur through the impermeable loading platen and dish. Fluid flux was, instead, permitted in the lateral surface of AC by setting the fluid pressure to zero at that side.

5.1.5 Contact Definitions

The solution to the analyses was obtained using the *sliding interface* contact to set up a non-penetration constrain between the bottom surface of the loading platen and the upper surface of AC. In order to avoid penetration the augmented Lagrangian method was employed instead of the Penalty method to use a smaller penalty factor and, thus, to avoid numerical instabilities (Maas, et al., 2010). After preliminary simulations, needed to find the best penalty factor to compute the Lagrangian multipliers, it resulted to be 10.

Compressive problem was defined as a *contact* between the rigid *master* surface of the loading platen and the deformable AC *slave* upper surface. Unfortunately, the augmented Lagrangian method increase the computational time more than the Penalty method, because at any increment the multipliers must be calculated (Maas, et al., 2010).

The interface was considered frictionless to reduce the computational time.

5.2 FE Implementation of the Thermal Analogy to Investigate Swelling

The evaluation of thermal analogy to analyze articular cartilage swelling was done on the FE software ABAQUS in an axysymmetric configuration. For this study the software ABAQUS was used instead of FEBio, because in the latter, the heat transfer has not been implemented yet. The FE implementation of thermal analogy is solved through two steps: (1) the initial concentration distribution within the tissue is obtained by solving the heat transfer analysis, after a change of concentration in the bath; (2) the swelling problem is computed applying to the transversely isotropic biphasic model the thermal analogy theory, knowing the concentration distribution measured in the previous step. The fluid and chemical expansion of the cartilage were replicated in this phase of the implementation.

Thus, a sequentially coupled thermal-stress analysis is activated, in which in the first step the temperature field does not depend on the stress field (Abaqus).

5.2.1 Diffusion Implementation

5.2.1.1 Geometry

The geometry used for the simulation of the heat transfer within the articular cartilage is very simple. Actually it consist only in the representation of the cartilage in a 2D axysymmetric configuration. The size of the considered sample was changed in each simulations in order to have an adequate correspondence between the numerical and experimental results.

5.2.1.2 Mesh

Cartilage was discretised with a structured mesh in ABAQUS/standard. DCCAX4 quadrilateral heat transfer elements were used, with four nodes for each element. A radial refinement was not considered in this analysis to avoid mismatch between the mesh used in the heat transfer analysis and the one utilized in the expansion simulation. A preliminary analysis was carried out to compare different mesh refinements so as to choose the mesh with the best compromise between accuracy and required computational time. In particular, the distance between two adjacent nodes were changed. The size of element used were 0.01, 0.025, 0.05 and 0.1 mm. As a result, the obtained total number of elements were 19800, 3180, 780 and 195. To apply the comparison the historical trend of temperature measured in the upper left corner was used. No particular change in the history of temperature was observed (not shown). Considering the value of temperature at the end of simulations, summarized in Table 5.2, a mesh with 780 elements was chosen in order to decrease the computational time.

Number of element	Concentration [mM]
195	22.5632
780	22.4819
3180	22.4604
19800	22.454

***Table 5.2**: Comparison between different temperatures (concentrations) measured in the upper-left corner of articular cartilage after 2500s for different meshes. The value were obtained with the same dimensions, material properties and boundary conditions, whereas the mesh was changed. Cartilage has a diameter of 3 mm and thickness of 1.319 mm.The material properties used are described in section 5.2.13.*

5.2.1.3 Material Properties

Considering the mathematical similarity between mass and thermal diffusion equation, as explained in Section 3.3.1.3, an analogy between thermal diffusivity (α) and the coefficient of diffusion for the mass diffusion can be done (Li, 2009). From the definition of thermal diffusivity is possible to calculate the isotropic thermal conductivity (k), as follows (Li, 2009; Probstein, 1994):

$$k = \alpha \rho c_p, \tag{5.4}$$

where ρ is the density of the solution and c_p is the specific heat. The diffusion coefficient of solution in cartilage was obtained from Maroundas's work (Maroundas, et al., 1977). The observed diffusion coefficient was found to be 0.58 x 10^{-9} m^2/s, thus, the thermal conductivity derived from equation 5.4 was 2.46 x 10^{-3} W/mK. The density and the specific heat of the solution were unknown, thus, the values of water were used. However, no change in the outcome history of temperature was observed by changing the values of these, because the thermal conductivity is a function of them.

The solution can diffuse only in the radial direction due to the presence of the loading platens in contact with the upper surface and of the sustaining dish in bottom one. Thus, the thermal conductivity coefficient was considered isotropic.

5.2.1.4 Boundary Conditions

Only boundary conditions in terms of concentration was set in this analysis. In particular, concentration was changed in the lateral side of the samples from 154mM to 15.4mM like in the experimental tests (Section 4.2.2). AC plugs were stored in PBS solution 154mM NaCl for approximately twelve hours before testing, thus the equilibrium was considered reached. Therefore, an initial value of concentration equal to 154mM was assigned to the entire cartilage.

5.2.2 Expansion Implementation

5.2.2.1 Geometry

The outlined geometries were: the loading platen, articular cartilage and the sustaining dish. Cartilage size was adapted in each simulations in order to have an adequate correspondence between the numerical simulations and experimental tests, and it was modelled like an axysymmetric deformable shell. Instead, due to the high stiffness of loading platens and of the sustaining dish compared to articular cartilage, them were designed as axysimmetric analytical rigid surface.

5.2.2.2 Mesh

The FE meshing technique used was *structured* and the mesh adopted for the models consisted of axisymmetric 8-node pore pressure elements (CAX8P) for the AC sample. Although Accardi's project showed that there were not a big difference in accuracy between the reaction force measured with linear (4-node) and quadratic (8-node) elements, 8-node elements were, however, considered to improve the accuracy of the measured stresses (Accardi, 2008). Together with the preliminary analysis on mesh refinement carried out for the heat transfer implementation, also for this analysis different mesh were studied. In order to increase accuracy all the nodes in the heat transfer and in the expansion simulation were overlapped. Hence, the same distance between nodes was used in both mesh sensitivity analyses. The size of elements used were so 0.02, 0.05, 0.1 and 0.2 mm. No relevant change in the trend of the history of reaction force was observed. Hence, considering the value of reaction force obtained at end of relaxation and of peak (Table 5.3) and the results showed in Section 5.2.1.2, a size of elements of 0.1 mm was chosen. As a result, cartilage was discretised in 195 elements.

Number of element	Reaction Force at equilibrium [N]	Reaction Force at peak [N]
56	0.1361	0.3793
195	0.1362	0.3806
780	0.1364	0.3809
4950	0.1368	0.3809

***Table 5.3**: Comparison between the reaction force measured at the end of relaxation (equilibrium) and at peak for different meshes. The value were obtained with the same dimensions, material properties and boundary conditions, whereas the mesh was changed. Cartilage has a diameter of 3 mm and thickness of 1.319 mm. The material properties used are described in section 5.2.2.3.*

5.2.2.3 Material Properties

Cartilage is modelled as a transversely isotropic biphasic material, according to the good agreement between the reaction force measured experimentally and numerically under unconfined compression configuration (Cohen, et al., 1998; DiSilvestro, et al., 2001). Although this model can accurately reproduce reaction force measured on cartilage after compression, it cannot replicate simultaneously both reaction force and lateral displacement (DiSilvestro, et al., 2001). However, in this work the interest was focused only on the prediction of reaction force. Thus, I believe that a transversely isotropic model can be used during this analysis.

As explained in Section 3.2.3, only five independent parameters (E_L, E_T, G_L, ν_{LT} and ν_{TT}) has to be defined for the transversely isotropic materials. In these simulation, fibers were considered to be all aligned in the same direction, parallel to the articular surface (called longitudinal direction). The transversal Young's modulus (E_T) was measured from the experimental tests at the end of relaxation. Actually, when the reaction force equilibrium is reached in an unconfined compression relaxation test, only the mechanical properties of the solid matrix of articular cartilage are measured. The shear modulus in the longitudinal direction (G_L) was unknown, because no tests to acquire this value was performed. Thus, a value equal to 0.37 MPa was considered from experiments conducted in the literature (Accardi, 2008; Donzelli, et al., 1999). The other three parameters were obtained from the comparison between the numerical prediction of the reaction force and the one measured

from the experimental test expressly conducted. In order to allow a better agreement with the experimental data strain dependent permeability was added to the TI model. First, the permeability (k') defined in the biphasic model (Mow, et al., 1980), has to be converted to the form required by the commercial software ABAQUS (k), with the following equation (Abaqus; Wu, et al., 1998):

$$k = \gamma k', \tag{5.5}$$

where, the volume weight of interstitial fluid (γ) is equal to 9.881 x 10^{-6} Nmm^{-3}. Actually, the permeability is commonly expressed in m^4/Ns, whereas ABAQUS requires the permeability expressed in the units m/s to compute the solutions. Thus, the conversion of units, expressed in equation 5.5, must be done. The strain dependent permeability is then assigned in ABAQUS using the possibility to implement it as a tabular input of permeability and void ratio. The relationship between permeability and void ratio utilized is expressed by equation 3.9. Hence, three parameters are required (as defined in Chapter 3): k_0, M, e_0. The initial void ratio considered was 4.2; the initial permeability was measured from the comparison between the experimental test and the numerical implementation so as to consider the relevant value for each sample; the parameter M was taken from literature and a value of 4.638 was considered (Accardi, 2008; Holmes, et al., 1990). In order to determine the range of void ratio needed to be input into ABAQUS (e), void ratio variation with time was requested from the equivalent BLE model with linear permeability.

To analyze the transient swelling of articular cartilage and for a better comprehension of the mechanisms that induce this phenomenon, Li presented an easy and fast FE implementation of the tissue expansion after a change in concentration in PBS bath (Li, 2009). She validated it through a comparison with confined compression experimental tests and other numerical implementation on swelling taken from literature (Wu, et al., 2002). She also demonstrated that thermal analogy is valid in both confined compression and unconfined compression tests. Unfortunately, all the mechanical parameters were obtained from the literature. Comparisons with experimental tests carried out in this project have produced more accurate mechanical parameters.

As explained in Chapter 3, there are two mechanisms that cause radial expansion of cartilage when a change in concentration is imposed: (1) the osmotic expansion, caused by

the increase of osmotic pressure inside the tissue; (2) chemical expansion, due to the presence of repulsive forces between negative charged GAGs. Hence, also in the thermal analogy analysis swelling is split into two type of expansion: thermal expansion and fluid expansion. The former is the implementation in the thermal analogy analysis of chemical expansion. The following equations will be expressed in terms of temperature, but of course temperature indicates concentration in the real system, due to analogy between the thermal expansion and cartilage swelling because of the concentration change. The total strain (ε) inside the tissue caused by thermal expansion are given by the sum of the solid strain (ε_s) associated to mechanical loading and the thermal strain (ε_{th}) , as follows (Wu, et al., 2002):

$$\varepsilon = \varepsilon_s + \varepsilon_{th} = \varepsilon_s + \alpha \Delta T \boldsymbol{I} . \quad (5.6)$$

If the material is isotropic elastic, the thermal stress can be calculated from Hooke's Law as (Abaqus):

$$\sigma_{th} = E\varepsilon_{th} = \alpha E \Delta T, \quad (5.7)$$

where E is the Young's modulus of the isotropic elastic materials, ΔT indicates the temperature change and α is the thermal expansion coefficient. This coefficient is defined as follows (Li, 2009; Wu, et al., 2002):

$$\alpha = \frac{T_C}{E\Delta T} , \quad (5.8)$$

where T_c indicates the chemical expansion. Considering equation 3.36 (Eisemberg, et al., 1987) equation 5.8 becomes:

$$\alpha = \frac{\beta_o e^{T/c_\beta}}{E\Delta T}, \quad (5.9)$$

where β_0 and c_β are material constants, T is the current temperature within the tissue, whose distribution is computed in the diffusion implementation. ABAQUS allows a tabular input of equation 5.9 in terms of thermal expansion coefficient and temperature. The appropriate value of E for each AC sample was obtained directly from the experimental data set at the end of relaxation, whereas the two material constants (β_0 and c_β) were changed in each simulations in order to obtain the best correlation between the experimental reaction force and the predicted one with the FE analysis. Furthermore, the osmotic expansion is implemented in this analogy as fluid expansion. In this parallelism,

the increase in water content of articular cartilage due to an increase of osmotic pressure within the tissue is represented by the volumetric fluid expansion due to a change of temperature. The pore-fluid expansion coefficient is defined as (Li, 2009):

$$\alpha = \frac{\Delta\pi}{\Delta T}, \tag{5.10}$$

Where $\Delta\pi$ is the osmotic pressure gradient, given by equation 3.23. Equation 5.10 can be rewritten in terms of internal and external temperature:

$$\alpha = \frac{\Phi_{int} RTT_{int} - \Phi_{ext} RTT_{ext}}{\Delta T}, \tag{5.11}$$

where T_{int} represents the current temperature as measured during the diffusion implementation; T_{ext} is the temperature in the bathing solution; Φ_{int} and Φ_{ext} correspond to respectively the internal and external osmotic coefficient, in particular, Φ_{ext} is extracted from literature and a value of 0.924 was considered (Wilson, et al., 2005), whereas Φ_{int} is obtained from the comparison between the numerical simulations and the experimental data-set; R is the universal gas constant and its value is 8.31J/molK; T is the absolute temperature, considered to be 298K. A self-consistent set of units must be used for this model, as summarized in table 5.4.

Set of units

Dimensions of the model	m	mm
R	8.31 J/molK	8.21 x 10^{-6}mJ/nmolK
T	K	K
T_{int}	mM	mM
T_{ext}	mM	mM
β_0	mM	mM
c_β	mM	mM

***Table 5.4**: a consistent set of units to be used in the thermal analogy model.*

5.2.2.4 Boundary Conditions

Displacement in radial direction and rotations of the loading platen were set to zero, whereas along the axial direction, a displacement equivalent to the one applied during the experimental tests was imposed (Chapter 4). Besides, all displacements and rotations of the sustaining dish were fixed to zero. On cartilage, due to symmetry conditions, displacement in the direction perpendicular to surface lying alongside the axis of symmetry were constrained. The unconfined compression model has impermeable boundary conditions at the top and bottom surfaces of the tissue sample as no fluid exudation can occur through the impermeable loading platen and dish. Fluid flux was, instead, permitted in the lateral surface of AC by setting the fluid pressure to zero at that side.

In order to simulate cartilage expansion due to swelling, the definition of the temperature (representing ionic concentration) distribution is required. Thus, the value of temperature in each node at different time, computed in the previous analysis, is given in the stress analysis as a predefined field.

5.2.2.5 Contact Definitions

Compressive problem was defined as a *node-to-surface contact* between the rigid *master* surface of the loading platen and the sustaining dish and, respectively, the deformable AC *slave* upper and bottom surfaces. To avoid penetration, a contact of type *hard* was chosen between the *slaves* and *masters* surfaces. Instead, the contact in the longitudinal direction was implemented considering the presence of friction between the specimen and loading platens interfaces. A coefficient of friction of 0.1 was chosen (see section 6.2.1.2).

5.3 FE Implementation to Investigate Friction

To investigate the effect of friction on the reaction force history predicted using the biphasic models, implementations on the FE software ABAQUS and on FEBio were done. A first analysis was actuated on ABAQUS to use a 2D geometry in which the friction coefficient was changed so as to decrease the computational time needed to compute the solution. Afterwards, simulations with the software FEBio were done to investigate which alterations introduce friction in the numerical reaction force predicted with BNLE and TIMRBNLE models in comparison with the case without friction.

5.3.1 Geometry

The geometry used in the implementation in FEBio is similar to the one presented in Section 5.1.1, but in this case the materials to be examined are three to allow the analysis of friction: the loading platen, articular cartilage and the sustaining dish.

Cartilage and the loading platen were modelled as described in section 5.1.1. The *dish* was modelled as a cylinder. As for the loading platen, stresses and strain within this material are not interesting for this study, thus the dimensions considered are different from the real ones. A diameter of 5 mm and a thickness of 0.3 mm were considered.

Again, to decrease the computational burden, only a quarter of the total geometry was considered due to the symmetry.

The same geometry was used for the simulations in ABAQUS, but in axysymmetric configuration. In particular, the loading platen and dish were considered as analytical surfaces, i.e. considered much more rigid than cartilage. As a result, only articular cartilage can be deformed. The diameter of articular cartilage plugs was considered equal to 3 mm (constant for all the sample), whereas a value equal to 1.07 mm in thickness was chosen (dimension of one AC sample utilized for the unconfined compression test).

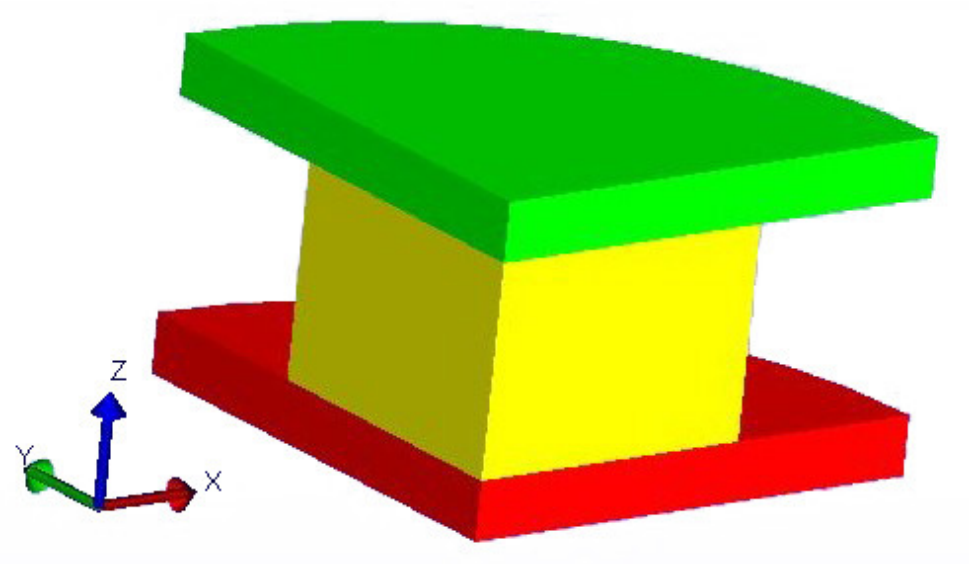

***Figure 5.6**: Simple three-dimensional geometry used in the FE implementation for the analysis of the effect of friction on biphasic materials. The dimensions are in [mm].*

5.3.2 Mesh

The type of mesh used in FEBio to implement this analysis is similar to the one described in section 5.1.2. Therefore, due to the large computational burden required by the implementation of friction in a three-dimensional geometry, a mesh with 640 elements was used to discretise the cartilage.

Instead, for the implementation in ABAQUS, the same mesh as the one summarized in Section 5.2.2.2 was used.

5.3.3 Material Properties

In FEBio the biphasic models used to reproduce cartilage were two: one isotropic (BNLE models) and the other one anisotropic (TIMRBNLE). The material parameters used are the same as the ones described in Section 5.1.3 to enable a comparison between the two simulations.

Moreover, the loading platen and the sustaining dish were modeled as a *rigid body*, thus, any material property was not required (Maas, et al., 2010).

Instead, in ABAQUS, only the material properties of the cartilage were assigned, because the loading platens and the sustaining dish were defined as *analytical rigid* surface. In order to improve the speed of simulation a BLE model was used to reproduce articular cartilage.

5.3.4 Boundary Conditions

The boundary conditions set for the analysis in FEBio are, again, the same as the one implemented for the comparison between different biphasic models. The dish was modelled as rigid body, with all the rotations and displacement constrained. Instead, for the loading platen all the displacement and rotation were set to zero, due to the symmetry of the material, except the displacement in the axial direction (z). In particular was imposed the same displacement applied in the step-wise unconfined compression relaxation test. On cartilage due to symmetry conditions, displacement was fixed in direction normal to the constrained surface. Fluid flux was permitted in the lateral surface of AC by setting the

fluid pressure to zero at that side, as happened in an unconfined compression tests with impermeable loading platen and dish.

In the simulations of ABAQUS the same boundary conditions described in Section 5.2.2.4 were set, without the definition of a temperature field.

5.3.5 Contact Definitions

The solution for the friction analysis with FEBio was obtained using the *sliding interface* contact with augmented Lagrangian method to avoid penetration (Maas, et al., 2010). The penalty factor used was the same used in the previous simulation, i.e. 10. With the BNLE model used to reproduce articular cartilage behavior in unconfined compression test a coefficient of friction of 0.1 was used. Instead, when the TIMRBNLE model was used a friction coefficient of 0.2 was implemented. As will be discussed in the following chapter, during this thesis work no experimental tests on friction were done. This coefficient is very hard to define because it is time-dependent, it changes with the type of solicitation and with the type of solution in which the sample is submerged. Thus, the friction coefficient is taken from the literature. This type of contact requires also the definition of the friction penalty factor. After preliminary simulations a coefficient of 10 was chosen. Compressive problem was defined as a *contact* between the rigid *master* surface of the loading platen and the deformable AC *slave* upper surface (Maas, et al., 2010).

Instead in ABAQUS, the same contacts as in the thermal analogy implementation (Section 5.2.2.5) were used, but the coefficient of friction was changed between 0 (frictionless interface) and 0.5.

5.4 FE Implementation to Investigate the Effect of *non-flat* Samples

FE implementation with the software FEBio was employed to investigate how much the use of an AC plug that is not perfectly flat influences the history of the reaction force predicted numerically.

During this analysis a BLE model was utilized to reproduce cartilage behaviour, due to the low computational burden required by this model. Mesh, material definition, boundary

condition and contacts were maintained constant during the analyses, only the orientation of articular cartilage plugs compared to the horizontal plane was changed.

5.4.1 Geometry

The modelled materials are two: the loading platen and articular cartilage. The supporting plate cartilage is not represented in order to decrease the number of nodes used in the model, and thus the computation burden. Actually, the entire geometry was considered (Figure 5.6). Cartilage was modeled as a cylinder with the same dimensions as one articular cartilage plug used for one experimental test. Thus, the considered diameter was of 3 mm whereas the thickness was 1.07 mm. To analyze the presence of slope in the superficial surface of AC plugs, cartilage was rotated with an angle between 0° (specimen completely flat) and 13°. The loading platen was also modelled as a cylinder, with a diameter of 5 mm and a thickness 0.3 mm.

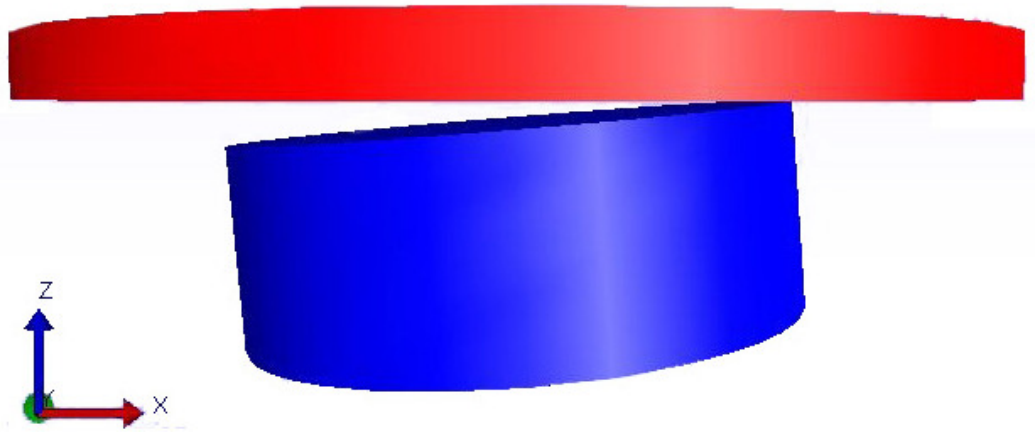

***Figure 5.6**: Simple three-dimensional geometry used in the FE implementation for the analysis of the effect of non-flat samples on the registered reaction force. The dimensions are in [mm].*

5.4.2 Mesh

No symmetry was considered, thus, a very fine mesh was not possible to be used due to the high computational time required. Therefore, a mesh with the same number of divisions and segments as the one used in section 5.3.1 was used to discretise the cartilage. 3D 8-node trilinear hexahedral brick elements were used (Maas, et al., 2010). The final mesh results in 2304 elements and 2986 nodes.

5.4.3 Material Properties

Cartilage was modelled as a poroelastic material with BLE model, because of its low computation burden required to compute the solutions. The material parameters applied to implement the BLE model are summarized in Table 5.5. Moreover, the loading platen was modeled as a *rigid body*, thus, any material property was not required (Maas, et al., 2010).

Material parameters	
E [MPa]	0.27
ν	0.1
k [mm^4/Ns]	0.04

***Table 5.5**: Material parameters of the BLE model obtained from a comparison between the measured reaction force and its numerical prediction.*

5.4.4 Boundary Conditions

All the displacements and rotations of the loading platen were set to zero, except the displacement in the axial direction (z) to apply the relaxation test on cartilage. In particular, was imposed a first step to allow the contact between the samples and the loading platens and then the same step-wise displacement employed in the unconfined compression experimental test. On the bottom surface of articular cartilage, displacement in all the direction (x, y and z) were set to zero, to fix in the space the AC plug. Fluid flux was permitted in the lateral surface of AC by setting the fluid pressure to zero at that side.

5.4.5 Contact Definitions

The solution was, again, obtained using the *sliding interface* contact with augmented Lagrangian method to avoid penetration (Maas, et al., 2010). The penalty factor used was the same used in the previous tests, i.e. 10. The interface between the loading platens and the articular cartilage was considered frictionless to reduce the computational time need to compute the solution. The bottom surface of the loading platen was defined as rigid *master* surface and deformable upper surface of AC as *slave*.

Chapter 6
Results

6.1 Experimental Results

6.1.1 Biphasic Models

From the step-wise unconfined compression relaxation test, it is possible to measure the Young's modulus of each bovine AC sample at the end of relaxation. Actually, at equilibrium, when all fluid flow has ceased, it is possible to consider the mechanical response of cartilage as composed by a single phase: the linearly elastic solid phase. Thus, the engineering constant E is easy to measure. The material property extracted from six samples (E = 0.22 ± 0.08 MPa), harvested from metacarpalphalyngeal joint of 7-day-old bovine calves, resulted to be lower than the values obtained from human cartilage in the literature. In general, elderly human articular cartilage has been found to be five times stiffer than adult bovine cartilage (Dèmarteau, et al., 2006), but exhibits the same deformation pattern (Brown, et al., 2009). Therefore, the parameters provided in this study, which have been derived for bovine tissue, can only be indicative of those that could be applied in the analyses of the human system. However, the aim of this study can be still achieved, because it is focused on the comparison between different biphasic models observing the historical pattern of the reaction force. The typical pattern of the reaction force measured in a step-wise unconfined compression test is shown in Figure 6.1.

6.1.2 Swelling Model

Six articular cartilage samples were tested, as described in Section 4.2.2, for a concentration transition from 0.154 M to 0.0154 M NaCl, with the sample thickness constrained to approximately 10% percent of its original value. After the addition of salt,

the load was observed to increase to an average of 40 % of its initial value, when the full thickness samples are considered (i.e. also the osteochondral bone layer is included in the samples). The measured load versus time for one sample is shown in Figure 6.2a.. Instead, if only the superficial layer are harvested from the full thickness articular cartilage, the measured equilibrium load attained in 0.0154 M NaCI was approximately 73 percent bigger than its value in 0.154 M NaCI (Figure 6.2b). According to Myers et al. (Myers, et al., 1984), the swelling of the tissue is smaller on the osteochondral bone layer, where the fiber are aligned, i.e. where the larger resistance of collagen network to swelling occurs.

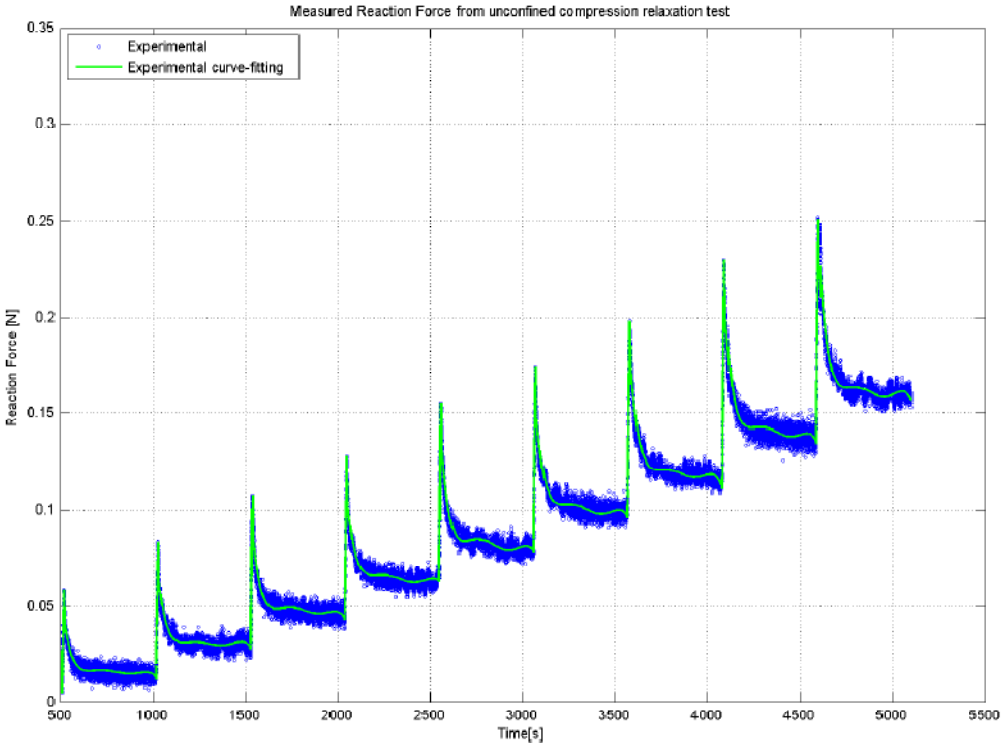

Figure 6.1*: Typical historical trend of the reaction force measured from the step-wise unconfined compression relaxation test described in chapter 4 . The reaction force is obtained from a full-thickness bovine AC sample with a diameter equal to 3mm and thickness equal to 1.07 mm. The experimental data set (blue) and its curve fit with a polynomial of 5 degrees (green) are shown.*

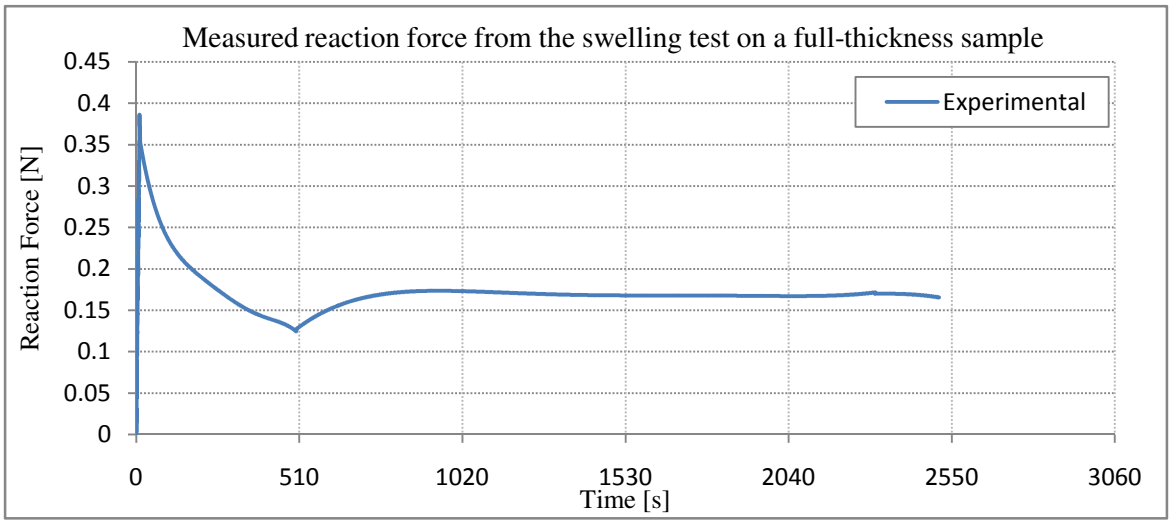

a)

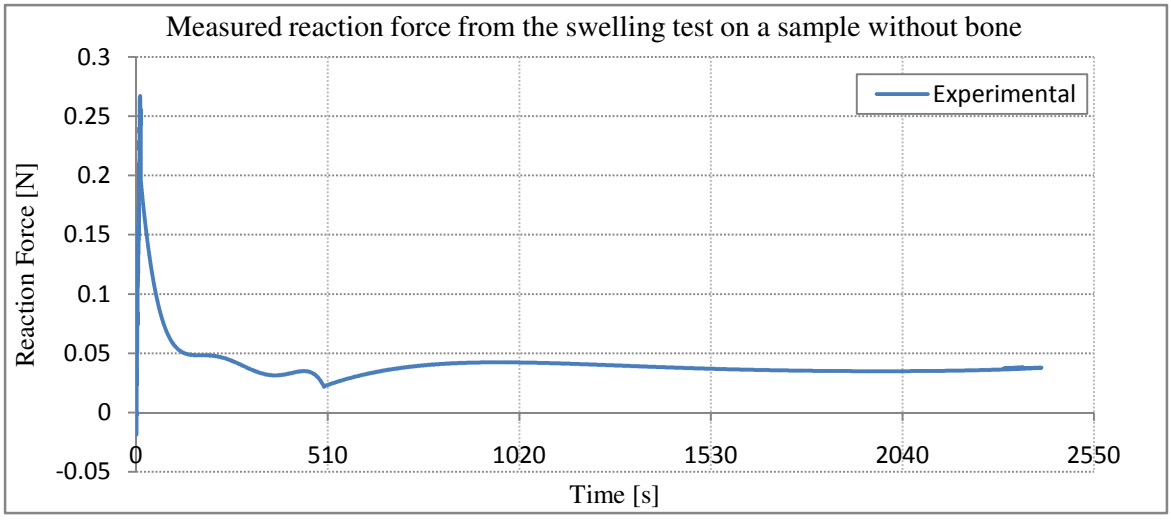

b)

Figure 6.2*: The figure shown the curve-fit of the reaction force measured from the unconfined compression relaxation test, where at 510s the PBS concentration was changed from 0.154MNaCl to 0.0154M NaCl. a) A full-thickness sample was tested, whose diameter was equal to 3 mm and thickness was 1.319 mm; b) no osteochondral bone was found in the AC plugs used in this test. The sample had the following dimensions: diameter of 3 mm and thickness of 0.539 mm.*

6.2 Finite Element Results

In the literature there are several models well validated to reproduce the mechanical behavior of articular cartilage during confined compression test, unconfined compression test and indentation test. In this chapter will be presented the biphasic models that were considered implementable using the information acquired from an unconfined compression

test. Besides a comparison will be described in order to analyze the differences of the predicted response of AC under unconfined compression test with different models.

Regarding the swelling models below will be presented the results obtained from the implementation of the thermal analogy models explained in the previous chapters.

6.2.1 Biphasic Models

6.2.1.1 Comparison Between Biphasic Models

The most simple and widely used biphasic model is the biphasic linear elastic model. In this model cartilage is modeled as composed of two phases: a linear elastic solid phase and a fluid phase. Even though the oversimplifications, this model is widely used due to the necessity of only three parameter to be defined (E, ν and k) and because the computational time requested to obtain the solution is very low. The easiness to implement it and the low computational burden, make this model the most used biphasic model in complex numerical simulation of joint.

In some FE implementations of the whole articulating knee joint, articular cartilage has been modeled as linear elastic (Li, et al., 1999; Plochocki, et al., 2009; Weiss, et al., 1996). This model allows a faster and easier FE analysis of the knee joint, however, it can adequately predict the mechanical response of cartilage only at the instant of load application when no fluid flows and at equilibrium, when the fluid flow has ceased. Thus, in order to reproduce more accurately AC response under mechanical loading, the time-dependent behavior of cartilage, due to the presence of the fluid phase, is required (Goldsmith, et al., 1996). Hence, the biphasic models resulted to be more accurate. However, this model cannot describe thoroughly the complex response of cartilage in compression, due to the numerous oversimplifications. First, the change in permeability with deformation due to the reduction of pores dimensions, is ignored (Mow, et al., 1980). This last lack could be overcome using the biphasic non linear elastic model, where the exponential change of permeability with deformation is implemented using equation 3.8 or 3.9 of Chapter 3, depending on the finite element software used. The comparison between the two models is shown in Figure 6.3. The instantaneous reaction force registered at the peak is larger for the BNLE model than for the BLE model. Actually, in the former one the permeability decreased exponentially with deformation, whereas in a BLE model the

permeability is maintained constant at the maximum value. Thus, the value of permeability in the biphasic linear model is greatly overestimated. As a result, AC relaxation is faster in the case of the BLE model due to a faster exudation of fluid out from the cartilage.

In conclusion, in a BLE model the permeability is overestimated, in particular this overestimation became bigger in case of large strain (Figure 6.3b) respect the case of small strain (Figure 6.3a). Consequently the BLE model is suggested only in case of small strain.

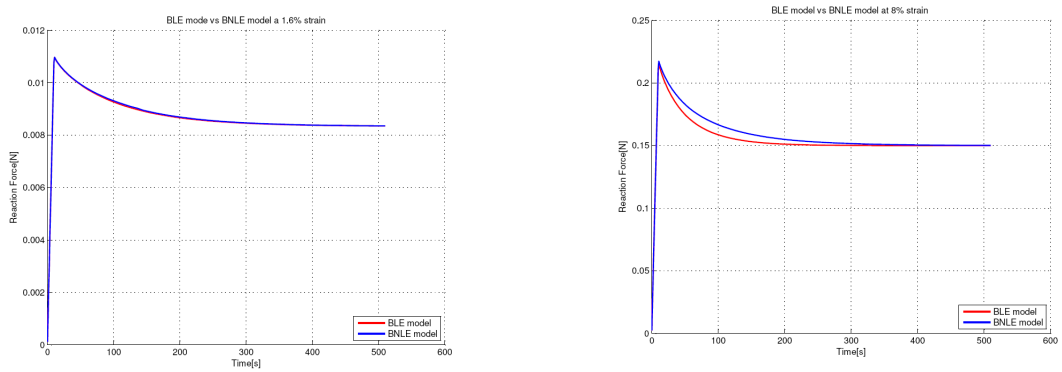

a) ***b)***

Figure 6.3: *Comparison between the history force obtained with the FE implementation of the BLE and BNLE models.* ***a)*** *A strain of 1.6% is implemented in the FE model;* ***b)*** *the applied strain is of 8%.*

Although the non-linearity due to the change of permeability with strain is considered, in a BNLE model, numerous inconsistencies with the structure and mechanical properties of articular cartilage still persist. Actually, the solid matrix is linear elastic and isotropic, thus, the model cannot describe the effect of anisotropy, inhomogeneity and viscoelasticity of the cartilage on the response of the tissue.

To avoid the discrepancy of anisotropy of the tissue a transversely isotropic biphasic model can be used. Essentially, a TIBLE model can well reproduce the indentation test, confined compression test and also the unconfined compression test, unlike both BLE and BNLE models (Cohen, et al., 1998; Li, et al., 1999). In particular, in the latter type of test, due to the radial expansion of the tissue under unconfined compression, the collagen fibers

are in tension and so the solid matrix in this direction is stiffer than in the transversal one. With a TI model it is easy to reproduce this mechanical behaviour, considering that the Young modulus is larger in the longitudinal direction than in the transversal one. However, DiSilvestro et al. (DiSilvestro, et al., 2001) provide that although TIBLE model can either reproduce the measured reaction force and lateral displacement, it is not able to account for both the variable simultaneously. Besides, this model has other disadvantages: the fibers are considered parallel to the articular surface and changes in orientation with depth are not taken into account; collagen fibers tension-compression non linearity is not assumed; the TIBLE models require seven independent parameters (five elastic constants and two permeability coefficients) that are not easy to find experimentally. Some of these disadvantages could be avoided using a transversely-isotropic Mooney-Rivlin biphasic model. In this model the tissue is described as composed by three phases: an isotropic matrix representing PGs; the fiber family corresponding to the collagen network and the fluid phase. The isotropic matrix is modeled using Mooney-Rivlin hyperelastic strain energy (equation 3.16). Considering C_2 equal to zero only two parameters are necessary, C_1 and K, that could be derived only knowing two engineering constants (as explained in Chapter 5): E and ν. To describe the *fluid-dependent* viscoelasticity, in case of constant permeability, only one additional parameter (k) has to be defined, otherwise if the Holmes-Mow permeability is considered (equation 3.8), other three parameters must be defined (φ_0, α and M). A further increase in the number of parameters required is added by the presence of fiber. Actually, another four parameters must be defined to fully describe the constitutive equation for the fibers. A big disadvantage is, thus, the number of parameters required (seven) to characterize the material, many more than the biphasic linear elastic (only three parameters). However, the increase in the ratio from peak to equilibrium using the TIMRBLE model than with the BLE and BNLE models (Figure 6.4) can justify the increase in the parameters required. As described above this improvement is due to the presence of the fibers that resist in tension during the unconfined compression test. Another advantage from the biphasic linear elastic model is due to how the constitutive equation for the fiber is defined (equation 3.19). Actually, the fibers are considered to resist only in traction, because of the buckling during compression. Besides, the relation between stress and strain is exponential, taking into account the realignment theory. Actually. due to the structure of the fibers, they present a toe-region, where the fibers are

not aligned and stretched yet. Once them are perfectly aligned and stretched, the traction strength increase and the fibers start to resist in traction.

In literature fiber reinforced models are well validated and widely used. Unfortunately, the definition of the preferred fibers orientations, generally, requires the selection of all the nodes one by one. This is going to be time consuming for the user. It is easy to understand how the application of this model is even more unlikely, for investigation on the whole knee joint. Instead, in the TIMRBLE model, the initial orientation of the fiber family on the software FEBio is easy to define. Actually, the fibers orientation can be specified by a vector in the space or by local node numbering. The software Preview allows the definition of the orientation for each element, thus, it is possible to vary this vector with throughout the different layers of AC, in order to consider the depth inohomogeneity of the tissue. Therefore, this is another advantage of the TIMRBLE model in comparison with the BLE and its extension to the strain-dependent permeability and TIBLE model.

As will be described better below, one disadvantage of this model is that the collagen network is represented with a single preferred fiber direction. This is far from the real structure of collagen network in articular cartilage, thus, this model cannot entirely predict all the experimental loading described in literature. Besides, inside the cartilage not only cartilage of type II exists, but also collagen of type IX and XI, and they both have an important role in the integrity of the cartilage.

This thesis work is part of a larger project on the analysis of a FE knee joint model. Thus, the objective of this study is the search of a model that is accurate in the reproduction of the response of articular cartilage, but at the same fast in the computation of the results. From the point of view of the computational speed of course the BLE model is the faster between the biphasic models. However, the computational time does not increase very much in comparison with the BNLE and TIBLE model. Instead, BLE model is much more faster than the TIMRBNLE model due to the lower futures of composition and structure of AC included. Hence, one should always try to use the simplest model that is sufficient to obtain the required data.

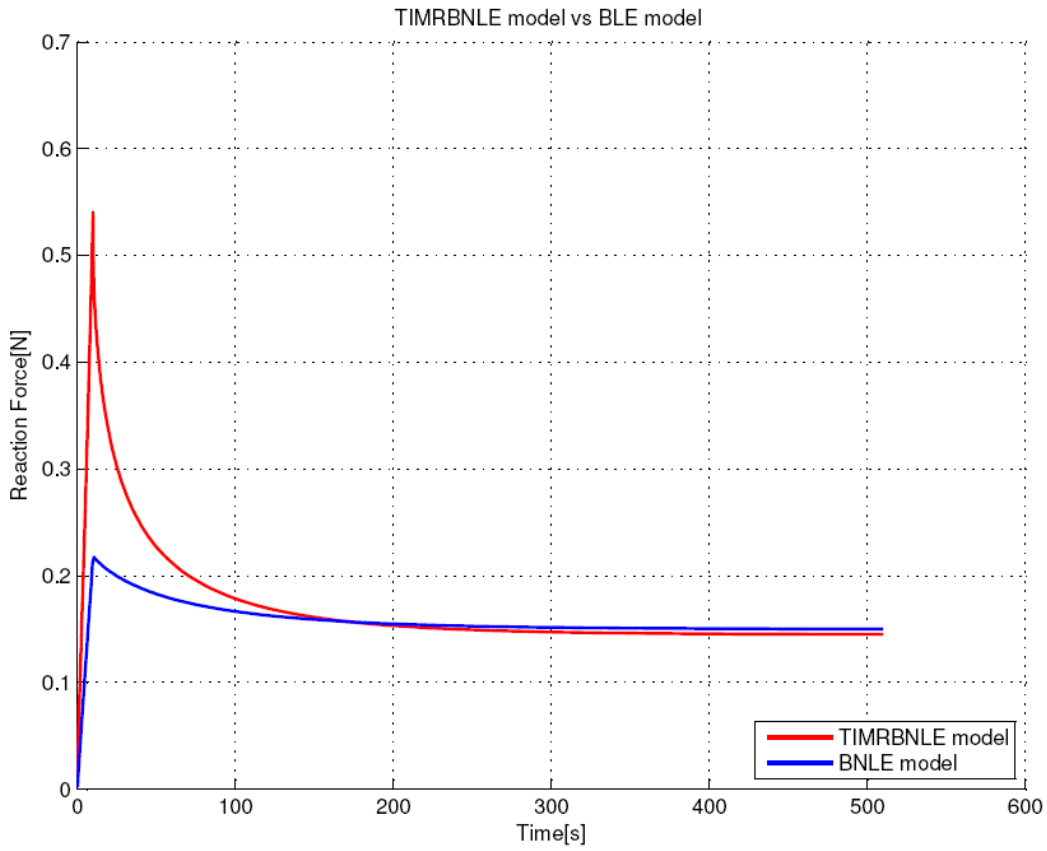

***Figure 6.4**: Comparison between the history of the reaction force obtained from the FE implementation of the BNLE and TIMRBNLE models, under strain of 8% during unconfined compression test.*

Here, a comparison between each model used in literature was done. At the end of this chapter a comparison between each model and the experimental data obtained from the unconfined compression test will be explained.

6.2.1.2 Effect of Friction on the Predicted Reaction Force

Is well known that cartilage has very good lubricant properties, however, when it is in contact with non lubricant material (for example, stainless steel) without the presence of a lubricant fluid (as the synovial fluid), friction between its surfaces and the loading indenter cannot be neglected. Thus, friction has to be considered also in FE implementation to improve the agreement between experimental tests and numerical simulations. Traditionally, the effect of friction between the samples and the loading indenter under unconfined compression tests was considered negligible, so as the material properties can be obtained curve-fitting the analytical model to the experimental data. Actually, in presence of friction the samples are compressed in a not uniform stress/strain state (Wu, et

al., 2004). However, even in ideally controlled experimental conditions, the friction in the specimen/platen interface in unconfined compression cannot be completely eliminated and friction is also needed to hold the specimens in place during the unconfined compression test. Consequently, the mechanical behavior of biomaterial, as observed via traditional unconfined compression tests, is influenced by the friction between the specimen and the platens (Wu, et al., 2003; Wu, et al., 2004). Spilker et al. (Spilker, et al., 1990) observed that the effect of friction varies with the samples aspect ratios: in specimens with a large aspect ratios (diameter/height = 3.57) friction effect is significant. Indeed, in this work all the samples have a large aspect ratio, thus, again, friction cannot be neglected.

However, due to the dimension of the specimens, it is hard to find experimentally a satisfactory friction coefficient. Besides, this coefficient change with time during pin-on-disc cyclic shear loading (Katta, et al., 2008) and also it depends on the applied loading. Actually it is observed that the friction coefficient could vary from a minimum value of 0.005 (± 0.003) to 0.153 (± 0.033) under static loading (Krishnan, et al., 2005). The authors proposed that this change might be due to the biphasic nature of AC. Basically, the presence of the fluid and his hydrostatic pressure influence the lubrication between the indenter and the specimens. When the load is transferred from the solid matrix to the fluid phase, the latter is able to reduce the coefficient of friction (Krishnan, et al., 2005). In addition, an increase in the applied load could reduce the minimum friction coefficient (Ateshian, et al., 2003).

Friction coefficient change not only with time and type of loading, but also with the bathing solution used to perform the compressive tests. Theoretical prediction demonstrated that increasing the concentration of the bathing solution reduces the minimum friction coefficient that can be reached, relative to its equilibrium value (Ateshian, et al., 2003).

Therefore, the dependence of friction coefficient to all these parameters cause difficulties in the identification of an accurate value to be included in the simulations. In this work for simplicity, medium values of 0.1 or 0.2 were chosen, according to the results obtained from previous work, changing the PBS solution (Ateshian, et al., 2003) and the loading protocol (Krishnan, et al., 2005). However, further analysis on this value will be necessary.

In the previous section was analyzed the lack of the biphasic model presented to reproduce the high ratio from peak to equilibrium, typical of AC samples under unconfined compression tests. This lack could be overcome considering friction, as can be seen in Figures 6.6 and 6.18. Goldsmith et al. (Goldsmith, et al., 1996) observed that the mismatch between the analytical solution and experimental tests were due to friction that was commonly neglected. As can be seen from Figure 6.5 and 6.6, the presence of interfacial friction was found to increase the peak and, at the same time, decrease the value at equilibrium of reaction force. Thus, a greater ratio from peak to equilibrium was found.

Besides, if the material properties of articular cartilage are obtained from a curve-fit between the experimental data and the numerical implementation without friction, the resulting material parameters are different from the real one. For example, if the BLE model is used (Figure 6.5), the curve-fitting between the numerical model without friction and the experimental test generate lower value of the Young's modulus (although the difference is small) and higher value of the permeability coefficient than the real mechanical properties. Probably for this reason, in the literature are reported higher values of permeability measured with numerical simulations than from permeation studies (Boschetti, et al., 2006).

Because of friction could not be neglected during the experimental test, in this analysis, friction between the specimens and indenter as well as between samples and sustaining dish were considered, but the material properties were obtained from the frictionless case, to decrease the computational time. Once, the material properties were obtained friction was added. Thus, in cases with friction it might be possible an overestimation of stress.

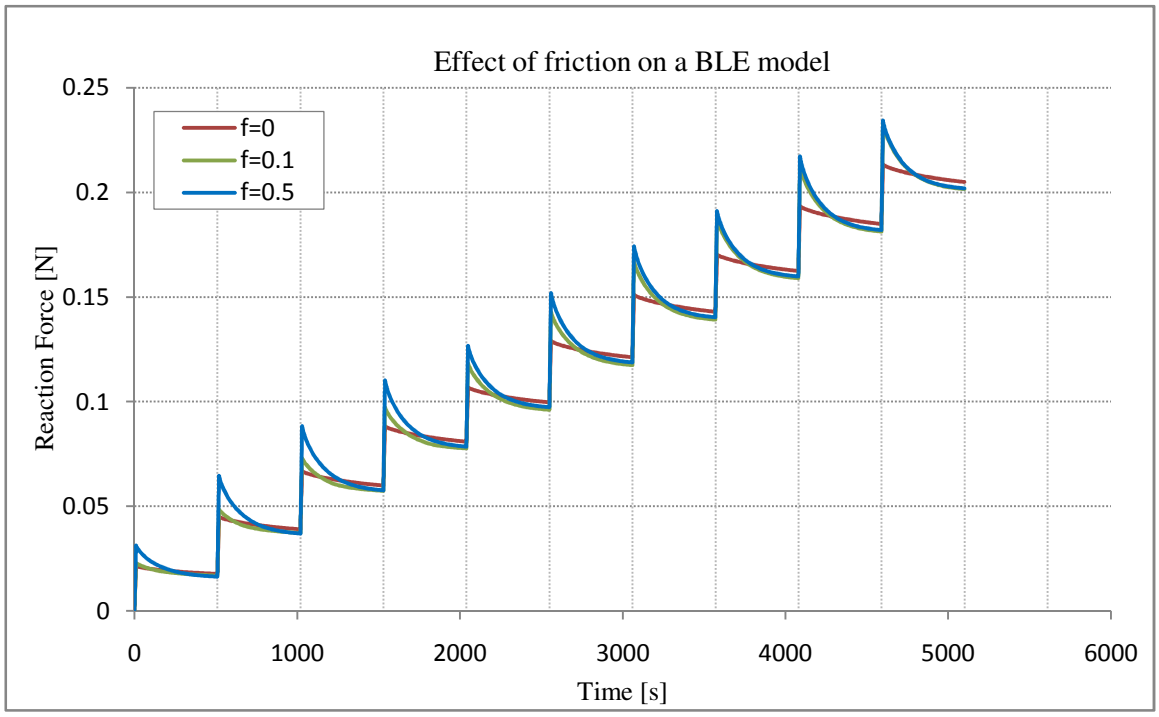

***Figure 6.5**: Numerical prediction of the reaction force obtained using a BLE model. Increasing the friction coefficient (f) the ratio from peak to equilibrium of the force increases.*

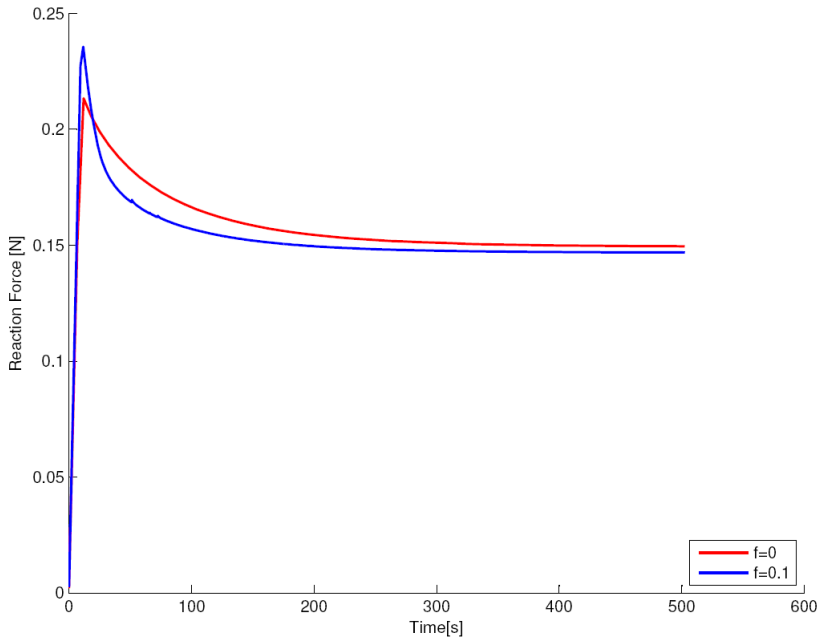

***Figure 6.6**: Comparison between the history of the reaction force obtained implementing the BNLE model without friction between the sample and the indenter and implementing the effect of friction (f=0.1). The relaxation increase adding friction.*

6.2.1.3 Effect of *non-flat* Samples on the Predicted Reaction Force

Another problem that can influence the measured mechanical properties is the presence of a slope between the specimen and the loading platens (Figure 6.7). Actually, if the sample is not flat, a discrepancy between analytical solution and experimental tests can occur, because for non-flat samples, the cross-section area, on which the load is applied, increase at each step. As a result, the reaction force observed increase non linearly with time and it also resulted to be smaller than the one measured for a flat specimens because the displacement is applied only on a little area of the articular surface. Furthermore, the initial peak is also much smaller when there is a smaller contact area (Figure 6.8).

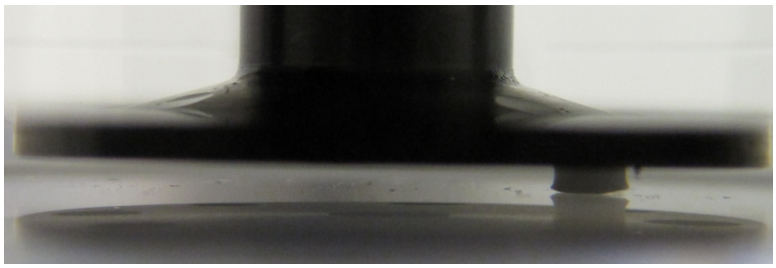

Figure 6.7*: Picture taken during the unconfined compression test to study swelling. In this photo the presence of non flat sample is clear. In this case not all the inferior surface is in contact with the sustaining dish producing a change of the cross-section area during the step-wise experimental test.*

Probably due to this problem, as well as the intrinsic non linearity of AC, the mechanical properties measured at the end of relaxation change at each step. Thus, one of the main problem observed and still unanswered is the necessity of flat samples.

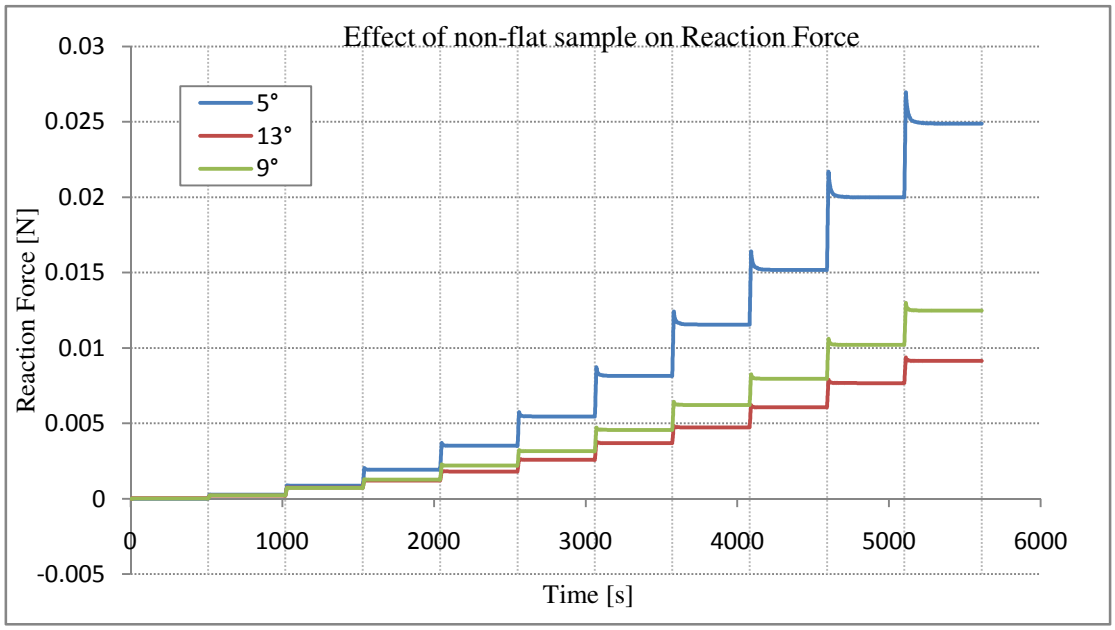

***Figure 6.8**: Numerical prediction of the reaction force obtained for non flat samples. The angle between the superficial surface of cartilage and the indenter was changed from 13° to 5°. If the sample is not flat the reaction force registered will be smaller and a non-linearity is registered that is not due to intrinsic property of cartilage, but is an error introduced by the user.*

6.2.2 Swelling Model

As already explained in Chapters 3, there are two mechanisms that cause swelling in cartilage: (1) the excess of mobile ions produce an increase in the osmotic pressure inside the tissue, called osmotic expansion; (2) repulsive forces between negative charges of GAGs, bounded to PGs, that produce a chemical expansion. FEM models could be useful for a better comprehension of the effect of swelling inside the tissue, actually is possible to consider the two mechanisms individually, as presented below.

6.2.2.1 Fluid Expansion

The response of the tissue due to the change in osmotic pressure under a change in concentration is shown in Figure 6.9. At 500s the external concentration was changed from the physiological value (0.154M NaCl) to a hypotonic one (0.0154M NaCl). The time for the change in concentration was considered 120s. The reaction force history measured is bimodal: the force initially rose sharply and then relaxed slowly until equilibrium. Indeed, due to concentration drop in the bathing solution, the osmotic pressure inside the

tissue increase, producing an inflow of solution inside the tissue (swelling). As a results, the isometric reaction force requested to maintain the tissue under isometric condition rises up. This increment is, then, followed by a decrease in reaction force because of the exudation of fluid, once the equilibrium in concentration is reached (Myers, et al., 1984).

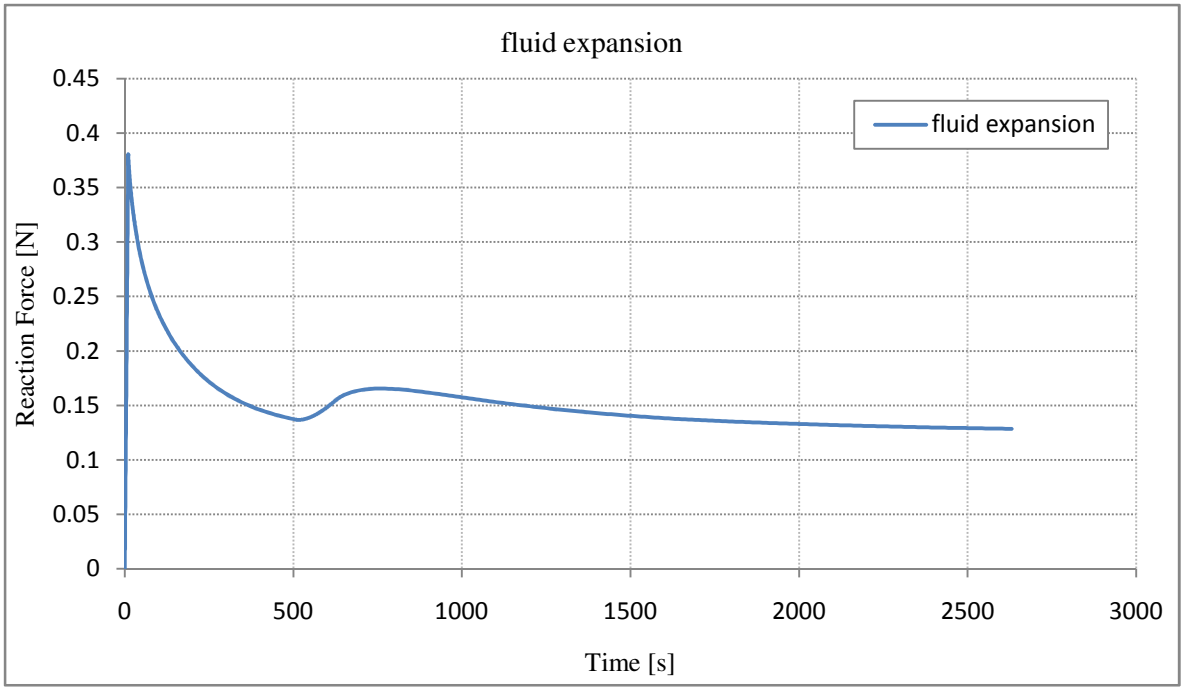

Figure 6.9: *Numerical prediction of the reaction force versus time registered due to the osmotic expansion under a change of salt concentration. The concentration was changed from 0.15M to 0.015M (hypotonic solution) obtained with α=-2E-4 1/°C, inducing swelling.*

6.2.2.2 Chemical Expansion

Figure 6.10 could be useful for a better comprehension of the mechanisms that occur inside the cartilage due to the repulsion between the negative charge of GAGs. Essentially, the reaction force after the change in concentration increase gradually until equilibrium is reached. This rose depends on the diffusion of Na^+ outside the tissue, so as to respect the electro-neutrality's law in the bathing solution. In fact, more and more cations diffuse out from the AC, more and more the repulsive force between negative charges increase. As a result, the isometric reaction force, needed to maintain the tissue with a fixed thickness, increase.

Beside, chemical expansion is useful to describe the change of stiffness of articular cartilage, with concentration. Compressive loading experiments on immature bovine

cartilage showed that the increase of concentration of the bathing solution, from 0.015M to 2M NaCl, produced a softer stress/strain response (Chahine, et al., 2004). Thus, transition of the concentration of PBS solution from 0.15M to 0.015M NaCl produce an increase in AC stiffness.

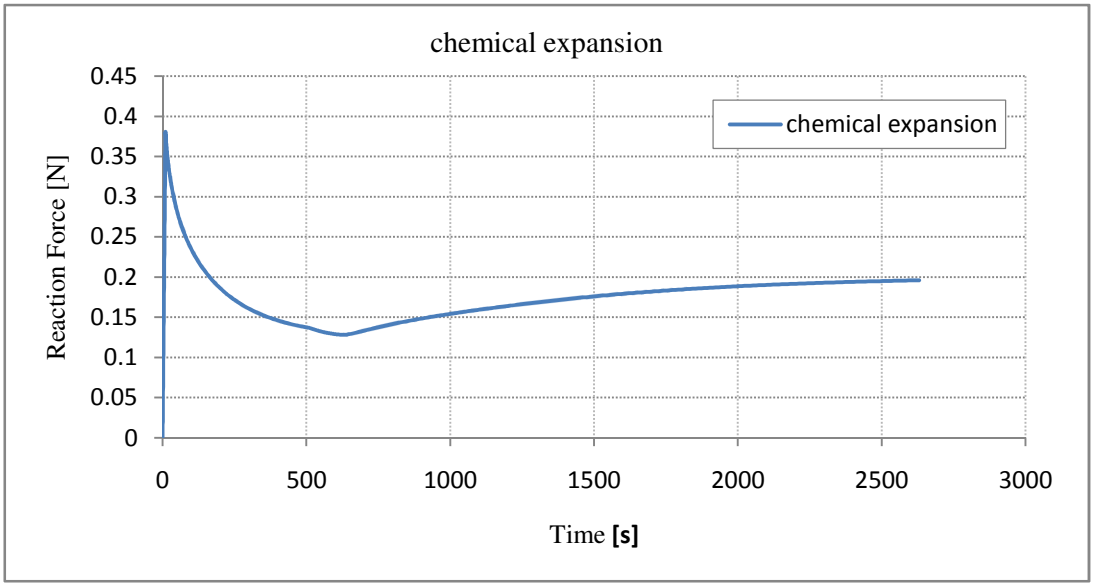

Figure 6.10: *Numerical prediction of the reaction force registered under a change of salt concentration from 0.15 to 0.015M due to charge-to-charge repulsion. The parameter used to obtain it are* β_0*=32kPa and* c_β*=10mM.*

6.2.2.3 Fluid and Chemical Expansion

A typical history of the force registered in the case both causes of swelling are considered, is shown in Figure 6.11. From the comparison with osmotic expansion and chemical expansion, it is easy to understand how the osmotic expansion affects the swelling during the first minutes, while chemical expansion influences the value of force obtained at equilibrium. It is easy to understand that the net reaction force is governed by osmotic expansion in case its coefficient is larger than the one obtained for the chemical expansion, while is the chemical expansion that affects the total force when the osmotic pressure goes to equilibrium (Wilson, 2005). From experimental tests was observed that the expansion coefficient of the two mechanism in an hypotonic solution has the same magnitude. The real reaction force resulting is, thus, similar to the one presented in Figure 6.11.

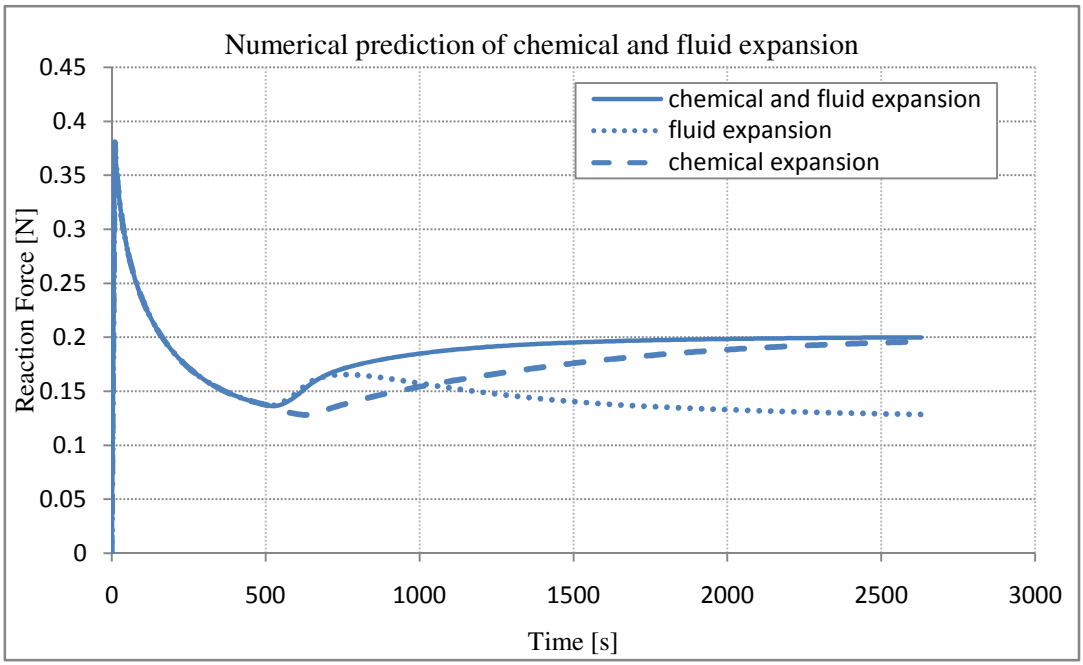

Figure 6.11: *Numerical prediction of the history of the reaction force registered under a decrease of concentration in the external bath due to either osmotic expansion, either chemical expansion and both the causes of swelling. The parameter used are β_0=32kPa and c_β=10mM for the chemical expansion, while for the fluid expansion a value of 2e-4 1/°C is used.*

6.3 Comparison Between Experimental Tests and Finite Element Models

6.3.1 Biphasic Models

In Section 6.2.1 a review on the comparison between some biphasic models was done, to understand which model is preferable to reproduce articular cartilage. From this review resulted that the more features of the composition are included, the more the structure of AC is reproduced, but the larger the number of material parameters that must be determined, and the more computationally expensive the model becomes. Hence, the requirements of a material model are highly dependent on the research question, in order to use the simplest and at the same time faster model to reproduce the mechanical behavior of the tissue. Below the comparison with the experimental data is shown, to help the choice of the more accurate biphasic model in reproducing the reaction force under unconfined compression test.

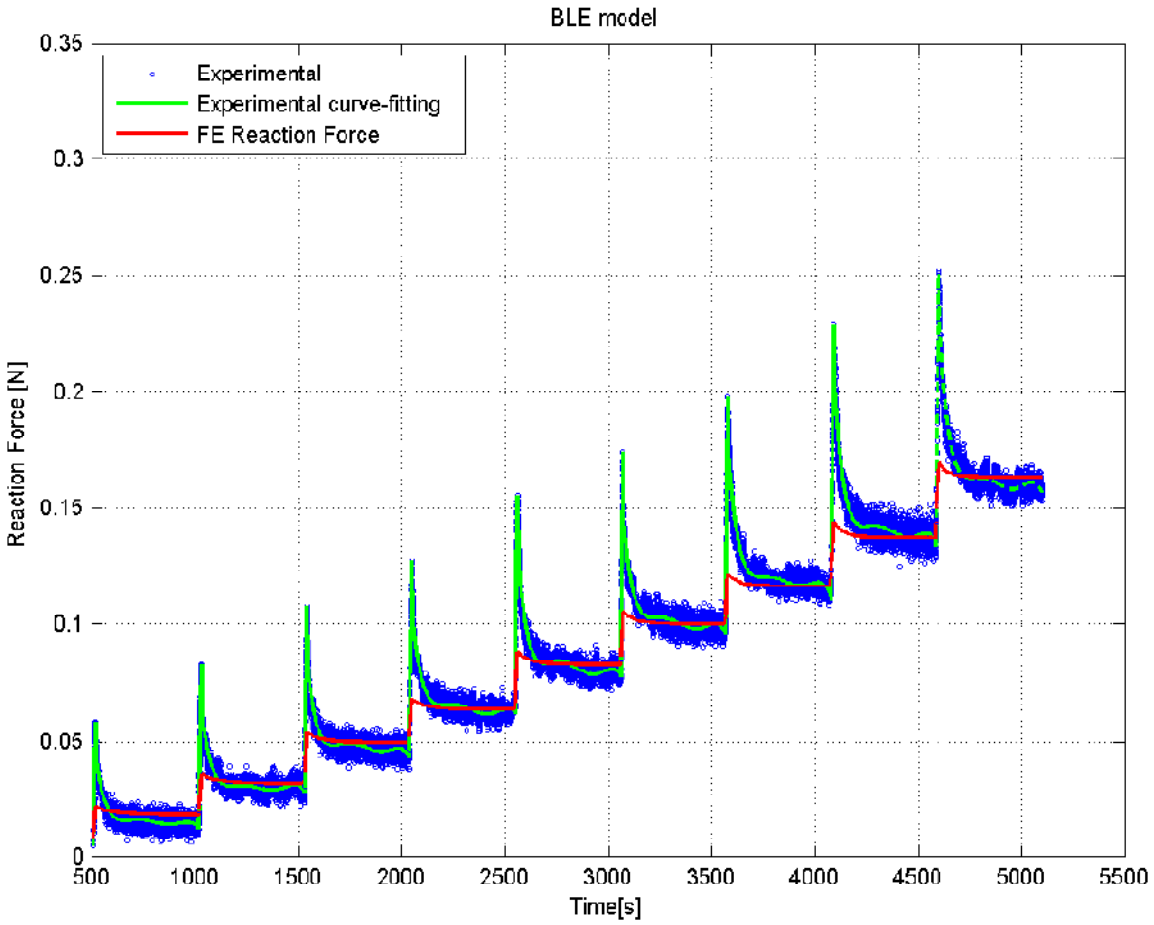

Figure 6.12: *Comparison between the reaction force obtained from the experimental data (blue) and its curve-fitting with a polynomial of 5th degrees (green) with a the numerical prediction obtained implementing the three-dimensional BLE model (red) in FEBio.*

The most widely used model to reproduce AC behavior is the BLE model. As explained above this model is very simple to use, actually it requires only three parameters (E, ν and k). From the unconfined compression test is possible to obtain the value of Young's modules, whereas the other material properties can be easily obtained from a curve-fit with the experimental data. Otherwise, other mechanical test can be applied to measure these parameters, for example a permeation study to investigate permeability or an optical analysis to measure the Poisson's coefficient. Although very fast and very simple in the implementation from the point of view of parameters needed, this model cannot reproduce the high ratio from peak to equilibrium of the force (Figure 6.12), as it is measured in the experimental tests. This means that the modeling of articular cartilage as composed by only two phases (solid and fluid), although can describe the time-dependent relaxation, is not

enough to accurately describe all the possible response of AC under different loading condition.

As mentioned above, the use of a transversely isotropic anisotropy can increase the relaxation of the reaction force, but as can be seen from Figure 6.13, the addition of one family of fiber to reproduce the anisotropy of AC is still not enough. Actually, the TIMRBNLE model cannot fully reproduce the reaction force obtained from the unconfined compression test. Ateshian et al. (Ateshian, 2007; Ateshian, et al., 2009) suggested that the use of a few discrete fiber bundles cannot fully reproduce all the mechanical test that can be done on cartilage. The same conclusion is suggested by other works where discrete fibers models that use more than three orthogonal family of fiber where used (Wilson, 2005; Julkunen, 2008). To prove these results, the random fiber model presented by Ateshian (Ateshian, 2007) was implemented in FEBio. Briefly, this model describes articular cartilage as composed of the solid matrix, the collagen network and the fluid phase. In particular, the former is implemented through the Mooney-Rivlin hyperelasticity constitutive relation, like the TIMRBLE model, but a more detailed representation of the structure of collagen network is, hence, done. Actually, the fibrillar matrix is described using a continuum fiber distribution, taking into account that the fibers can only support traction. The fiber constitutive relation used is a power-law, in order to implement the simplest relation that may capture the experimental response of cartilage, whereas the fibers are randomly distributed in the space. As can be seen from Figure 6.14 the continuum angular distribution model can actually reproduce better the high relaxation of cartilage. However, this model resulted to be computationally very expensive, thus, the application of this model in a knee joint model is not suggested. Therefore, in this work the random fiber material parameters needed to reproduce articular cartilage behavior in unconfined compression, were obtained only for one step.

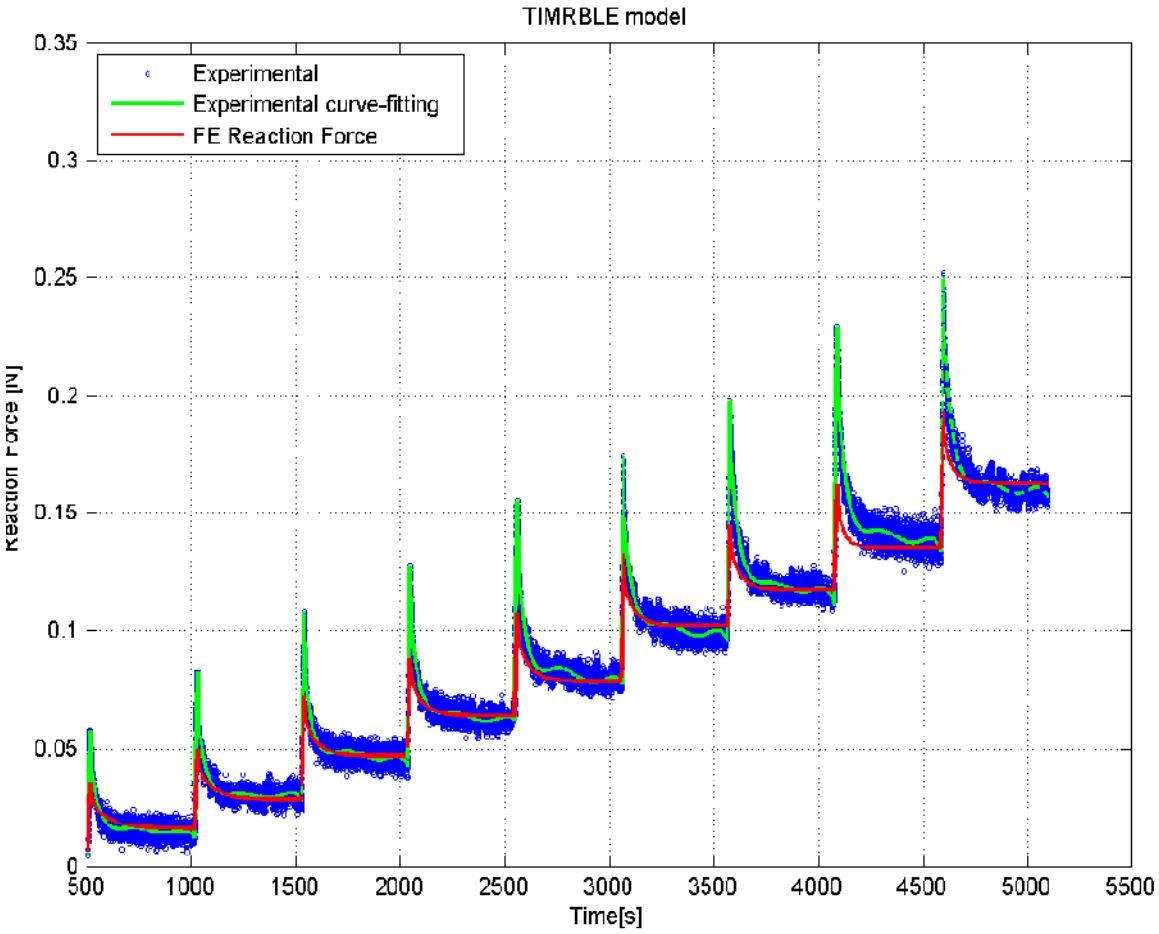

Figure 6.13: *Comparison between the reaction force obtained from the experimental data (blue) and its curve-fitting with a polynomial of 5^{th} degrees (green) with a the numerical prediction obtained implementing the three-dimensional TIMRBLE model (red) in the FEM FEBio.*

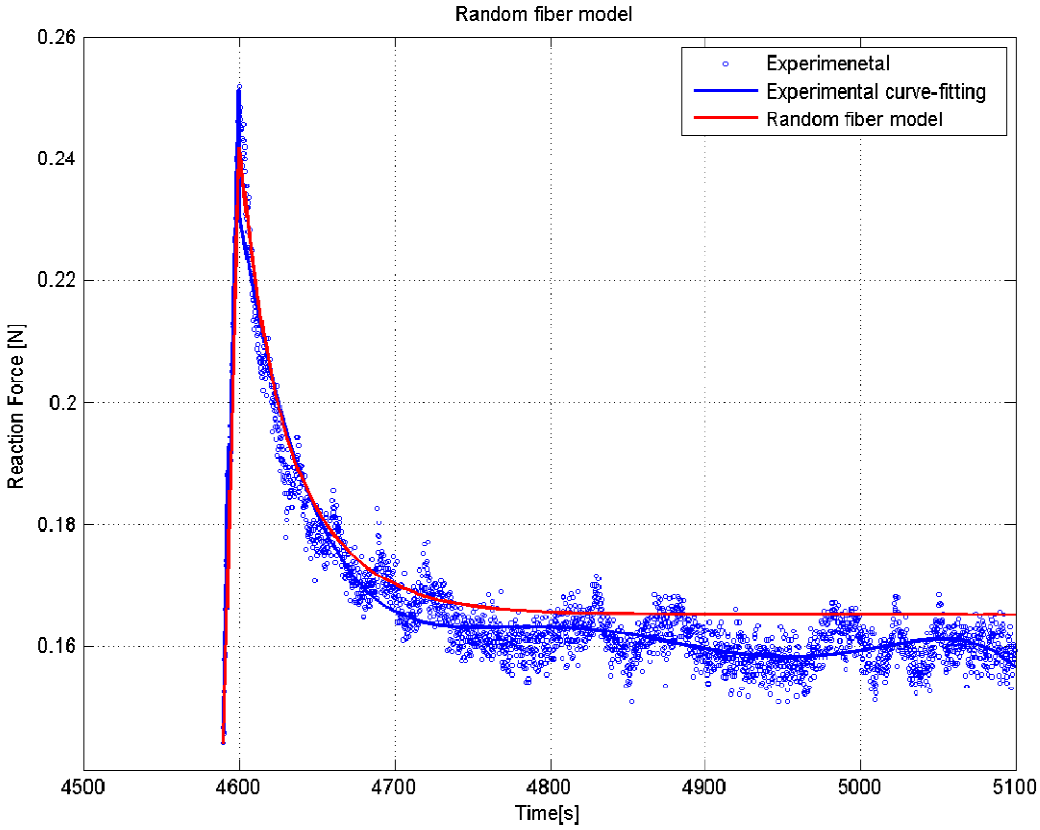

Figure 6.14: *Comparison between the reaction force obtained from the experimental data (blue) and its curve-fitting with a polynomial of 5th degrees with a the numerical prediction obtained implementing the three-dimensional random fiber model (red) in the FEM FEBio. In this figure is showed only the 10th step (i.e 8% strain) under the step-wise unconfined compression.*

a) *b)*

Figure 6.15: *In this figure is shown the difference between the collagen architecture of human (a) and bovine (b) cartilage. The images of both samples represent the orientation (OR) distribution of collagen network obtained from polarized light microscopy (on the left) and spatial T2 distribution from magnetic resonance imaging (in the middle). On the right there are illustrations showing the collagen arrangement for a better comprehension. (Adapted from Julkunen, 2008)*

The use of imaging techniques such as polarized light microscopy or magnetic resonance imaging (MRI) may be useful to investigate the arrangement of collagen fibers. From studies with these techniques can be observed that the collagen fibers in bovine cartilage are randomly arranged in many layers (Figure 6.15). Therefore, a distribution of fibers with a preferred orientation and the description of the collagen network with only one family of fibers, is considered not appropriate to adequately describe the whole structure of collagen (Julkunen, 2008). Probably, TIMRBLE model can predict more accurately the reaction force obtained with an unconfined compression test on human cartilage, due to the higher level of alignment of fiber in each layer in human cartilage than in the bovine one.

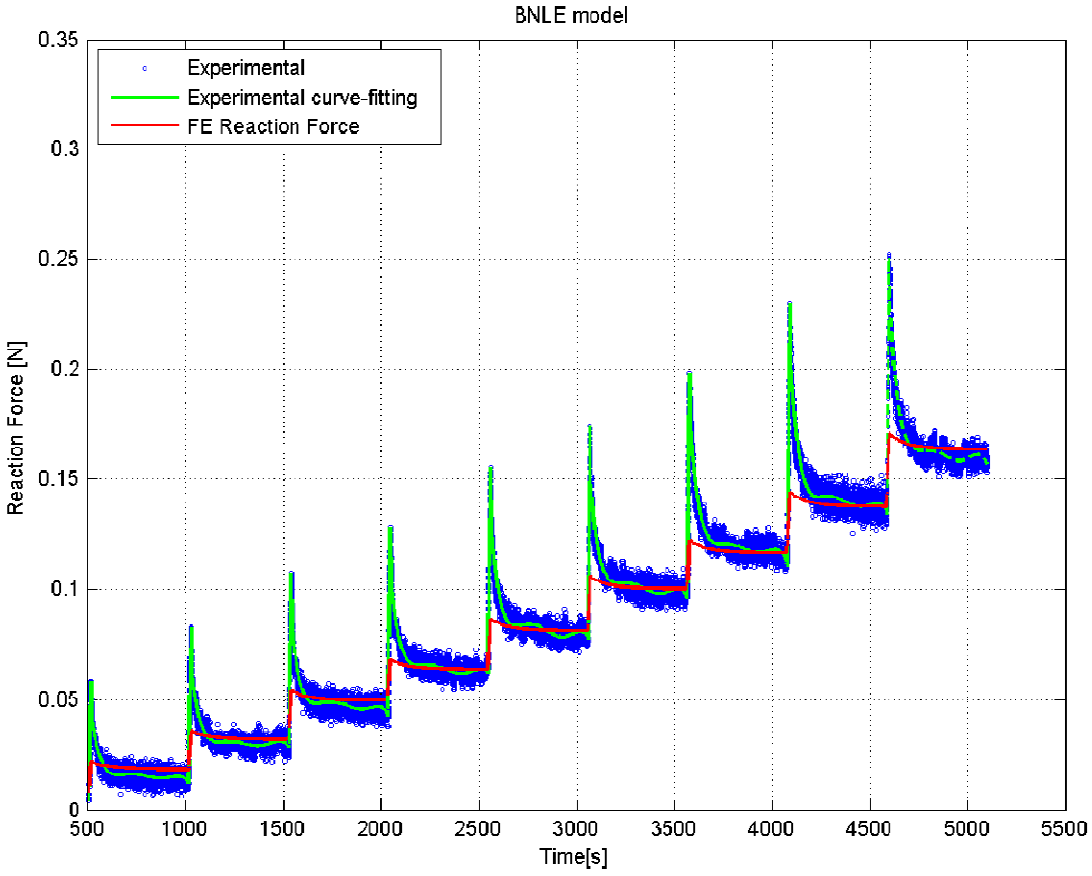

Figure 6.16: *Comparison between the reaction force obtained from the experimental data (blue) and its curve-fitting with a polynomial of 5th degrees (green) with a the numerical prediction obtained implementing the three-dimensional BNLE model (red) in the FEM FEBio.*

The addition of strain dependent permeability is strongly suggested to replicate articular cartilage behavior, especially at high strain. Actually, as can be seen in Figure 6.16 and 6.17, the addition of Holmes-Mow permeability increase the accuracy in the reproduction of the reaction force under unconfined compression step-wise relaxation test. The addition of this feature, in fact, increase the level of accuracy in the description of AC mechanical properties, even if the computational time and resources needed to compute the solution remain almost identical to the case with constant permeability.

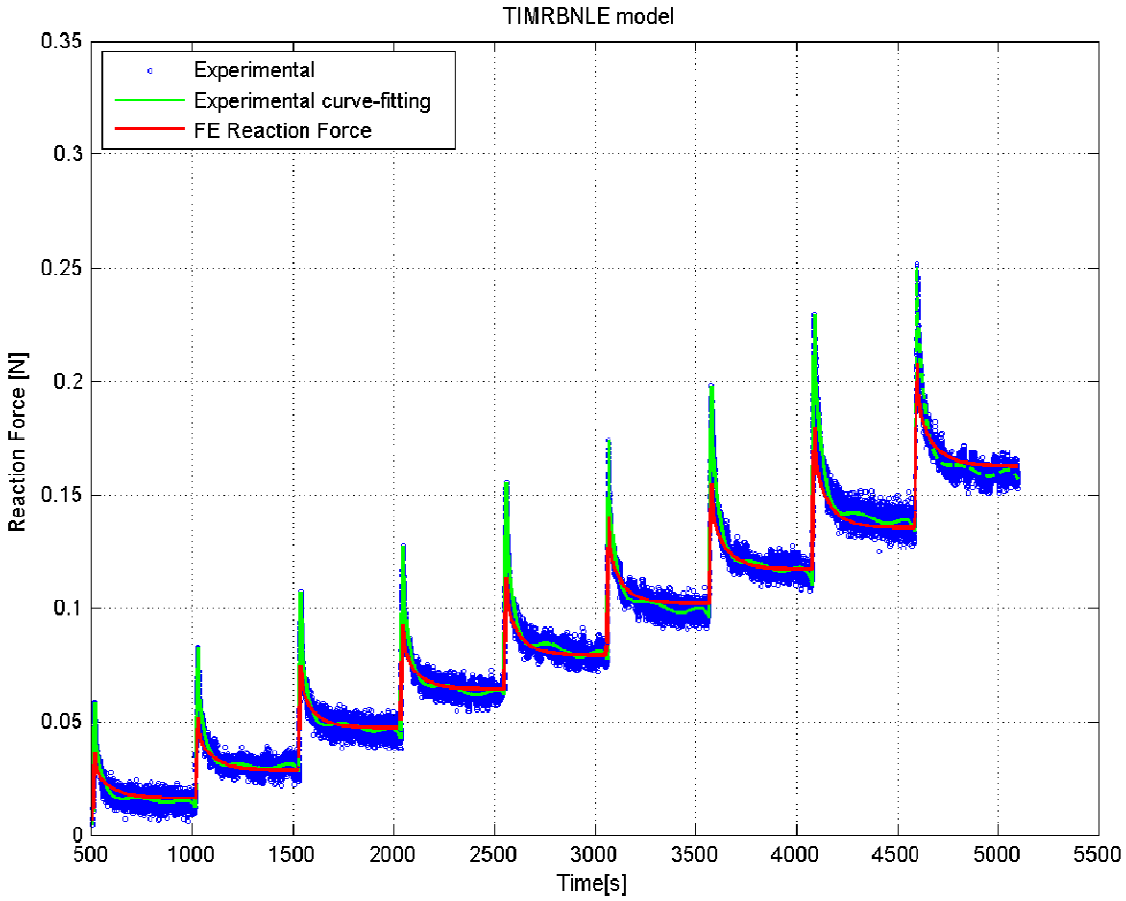

Figure 6.17: *Comparison between the reaction force obtained from the experimental data (blue) and its curve-fitting with a polynomial of 5th degrees (green) with a the numerical prediction obtained implementing the three-dimensional TIMRBNLE model (red) in the FEM FEBio*

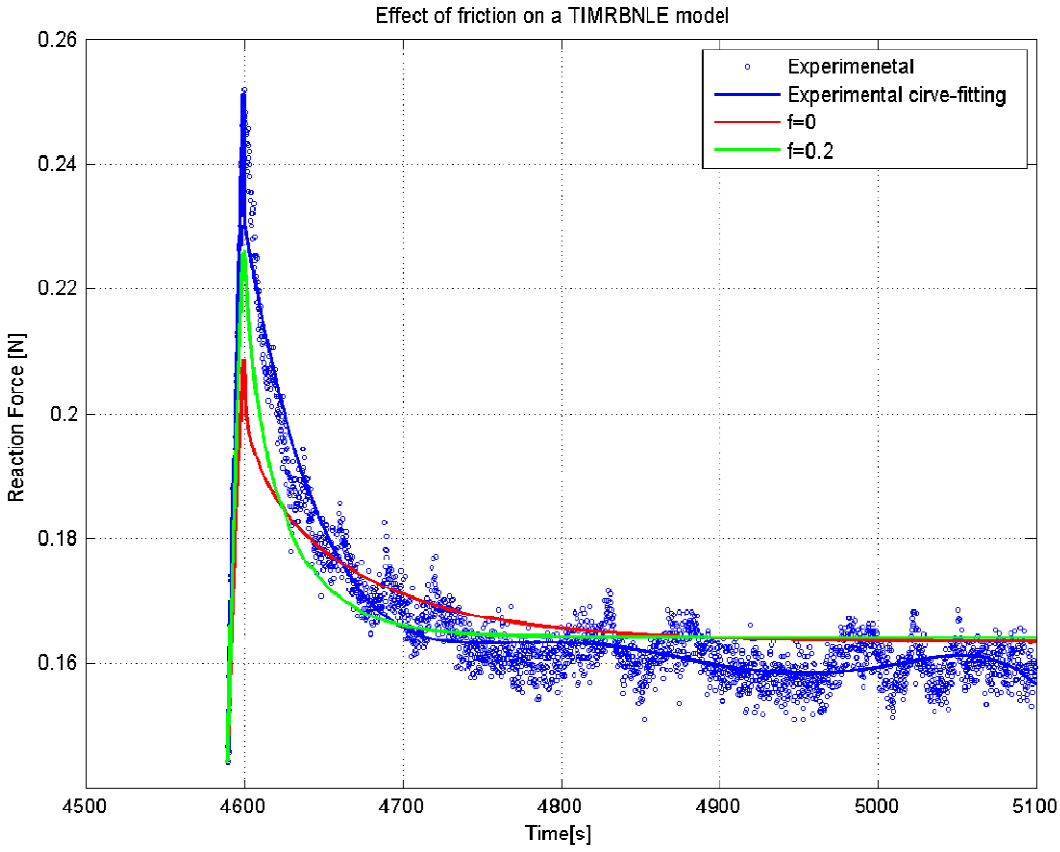

Figure 6.18: *Comparison between the reaction force obtained from the experimental data (blue) and its curve-fitting with a polynomial of 5th degrees with a the numerical prediction obtained implementing the three-dimensional TIMRBNLE model (red) in the FEM FEBio and the same model at which friction (f=0.2) was added (green) . In this figure is showed only the 10th step (i.e 8% strain) of the step-wise unconfined compression.*

As well discussed above, traditionally, in unconfined compression test, the effect of friction between the samples and the loading plates is considered negligible, such that the specimens are considered to deform uniaxially the material properties are easily obtained by a curve-fit between the experimental data and the analytical model (Wu, et al., 2004). However, even in ideally controlled experimental conditions, the friction in the specimen/platen interface in unconfined compression cannot be completely neglected (Wu, et al., 2004; Wu, et al., 2003).

Above was analyzed the lack of the biphasic model to reproduce the high ratio from peak to equilibrium of the reaction force, typical of AC samples under unconfined compression relaxation tests. This lack could be overcome considering friction (Li, et al., 1999; Spilker,

et al., 1990) as can be seen also from Figure 6.18. A bigger ratio from peak to equilibrium could be reached considering friction in either the case of isotropic (Figure 6.6) and anisotropic material (Figure 6.18), but still the mismatch between experimental data and numerical solution persist.

From the results of the FE analysis on friction, presented in Section 6.2.1.2, it is possible to conclude that if the material properties of articular cartilage are obtained from a curve-fit between the experimental data and the numerical implementation without the consideration of friction, the resulting material parameters are lower than the true mechanical properties. Thus, in conclusion, although the resulting computational time increase conspicuously, the effect of friction cannot be neglected during the FE analysis to measure the mechanical properties of articular cartilage under unconfined compression test.

To increase the accuracy between the reaction force measured from the unconfined compression test and its numerical prediction, the mechanical parameters used to reproduce AC behavior under compression, were changed in each step. As suggested before, this is probably because the upper surface of the sample is not parallel to the loading platens. Thus, if the angle between the two surfaces are considered in the FE analysis, a bigger accuracy between the experimental reaction force and the numerical one at each step may be found without changing the material properties at each step (Figure 6.19). During the sample preparation, great afford was made to obtain specimen flatter than possible. But the intrinsic variation of AC thickness in the joint as well as errors introduced during the manipulation by the user could be lead to the preparation of non flat samples. Although the drilling of the AC plugs from 6 mm to 3 mm in diameter produces sample with surfaces that seems more parallel than in the case of bigger diameter, the problem of the flatness still persist. Figure 6.19 shows how big is the change in the reaction force measured, also in the case that the articular surface is skew only of one degree. Only observing with the eye is not possible to perceive that the sample is not flat, but the experimental data obtained are affected by this problem.

Finally, a comparison between axisymmetric and three-dimensional simulations (Figure 6.20) was conducted, using the same material properties on different FE software (respectively, ABAQUS and FEBio). The results showed that the accuracy of the reproduction of the reaction force at the end of relaxation is bigger for a three-dimensional

analysis than the axisimmetric one, especially at larger strain. It is possible to conclude that the mechanical parameters obtained from three-dimensional simulations through a curve-fit with the experimental data, are more accurate than the ones measured with axisymmetric simulations. Besides, 3D simulations make it possible to compute more accurate stress and strain within the tissue.

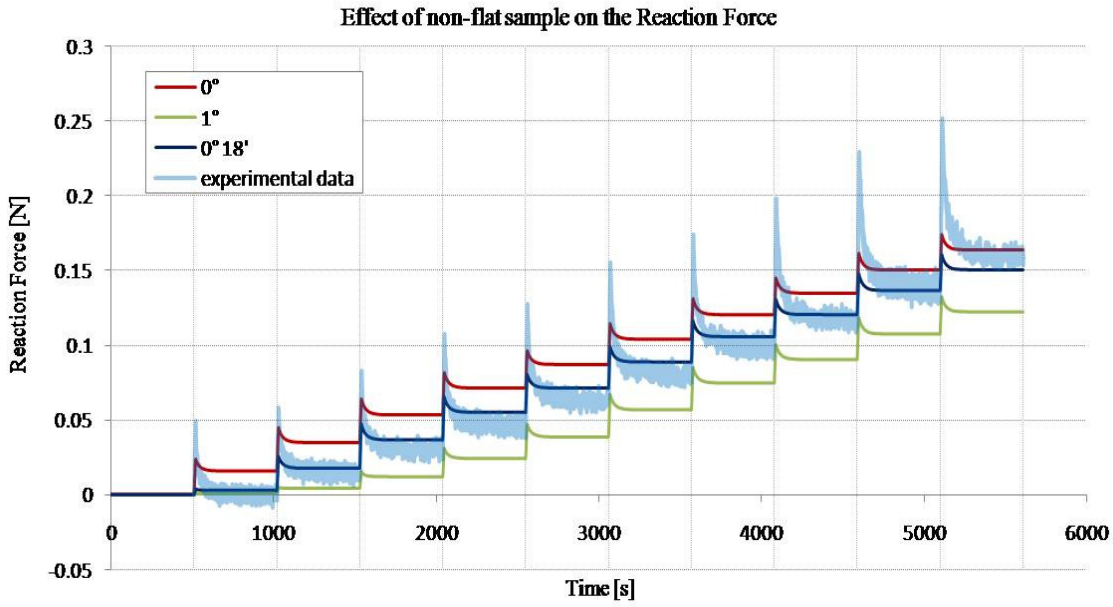

Figure 6.19: *Numerical prediction of the reaction force obtained for non flat samples. The angle between the superficial surface of cartilage and the indenter was changed from 1° to 0°. Note how much change the reaction force registered with small change in the orientation of the sample.*

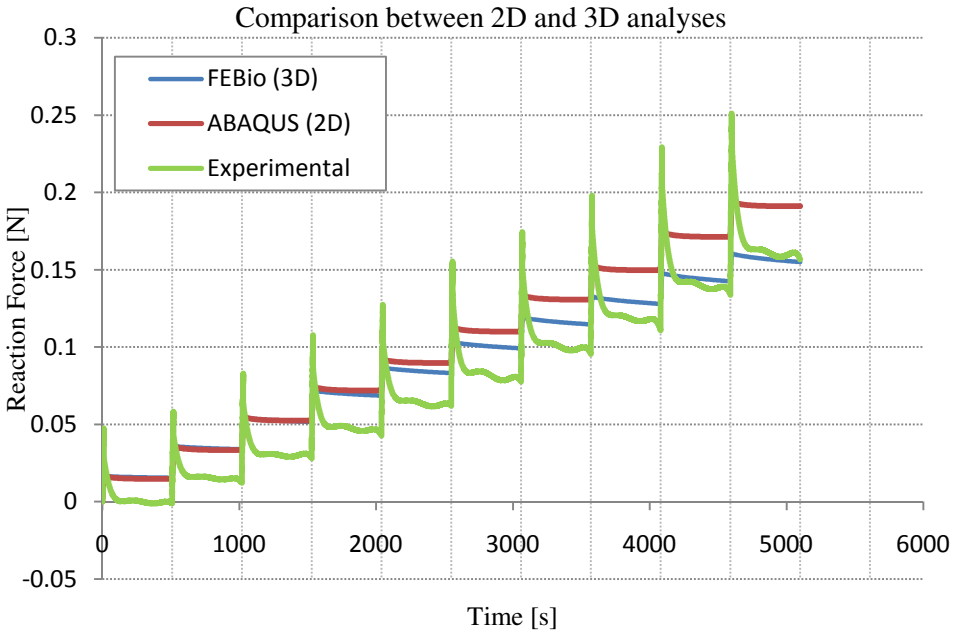

***Figure 6.20**: comparison between 2D and 3D models.*

6.3.2 Swelling Model

During an experimental tests on swelling is impossible to divide the effect of the presence of mobile ions inside the tissue from the one due to the presence of charge-to-charge repulsive forces, without damaging the cartilage. However, it is possible to obtain a good approximation of the material constants of equation 5.9 for the chemical expansion, from curve-fit between the numerical and experimental reaction force at equilibrium (Figure 6.21). Whereas the materials constants of equation 5.11 for the fluid expansion can be obtained from the curve–fit at the beginning of swelling (Figure 6.21). The materials constants obtained are shown in Table 1. Thermal analogy to analyze swelling is able to fit the observed reaction force obtained from the experimental tests presented in chapter 4 (Figure 6.22).

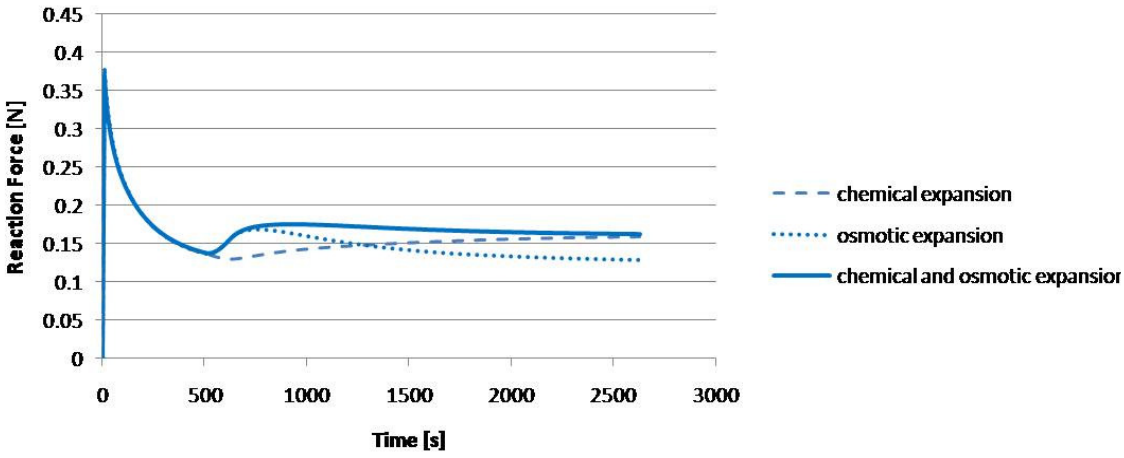

***Figure 6.21**: Numerical prediction of the osmotic expansion and chemical expansion. The parameters used are in Table1.*

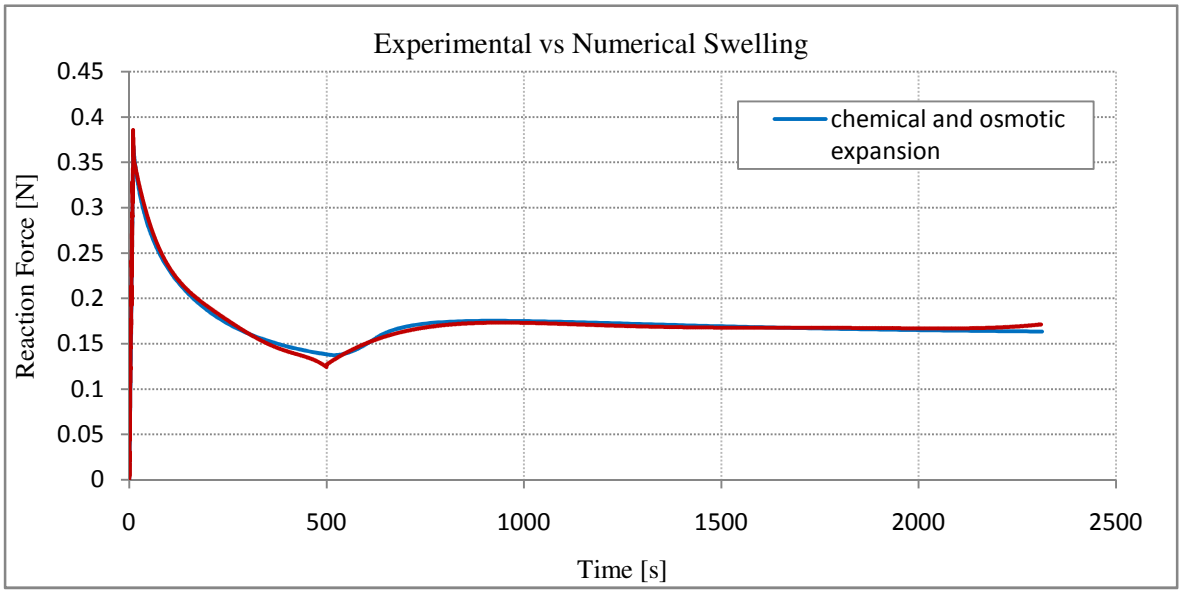

***Figure 6.22:** Comparison between the experimental reaction force obtained from the swelling test and the thermal analogy model.*

	Sample A	Sample B	Sample C	Sample D
ξ_{int}	0.259	0.257	0.253	0.245
ξ_{ext}	0.924	0.924	0.924	0.924

Table 1: *Material parameters for the osmotic expansion obtained from the curve- fit between the experimental reaction force and the numerical one.*

	Sample A	Sample B	Sample C	Sample D
β_0 [kPa]	15	10	6	8
c_β [mM]	10	10	10	10

Table 2: *Material parameters for the chemical expansion obtained from the curve- fit between the experimental reaction force and the numerical one.*

Numerous hypothesizes were done to simplify the complex triphasic model. In particular, the major difference between the proposed approach and the triphasic formulation (Lai, et al., 1991) is that the friction between ions and fluid was neglected in thermal analogy model. However, can be considered that the effects of the friction between ions and fluid are included in the diffusion coefficient. Thus, the thermal analogy represents a reasonable approximation of complex biological systems, since the friction between ions and fluid cannot be measured directly, whereas the diffusion coefficient can be determined experimentally.

Besides, in the present simulations, a constant osmotic coefficient, hydraulic permeability, and diffusion coefficient was used. However, in reality, these coefficients are not constant. Deformation-and ion concentration-dependent coefficients (osmotic coefficient, hydraulic permeability, and diffusion coefficients) can be incorporated into the proposed approach.

In the present simulations, no convention was taken into account to simplify the model. However, comparison with Wu's model (Wu, et al., 2002), in which convection was

considered, demonstrated that not a big difference there is between the two models (Li, 2009).

In conclusion, from the great accuracy registered between the reaction force measured in the experiment and the predicted one, AC swelling can be accurately reproduced in a commercial FE software, with the thermal analogy method.

Chapter 7
Conclusion and Future Work

The purpose of this study was to validate numerous biphasic models used to reproduce the mechanical properties of cartilage and investigate the interaction between each component of the tissue, for a better comprehension of the mechanisms that could induce diseases. To validate the biphasic models present in the literature, a comparison was led between the numerical implementation in the FE softwares FEBio v.1.2.0 (Musculoskeletal Research Laboratories, University of Utah) and ABAQUS v.6.8.1 (ABAQUS Inc., Providence, USA) and unconfined compression relaxation tests. Results of this type of test show that is possible to calculate the mechanical properties of the tissue directly from a curve-fit between the numerical prediction of reaction force and the measured one.

This work is part of a larger project aimed at modeling the knee joint. Thus, accurate stress and forces acting on each component of the knee during daily activity have to be investigated, on order to reach a better comprehension of the structure of the healthy knee joint and its alteration during injury. To precisely reproduce the behaviour of the AC during loading, it is essential to describe each component of cartilage. However, adding more features of the AC composition increases the number of material parameters that must be determined making the model the more computationally expensive. Hence, this thesis work started by analyzing the simplest model (BLE), increasing evermore the level of the complexity of the structure until a good agreement between the numerical results and experimental data was found. The BLE model can be easily used in a knee joint FE model due to the low computational burden and the use of only three parameters to define the mechanical properties of cartilage. However, it is well known that the description of cartilage as a poroelastic material is not enough to reproduce numerically the response of articular cartilage under the unconfined compression relaxation test, because the anisotropy

of cartilage is not taken into account (Boschetti, et al., 2006; Cohen, et al., 1998; Li, et al., 1999; Wilson, et al., 2005). The addition of anisotropy through the introduction of a single preferred fiber direction (TIMRBLE and TIMRBNLE models) is still not enough to reproduce the registered history of the reaction force of articular cartilage under the unconfined compression test. This is probably due to the consideration of a single family of fibers and due to the use of a discrete fiber distribution (Ateshian, et al., 2009; Wilson, 2005). In fact, the continuum angular distribution is able to replicate the history of reaction force of the AC under the unconfined compression test. Though it adds a major disadvantage to the computational burden, in terms of time and resources required to compute the internal stress and strain of articular cartilage. In addition, both require the identification of a large number of parameters (seven for TIMRBLE model and nine for the continuum angular fiber distribution model), considerably higher than the number of parameters (only three) demanded by the BLE model.

The addition of the strain-dependent permeability made it possible to replicate, with more accuracy, the reaction force of the articular cartilage under unconfined compression step-wise relaxation test.

Because, PGs determine the response in compression, an accurate model for cartilage must also take into account the presence of PGs, especially their negative charge (FCD). To include their presence in a FE analysis a thermal analogy model was developed in order to simulate swelling, from Wu's (Wu, et al., 2002) and Li's (Li, 2009) works. This model was then validated by comparing the predicted numerical reaction force with the measured reaction force obtained through a specially designed unconfined compression test. The results show that such tests are successful in analyzing the effect of change of concentration in the bath on the cartilage. In particular, these tests proved to be easy to apply and they required the same experimental set-up used to validate the biphasic models.

An interesting question arose during the development of this work concerning the effect of friction between cartilage and the materials in contact with it (dish and loading platens). Traditionally, the effect of friction between the samples and the loading indenter is considered negligible, so as the material properties are easily obtained by a curve-fit between the experimental data and the numerical model. However, even in ideally controlled experimental conditions, the friction in the specimen/platen interface in

unconfined compression cannot be completely eliminated. Consequently, the mechanical behavior of biomaterial, as observed via traditional unconfined compression tests, is influenced by the friction between the specimen and the platens (Wu, et al., 2003; Wu, et al., 2004). Thus, if the material properties of articular cartilage are obtained from a curve-fit between the experimental data and the numerical implementation without friction, the resulting material parameters are lower than the true mechanical properties. A bigger ratio from peak to equilibrium could be reached considering friction in either the case of isotropic (Figure 6.4) and anisotropic material (Figure 6.14), but still the mismatch between experimental data and numerical solution persisted due to the poor accuracy of the modeling of AC structure.

During the preparation of the sample and the execution of the unconfined compression tests, another problem emerged: articular cartilage plugs have to be flat. If actually the samples are not flat, the registered reaction force will be lower than those measured on flat samples and the initial peak of reaction force is also much smaller when there is smaller contact area. Thus, a smaller relaxation occur in the cartilage. As a result, the mechanical parameters obtained from the curve-fit may be different from the real mechanical properties. Thus, one of the main problems observed, and still unanswered, is the need for flat samples. For this reason, it is required to develop a custom made device in order to obtain flatter samples without altering the structure of AC.

A big effort must be made in the research of a constitutive model that could thoroughly reproduce the response of cartilage under different loading and that could be applied in a three-dimensional knee joint FE model.

In this thesis work, the numerical results from thermal analogy to analyze swelling were compared with experimental tests. Further studies have to be made to fully validate this model. In particular, it is necessary to corroborate the hypothesis at the base of this model, i.e. that the thermal diffusion is equivalent to mass diffusion. A study on this topic has just started.

Further experimental studies on friction in the specimen/platen interface have to be made to obtain more accurate values, due to the impossibility of defining the best value through analytical study. Actually, numerous factors influence the friction coefficient: it is time-dependent and it changes both with the concentration of bath and the type of loading.

In summary, the AC constitutive relation for a FE knee joint model requires a compromise between accuracy in the response reproduction of the tissue under different loading and speed in the results computation. Actually, in order to replicate all the mechanical behavior of cartilage under different experimental test, the description of cartilage as only composed of a linearly elastic solid matrix and a fluid phase is not enough. To improve accuracy, it is required an accurate description of the real structure of collagen network, but obviously to the detriment of calculation speed. Moreover, a purely fibrillar matrix, where fiber can only support tensile loading, is completely unstable. The stability of such structure is provided by the negative charged PGs, represented here by the fluid and chemical expansion through the thermal analogy model. This model proved to be very accurate in the reproduction of swelling, also in the transient phase. Again, the increase in the detail of the description of the structure decrease the computational speed. Finally, results suggested that the presence of friction between sample/platens interfaces, the use of samples that are not flat and the storing method affect the measured mechanical properties of articular cartilage. This study propose a FE approach to neglect their influence on the mechanical properties.

References

Abaqus documentation.

Accardi, M. (2008). *Mechanical behaviour of cartilage for human joint.* 4M Final year report, Imperial collage.

Accardi, M. (2007). *Soft tissue tribology: mechanical response and modelling of cartilage.* Litterature research, Imperial collage.

Ateshian, G. (2007). Anisotropy of fibrous tissues in relation to the distribution of tensed and buckled fibers. *Transaction of the ASME , 129*, p. 240-249.

Ateshian, G., Rajan, V., Chahine, N., Canal, C., & Hung, C. (2009). Modeling the matrix of articular cartilage using a continuous fiber angular distribution predicts many observed phenomena. *Journal of biomechanical engineering , 131*, p. 1-10.

Ateshian, G., Soltz, M., Mauck, R., Basalo, I., Hung, C., & Lai, W. (2003). The role of osmoric pressure and tension-compression nonlinearity in the frictional responce of articular cartilage. *Transport in porous media , 50*, p. 5-33.

Boschetti, F., Gervaso, F., Pennati, G., Peretti, G., Vena, P., & Dubini, G. (2006). Poroelastic numerical modelling of natural and engineering cartilage based on in vitro tests. *Biorheology , 43*, p. 235-247.

Brown, C. P., Nguyen, T. C., Moody, H. R., Crawford, R. W., & Oloyede, A. (2009). Assessment of common hyperelastic constitutive equation for describing normal and osteoarthritic articular cartilage. *Journal of engineering in medicine , 223* (H), p. 643-652.

Chahine, N., Wang, C., Hung, C., & Ateshian, G. (2004). Anisotropic strain-dependent material properties of bovine articular cartilage in the transitional range from tension to compression. *Journal of Biomechanics , 37*, 1251-1261.

Chen, A., Bae, W., Schinagl, R. M., & Sah, R. (2001). Depth- and strain-dependent material properties of bovine articular cartilage in the transitional range from tension to compression. *Journal of Biomechanics , 34*, 1-12.

Cohen, B., Lai, W. M., & Mow, V. C. (1998). A transversely isotropic biphasic model for unconfined compression of growth plate and chondroepiphysis. *Journal of biomechanical engineering , 120*, 491-496.

Dèmarteau, O., Pillet, L., Inaebnit, A., Borens, O., & Quinn, T. (2006). Biomechanical characterization and in vitro mechanical injury of elderly human femoral head cartilage: comparison to adult bovine humeral head cartilage. *OsteoArthritis and Cartilage , 14*, p. 589-596.

DiSilvestro, M. R., & Suh, J. F. (2001). A cross-validation of the biphasic poroviscoelastic model of articular cartilage in unconfined compression, indentation, and confined compression. *Journal of biomechanics , 34*, 519-525.

DiSilvestro, M. R., Zhu, Q., & Suh, J. F. (2001). Biphasic poroviscoelastic simulation of the unconfined compression of articular catilage: II-effect of variable strain rates. *Journal of biomechanical engineering , 123*, 198-200.

DiSilvestro, M. R., Zhu, Q., Wong, M., Jurvelin, J. S., & Suh, J. F. (2001). Biphasic poroviscoelastic simulation of the unconfines compression of articular cartilage: I - simultaneous prediction of reaction force and lateral displacement. *Journal of biomechanical engineering , 123*, p. 191-197.

Donzelli, P., Spilker, R., Ateshian, G., & Mow, V. (1999). Contact analysis of biphasic transversely isotropic cartilage layers and correlations with tissue failure. *Journal of biomechanics , 32*, p. 1037-1047.

Eisemberg, S., & Grodzinsky, A. (1987). The kinetics of chemically induced nonequilibrium swelling of articular cartilage and corneal stroma. *journal of biomedical engineering , 109*, p. 79-89.

Federico, S., Grillo, A., La rosa, G., Giaquinta, G., & Horzog, W. (2005). A trasversely isotropic, trasversely homogeneus microstructural-statistical model of articular cartlage. *Journal of biomechanics , 38*, 2008-2018.

Fung, Y. C. (1993). *Biomechanics:mechanical properties of living tissue.* Springer.

Goldsmith, A., Hayes, A., & Clift, S. (1996). Application of finite elements to the stress analysis of articular cartilage - A review. *Med. Eng. Phys. , 18* (2), p. 89-98.

Holmes, M. H., & Mow, V. C. (1990). The nonlinear characteristics of soft gels and hydrated connective tissues in ultrafiltration. *Journal of biomechanics , 23* (11), p. 1145-1156.

Julkunen, P. (2008). *Relationships between structure, composition and function of articular cartilage - Studies based on Fibril Reinforced Poroviscoelastic modeling.* Doctoral dissertation, University of Kuopio, Department of Physics.

Jurvelin, J. S., Buschmann, M. D., & Hunziker, E. B. (2003). Mechanical anisotropy of the human knee articular cartilage in compression. *Proc. Inc. Mech. Eng , 217* (H), 215-219.

Katta, J., Zhongmin, J., Ingham, J., & Fisher, J. (2008). Biotribology of articular cartilage - A review of the recent advances. *Medical engineering & physics* .

Kennedy, E., Tordonado, D., & Duma, S. (2007). Effects of freezing on the mechanical properties of articular cartilage. *Biomedical science instrument , 43*, p. 342-347.

Korhonen, R., Laasanen, M., Toyras, J., Rieppo, J., Hirvonen, J., Helminen, H., et al. (2002). comparison of the equilibrium responce of articula cartilage in unconfined compression, confined compression and indentation. *Journal of biomechanics , 35*, p. 903-909.

Krishnan, R., Mariner, E., & Ateshian, G. (2005). Effect of dynamic loading on the frictional responce of bovine articular cartilage. *Journal of biomechanics , 38*, p. 1665-1673.

Lai, W. M., Hou, J. S., & Mow, V. C. (1991). A Triphasic Theory for the Swelling and Deformation Behaviors of Articular Cartilage. *Journal of biomachanical engineering , 113*, 245-258.

Li, G., Gil, J., Kanamori, A., & Woo, S. (1999). A validated three-dimensional computational model of a human knee joint. *Journal of biomechanical engineering , 121*, p. 657-662.

Li, J. (2009). *Mechanical behaviour of articular cartilage for human joint.* 4M Final year report, Imperial college.

Li, L. P., Soulhat, J., Buschmann, M., & Shirazi-Adl, A. (1999). Nonlinear analysis of cartilage in unconfined ramp compression using a fibril reinforced poroelastic model. *Clinical biomechanics , 14*, 673-682.

Li, L., Cheung, J., & Herzog, W. (2009). Three-dimensional fibril-reinforced finite element model of articular cartilage. *Med Biol Eng Comput , 47*, p. 607-615.

Maas, S., Rawlins, D., Weiss, J., & Ateshian, G. (2010). *FEBio theory manual.*

Maas, S., Rawlins, D., Weiss, J., & Ateshian, G. (2010). *Febio user's manual.*

Mansour, J. M. (2003). Biomechanics of Cartilage. In C. A. Oatis, *Kinesiology: the mechanics and pathomechanics of humen movement* (p. Chapter 5, 66-79). Lippincott William and Wilkins, Philadelphia.

Maroundas, A., & Venn, M. (1977). Chemical composition and swelling of normal and osteoarthrotic femoral head cartilage. *Annals od the Rheumatic diseas , 36*, p. 399-406.

Mow, & Lai. (2000). Basic biomechanics of the musculoskeletal system. In Nordin, & Frenkel.

Mow, V. C., Kuei, S. C., Lai, W. M., & Armstrong, C. G. (1980). Biphasic creep and stress relaxation of articular cartilage in compression: theory and experiments. *Journal of biomechanical engineering , 102*, 73-84.

Muldrew, K., Novak, K., Yang, H., Zernicke, R., Schachar, N., & McGann, L. (2000). Criobiology of articular cartilage:ice morphology and recovery of chondrocytes. *Cryobiology , 40*, p. 102-109.

Myers, E., Lai, W., & Mow, V. (1984). A continuum theory and an experiment for the ion-induced swelling behaviour of articular cartilage. *Journal of biomechanical engineering , 106*, p. 151-158.

Plochocki, J., Ward, C., & Smith, D. E. (2009). Evaluation of the chondral modeling theory using fe-simulation and numeric shape optimization. *Jourbnal of anatomy , 214*, p. 768-777.

Probstein, R. (1994). *Physicochemical hydrodynamics - An introduction* (2nd Ed. ed.). John Willy&sons,Inc.

Spilker, R. L., Suh, J., & Mow, V. C. (1990). Effects of friction on the unconfined compressive responce of articular cartilage: a finite element analysis. *Journal of biomechanics , 112*, p. 138-146.

Wang, Q., & Zheng, Y. (2007). Ultrasound measurement of swelling behaviors of articular cartilage in situ. In *Biomechanical systems technology* (p. 271-295). Cornelius T Leondes (University of California, Los Angeles, USA).

Weiss, J., Maker, B., & Govindjee, S. (1996). Finite element implementation of incompressible, trnsversely isotropic hyperelasticity. *Vomputer methods in applied mechanics and engineering , 135*, p. 107-128.

Willett, T., Whiteside, R., Wild, P., Wyss, U., & Anastassiades, T. (2005). Artefacts in the mechanical characterization of porcine articular cartilage due to freezing. *Journal of engineering in medicine , 219*, p. 23-29.

Wilson, W. (2005). *An explanation for the onset of mechanically induced cartilage damage.* Doctoral dissertation, Technische Universiteit Eindhoven.

Wilson, W., van Donkelaar, C., van Rietbergen, R., & Huiskes, R. (2007). The role of computational models in the search for the mechanical behavior and damage mechanisms of articular cartilage. *Medical Engineering & Phisics , 27*, 810-826.

Wilson, W., van Donkellaar, C., & Huyghe, J. (2005). A comparison between mechano-elecrochemical and biphasic swelling theories for soft hydrated tissues. *journal of biomechanical engineering , 127*, p. 158-155.

Wu, J. Z., & Herzog, W. (2002). *Simulating the swelling and deformation behaviour in soft tissues using a convective thermal analogy.* Tratto da http://www.biomedical-engineering-online.com/content/1/1/8.

Wu, J. Z., Dong, R. G., & Schopper, A. W. (2004). Analysis of effects of friction on the deformation behaviour of soft tissue in unconfined compression tests. *Journal of biomechanics , 37*, p. 147-155.

Wu, J. Z., Dong, R. G., Smutz, W. P., & Schopper, A. W. (2003). Effect of speciment/platen friction in unconfined compression of soft tissue is non-negligible.

Wu, J., Dong, R., & Smutz, W. (2004). Elimination of the friction effects in unconfined compression tests of biomaterials and soft tissues. *Journal of engineering in medicine , 218* (H), p. 35-40.

Wu, J., Herzog, W., & Epstein, M. (1998). Evaluation of the Þnite element software ABAQUS for biomechanical modelling of biphasic tissues. *Journal of biomechanics , 21*, p. 165-169.

Zheng, S., Xia, Y., Bidthanapally, A., Badar, F., Ilsar, I., & Duvoisin, N. (2009). Damages to the extracellular matrix in articular cartilage due to cryopreservation by microscopic magnetic resonance imaging and biochemistry. *Magnetic resonance imaging , 27*, p. 648-655.

Ringraziamenti

Arrivata alla fine di questo meraviglioso anno desidero ringraziare tutti coloro che mi hanno permesso di realizzare questo lavoro e di vivere una bellissima esperienza a Cardiff. Innanzitutto desidero ringraziare il Prof. Vena per avermi dato l'opportunità di svolgere questa mia tesi all'estero, in un ambiente stimolante in qualsiasi campo di ricerca. Un grazie particolare va al Prof. Evans per avermi sempre dato geniali suggerimenti per risolvere qualsiasi tipo di problema, per aver sopportato le mie numerose e-mail giornaliere, per aver avuto tanta pazienza nel leggere la mia tesi nel mio "inglese", ma soprattutto per avermi concesso di svolgere la tesi a Cardiff.

Come non ringraziare la Dott.ssa Emma Blain per avermi aiutata nelle prove sperimentali pur perdendo tanto tempo nel camminare tra infiniti corridoi e ancor più numerose porte almeno 20 volte al giorno tra un esperimento e l'altro, ma soprattutto per aver sperato con me che ogni prova riuscisse, anche senza la supervisione attenta del Prof. Evans.

Grazie a tutti coloro a che mi hanno dato un caloroso benvenuto all'università di Cardiff. In particolare, grazie alla Dott.ssa Cathy Holt per il sostegno, le innumerevoli risate e per avermi mostrato come sia facile instaurare una relazione di scherzi e risate tra professori e studenti. A tutti i PhD che hanno sempre sopportato le mie "chiacchere" che li distraevano dal loro lavoro e per avermi sempre coinvolto in cene e uscite ai pub per farmi sentire a casa. Cercherò di nominarvi tutti sebbene siate tanti (spero di non aver dimenticato nessuno): Rachel, Lindsay, Joanna, Barry, Wayne, Dan, Gemma, Phil, June, Holly e Jamal.

Un grande e speciale ringraziamento va alla mia famiglia. A mia mamma e mio papà, anche se non siate i primi in questa pagine siete sempre i primi nel mio cuore per avermi sempre sostenuto nelle mie scelte, per avermi sempre incoraggiata a superare le difficoltà, per credere sempre in me, per aver investito in me in tutti questi anni e per essermi sempre vicino. Grazie!!!

Un grazie speciale a Fabio per essermi sempre vicino soprattutto durante le mie crisi di panico in cui tutto mi sembra impossibile, ma poi grazie ai tuoi consigli e alla tua vicinanza tutto passa. Grazie!!!

Grazie a tutti gli amici che ho conosciuto in questi anni di università che mi hanno sempre permesso di affrontare interminabili ore di viaggio tra Milano e Varese e stressanti giornate in università con il sorriso. Senza di voi e la vostra vena di follia Virgi, Richi, Gigio, Gio ed Evi non ce l'avrei mai fatta. A tutti quelli che mi hanno permesso di trovare la noiosa Varese felice e divertente. Grazie!

Come dimenticare la mia "famiglia" spagnola che ho conosciuto a Cardiff. Gli Amici con la A maiuscola che mi sono sempre stati vicini, perché gli amici si vedono sì nel momento del bisogno ma è soprattutto nella vita di tutti i giorni. Grazie per le innumerevoli splendide serate passate insieme (sia quelle a casa davanti a Youtube sia in qualche festa a scatenarsi), per farmi sentire ancora parte di quella meravigliosa famiglia nonostante la lontananza e per i momenti che affronteremo insieme. E a tutte le meravigliose persone che ho conosciuto a Cardiff…Grazie, grazie, grazie!!